

**THE INFLUENCE OF SCALE AND PARENT MATERIAL ON  
HILLSLOPE HYDROLOGICAL PROCESSES IN KRUGER  
NATIONAL PARK**

**FT Jumbi**

Submitted in partial fulfillment of the requirements for the degree of MSc Hydrology

Centre for Water Resources Research  
University of KwaZulu-Natal  
Pietermaritzburg  
April 2014

## ABSTRACT

Semi-arid savannas are dynamic and complex systems controlled by fire, nutrient and water availability where water is the major driving force controlling the biological activity in these systems. Knowledge of hydrological processes is therefore, crucial for the prediction of ecosystem changes, given the prospect of climate change and the ever-increasing anthropogenic pressure on resources. There have been numerous advances in hydrological studies especially at the hillslope scale. Many of them have however, been site-specific and mostly comprising of a series of point measurements, thereby making it difficult to link processes at different scales in other sites. Some form of classification system would therefore, enable process integration, which is crucial in understanding and linking processes at various scales. For effective management and water resource planning, knowledge of how a system functions is crucial especially in savannas. It also helps in better prediction of behavior in ungauged systems that are in similar settings since many people rely on savannas for various ecosystem goods and services, the sustainability of livelihoods and biodiversity.

Meanwhile, ephemeral systems contribute significantly to how savanna systems work. However, hydrological processes operate at different scales even in these ephemeral systems involving controls such as landscape morphology, geology and climatic conditions in different environments. The effect of scale on hydrological processes is one unresolved issue in hydrological studies and knowledge of how processes vary at different scales is fundamental in understanding scale-dependent processes and those that are not. This also helps in understanding the thresholds and controls at which the processes operate. Hydrological processes were observed and quantified at the hillslope scale in contributing areas to 1<sup>st</sup>, 2<sup>nd</sup> and 3<sup>rd</sup> order ephemeral streams in the Kruger National Park (KNP) landscapes on basalt and granite parent materials. Processes include subsurface lateral and vertical flow, overland flow and potential recharge to groundwater. These were focused on the KNP supersites, which are sites that were especially selected for multidisciplinary research. This would allow the description and measurement of processes and patterns at different scales, rainfall gradients and geological settings within the landscapes.

Hillslope hydrological processes are dynamic and very complex but they are nonetheless vital, due to their interactions with surface and groundwater. Hillslope mechanisms of flow and subsurface moisture content are highly variable at both spatial and temporal scales. In order to gain insights into this variability, a number of techniques were used, such as measurement of soil water potential at different depths, geophysical surveys and numerical modelling. From the hydrometry data and modelling exercise, fluxes and water balances were derived in order to derive the hillslope response functions and potential connectivity with the underlying aquifers and/or adjacent streams. Since soils and hydrology have an interactive relationship, hillslope soil type responses were characterized through qualitative hydropedological descriptions.

Results showed that hillslope hydrological responses, such as flow mechanisms and connectivity are dependent on scale (incremental stream orders). Hydrological connectivity was highly driven by rainfall intensity on hillslopes associated with high order streams (2<sup>nd</sup> and 3<sup>rd</sup>). The major driver of hillslope storage was shown to be ET demand rather than soil depth, in these savanna ecosystems. The initial perception was that deeper soils will have greater storage capacity, but results obtained in this study proved otherwise. This also proved the ability of savanna vegetation to extract large amounts of soil water when available in the soil profile. This study showed that flow mechanisms were mainly influenced by topography and soil hydraulic properties and to a lesser extent the parent material.

## PREFACE

I..... declare that:

- (i) The research reported in this thesis, except where otherwise indicated, is my original work.
- (ii) This thesis has not been submitted for any degree or examination at any other university.
- (iii) This thesis does not contain other persons' data, pictures, graphs or other information, unless specifically acknowledged as being sourced from other persons.
- (iv) This thesis does not contain other persons' writing, unless specifically acknowledged as being sourced from other researchers. Where other written sources have been quoted, then:
  - (a) their words have been re-written but the general information attributed to them has been referenced;
  - (b) where their exact words have been used, their writing has been placed inside quotation marks, and referenced.
- (v) This thesis does not contain text, graphics or tables copied and pasted from the Internet, unless specifically acknowledged, and the source being detailed in the thesis and in the References sections.

Signed:.....

Student: Faith Tatenda Jumbi

Signed:.....

Supervisor: DR ES Riddell

Signed:.....

Co-supervisor: Prof SA Lorentz

## ACKNOWLEDGEMENTS

First and foremost, I would like to thank the Lord Almighty, who has and will always be my rock and strength, for guiding me throughout this research. I would also like to thank the following:

Water Research Commission - for funding the project.

Dr ES Riddell - Honorary Research Fellow, University of Kwa-Zulu Natal. Thank you for your supervision and support throughout the project. This would not have been possible if it had not been for all your tireless efforts.

Professor SA Lorentz - Honorary Associate Professor, Centre for Water Resources Research, University of KwaZulu-Natal, for his effort and time in supervising this project.

Mr. Thomas Rowe, Centre for Water Resources Research, University of KwaZulu-Natal - for assistance with SEBAL data and HYDRUS.

Colleagues - Ms. Tercia Strydom, Mr. Daniel Fundisi, Mr Ashton van Niekerk, for assistance with fieldwork, general logistics, ideas and companionship through the hard times.

Mr Kobus Coetzee and colleagues - University of Free State. Thank you for the assistance with soil surveys, classification and collection of samples.

Dr George van Zijl and Dr le Roux - University of Free State. Special thanks for the assistance with the soil surveys and hydro-pedological classification on the southern supersites.

Dr Johan van Tol – University of Fort Hare, for the valuable insights on hydro-pedology classification.

Professor Richard Stirzaker and Mr Johannes Hachmann – for valuable insights on soil water data and HYDRUS, respectively.

Mr JJ Pretorius - Senior Technician, Centre for Water Resources Research, University of KwaZulu-Natal, for organizing and assisting with field equipment

SANParks Scientific Services and - For permission to work in the park.

Mr A Mashele - SANParks Scientific Services, for keeping us safe in the field and assistance with the field work.

Special thanks also go to my family for their prayers and financial support.

## **SUPERVISOR'S APPROVAL**

As the candidate's supervisor, I have approved this thesis for submission

Signed .....

Name Dr ES Riddell

Date April 2014

# TABLE OF CONTENTS

ABSTRACT .....	ii
PREFACE.....	iv
ACKNOWLEDGEMENTS .....	v
SUPERVISOR’S APPROVAL .....	vi
LIST OF TABLES .....	xii
LIST OF FIGURES .....	xiii
LIST OF ABBREVIATIONS .....	xvi
1. INTRODUCTION.....	1
2. LITERATURE REVIEW .....	4
2.1 The Savanna Ecosystem .....	4
2.2 Hydrological Processes at the Hillslope Scale.....	4
2.3 Hillslope Flow Paths .....	6
2.3.1 Overland flow .....	7
2.3.2 Subsurface flow .....	8
2.3.3 Bedrock flow.....	9
2.4 The Influence of Macropores and Soil Pipes on Hillslope Storage .....	9
2.5 The Hillslope Water Budget .....	10
2.6 Hillslope Hydrological Connectivity.....	11
2.7 Hydropedological Soil Types and the Use of Pedotransfer Functions.....	11
2.8 The Significance of Conducting Research at Multiple Scales.....	13
2.9 The Use of Models in Hydrological Studies.....	14
2.10 Model Sensitivity Analysis.....	14

2.11	Evapotranspiration: Conventional/Remote Sensing Techniques.....	15
2.12	Review of Methods .....	16
2.13	Conclusion .....	19
2.14	Study Objectives, Key Question and Development of Hypothesis.....	20
3.	<b>STUDY SITES AND METHODOLOGY.....</b>	<b>22</b>
3.1	Location: Kruger National Park (KNP).....	22
3.2	Climate.....	22
3.3	KNP Geology and Soils.....	23
3.4	Drainage.....	24
3.5	Vegetation.....	25
3.6	Overview: Supersites.....	25
3.7	Methodology Roadmap.....	27
3.8	Instrumentation Network.....	28
3.8.1	Meteorological Station.....	29
3.9	Characterization of Soil Hydraulic Properties .....	30
3.9.1	Field measurement of unsaturated hydraulic conductivity ( $K_{\text{unsat}}$ ).....	30
3.9.2	Field measurement of saturated hydraulic conductivity ( $K_{\text{sat}}$ ) .....	31
3.9.3	The double ring infiltrometer.....	32
3.9.4	The mobile permeameter .....	33
3.10	Soil Classification .....	34
3.11	Monitoring of Subsurface Soil Water Dynamics .....	37
3.11.1	Laboratory-derived soil water potential.....	39
3.12	Geophysical Surveys .....	40
3.13	Simulation of Flow and Catena Element Water Balances Using HYDRUS 1D .....	43
3.13.1	Water flow simulation and its governing equations.....	44

3.13.2	Simulation period .....	45
3.13.3	Location, domain set-up and boundary conditions .....	45
3.13.4	The residual and saturated soil water content .....	46
3.14	Actual Evapotranspiration from Satellite Imagery.....	47
3.14.1	Partition of evapotranspiration into soil and root components .....	48
3.15	Model Validation (sensitivity analysis) .....	49
4.	<b>HILLSLOPE PROCESS CHARACTERIZATION RESULTS AND DISCUSSION .....</b>	<b>51</b>
4.1	Southern Granite Hydraulic Characterization.....	51
4.1.1	1 <sup>st</sup> order hillslope.....	51
4.1.2	2 <sup>nd</sup> order hillslope .....	54
4.1.3	3 <sup>rd</sup> order hillslope.....	56
4.2	Subsurface Soil Water Dynamics on Southern Granite Supersite .....	58
4.2.1	1 <sup>st</sup> order hillslope.....	58
4.2.2	2 <sup>nd</sup> order hillslope.....	61
4.2.3	3 <sup>rd</sup> order hillslope .....	63
4.3	Soil Water Potential (lab results) .....	66
4.4	Results from Geophysical surveys (ERT) on Granite Supersite.....	66
4.4.1	1 <sup>st</sup> order hillslope ERT .....	66
4.4.2	2 <sup>nd</sup> order hillslope ERT.....	68
4.4.3	3 <sup>rd</sup> order hillslope ERT .....	69
4.5	Hydropedological Hillslope Interpretations on Southern Granite Supersite .....	71
4.5.1	1 <sup>st</sup> order hillslope conceptual model .....	71
4.5.2	2 <sup>nd</sup> order hillslope conceptual model.....	72
4.5.3	3 <sup>rd</sup> order hillslope conceptual model .....	73
4.6	Southern Basalt Characterization Results.....	74

4.6.1	1 <sup>st</sup> order hillslope.....	74
4.6.2	2 <sup>nd</sup> order hillslope.....	75
4.6.3	3 <sup>rd</sup> order hillslope .....	77
4.7	Subsurface Soil Water Dynamics on the Southern Basalt Supersite .....	78
4.7.1	1 <sup>st</sup> order hillslope .....	78
4.7.2	2 <sup>nd</sup> order hillslope.....	80
4.7.3	3 <sup>rd</sup> order hillslope .....	82
4.8	Conceptual Models Derived from Hydropedological Interpretations on Southern Basalt Supersite .....	84
5.	QUANTIFICATION RESULTS AND DISCUSSION .....	85
5.1	Rainfall Distribution on the Granite Site.....	85
5.2	Measured Actual ET.....	86
5.3	Rainfall Distribution on the Basalt (Nhlowa) Site .....	88
5.4	Modelled Hydrological Fluxes .....	91
5.4.1	Simulated results for 1 <sup>st</sup> order granite hillslope.....	92
5.4.2	Simulated results for 2 <sup>nd</sup> order granite hillslope .....	94
5.4.3	Simulated results for 3rd order granite hillslope .....	97
5.4.4	Simulated results for basalt 3rd order hillslope .....	99
5.5	Model Validation.....	102
5.5.1	Observed vs Simulated Matric Potential .....	108
5.5.2	Model Sensitivity Analysis.....	108
5.6	Updated Conceptual Models from Observed and Simulated Data .....	110
6.	SYNTHESIS.....	115
7.	CONCLUSIONS.....	120
7.1	General Conclusions .....	121

7.2	Recommendations.....	121
8.	REFERENCES.....	122
9.	APPENDICES .....	137
9.1	Appendix A: Results from Geophysical Surveys (ERT) on Basalt Supersite.....	137
9.2	Depth of Installed Soil Moisture Sensors and Taxonomical Classification .....	140
9.3	$K_{sat}$ Replicates on Granite Supersite .....	140

## LIST OF TABLES

		Page
Table 3.1	Hydropedological hillslope classes (after van Tol <i>et al.</i> , 2013)	36
Table 3.2	Derived constants for parameter A-G	37
Table 4.1	Soil classification per catena element on granite 1 <sup>st</sup> order hillslope	53
Table 4.2	Soil classification per catena element on granite 2 <sup>nd</sup> order hillslope	55
Table 4.3	Soil classification per catena element on granite 3 <sup>rd</sup> order hillslope	57
Table 4.4	Soil classification per catena element on basalt 1 <sup>st</sup> order hillslope	74
Table 4.5	Soil classification per catena element on basalt 2 <sup>nd</sup> order hillslope	76
Table 4.6	Soil classification per catena element on basalt 3 <sup>rd</sup> order hillslope	77
Table 5.1	Catena element water budgets for 1 <sup>st</sup> order granite hillslope	92
Table 5.2	Catena element water budgets for 2 <sup>nd</sup> order granite hillslope	95
Table 5.3	Catena element water budgets for 3 <sup>rd</sup> order granite hillslope	98
Table 5.4	Catena element water budgets for 3 <sup>rd</sup> order basalt hillslope	100
Table 5.5	Sensitivity analysis using 2 <sup>nd</sup> order granite midslope catena element	108
Table 9.1	Catena elements taxonomy classes, diagnostic horizons and sensors	140

## LIST OF FIGURES

	Page
Figure 2.1	Dominant hillslope processes and flow paths (Anderson and Burt, 1990) 7
Figure 2.2	Macropore flow - Soil pipe outlet (photo by le Roux, 2006) 10
Figure 3.1	Rainfall distribution in KNP and location of supersites 23
Figure 3.2	Geology of KNP and location of supersites within the land systems 24
Figure 3.3	Southern granite supersite (a), southern basalt supersite (b) stream orders 26
Figure 3.4	Methodology roadmap 27
Figure 3.5	Monitoring stations and geophysics transects on granite supersite 28
Figure 3.6	Monitoring stations and geophysics transects on basalt supersite 29
Figure 3.7	(a) Schematic of a TDI, (b) TDI set-up in the field 31
Figure 3.8	Field measurement of $K_{sat}$ using the double ring infiltrometer and permeameter, respectively 32
Figure 3.9	Schematic of the measurement of $K_{sat}$ using the mobile permeameter 34
Figure 3.10	Taxonomical soil classification on catena elements 35
Figure 3.11	Hydrological soil types (after van Tol <i>et al.</i> , 2013) 36
Figure 3.12	(a) Soil moisture sensor (Cal Africa, 1978) and (b) Schematic of sensors 38
Figure 3.13	WPA Dewpoint PotentialMeter to measure soil water potential 40
Figure 3.14	ERT instrumentation ABEM Terrameter (ABEM [2005]: Instruction Manual 40
Figure 3.15	Resistivity ranges of various sediments and rock types (after Loke, 2004) 41
Figure 3.16	Basic electrical resistivity circuit from (a) one (b) two electrodes (after Todd 1980) 42
Figure 3.17	A schematic illustration of diagnostic horizons and boundary conditions 42
Figure 3.18	Iteration criteria on HYDRUS 1D 46
Figure 3.19	Boundaries of catena elements demarcated on Google Earth 48
Figure 4.1	Characterization chapter roadmap 51
Figure 4.2	Soil texture triangle, site map, $K_{unsat}$ at soil surface, $K_{sat}$ on SGR1 53
Figure 4.3	Soil texture triangle, site map, $K_{unsat}$ at soil surface, $K_{sat}$ on SGR2 55
Figure 4.4	Soil texture triangle, site map, $K_{unsat}$ at soil surface, $K_{sat}$ on SGR3 57

Figure 4.5	Soil moisture responses and % ED curves for granite 1 <sup>st</sup> order hillslope	60
Figure 4.6	Soil moisture responses and % ED curves for granite 2 <sup>nd</sup> order hillslope	62
Figure 4.7	Soil moisture responses and % ED curves for granite 3 <sup>rd</sup> order hillslope	65
Figure 4.8	A comparison of water potential between the 3 <sup>rd</sup> order hillslopes	66
Figure 4.9	Time series ERT for granite 1 <sup>st</sup> order hillslope	67
Figure 4.10	Time series ERT for granite 2 <sup>nd</sup> order hillslope	69
Figure 4.11	Time series ERT for granite 3 <sup>rd</sup> order hillslope	70
Figure 4.12	Hydrological soil types (after van Tol <i>et al.</i> , 2013)	71
Figure 4.13	Hydrological soil types and flow paths on granite 1 <sup>st</sup> order hillslope	71
Figure 4.14	Hydrological soil types and flow paths for granite 2 <sup>nd</sup> order hillslope	73
Figure 4.15	Hydrological soil types and flow paths for granite 3 <sup>rd</sup> order hillslope	73
Figure 4.16	Unsaturated hydraulic conductivity on 1 <sup>st</sup> order hillslope	75
Figure 4.17	Unsaturated hydraulic conductivity on 2 <sup>nd</sup> order hillslope	76
Figure 4.18	Unsaturated hydraulic conductivity on 3 <sup>rd</sup> order hillslope	78
Figure 4.19	Soil moisture responses and % exceedence curves for 1 <sup>st</sup> order hillslope	80
Figure 4.20	Soil moisture responses and % exceedence curves for 2 <sup>nd</sup> order hillslope	81
Figure 4.21	Soil moisture responses and % exceedence curves for 3 <sup>rd</sup> order hillslope	83
Figure 4.22	Hydrological soil types and flow paths on basalt hillslopes	84
Figure 5.1	Roadmap for results presentation	85
Figure 5.2	SGR rainfall intensities over the modelling period	86
Figure 5.3	aET per catena element for granite 1 <sup>st</sup> order hillslope	87
Figure 5.4	aET per catena element for granite 2 <sup>nd</sup> order hillslope	87
Figure 5.5	aET per catena element for granite 3 <sup>rd</sup> order hillslope	88
Figure 5.6	SBAS rainfall intensities over the modelling period	89
Figure 5.7	aET per catena element for basalt 1 <sup>st</sup> order hillslope	89
Figure 5.8	aET per catena element for basalt 2 <sup>nd</sup> order hillslope	90
Figure 5.9	aET per catena element for basalt 3 <sup>rd</sup> order hillslope	91
Figure 5.10	Simulated cumulative evapotranspiration fluxes on SGR1 hillslope	93
Figure 5.11	Simulated cumulative free drainage fluxes on SGR1 catena elements	94
Figure 5.12	Cumulative surface runoff on SGR2 hillslope catena elements	95
Figure 5.13	Simulated cumulative evapotranspiration fluxes on SGR2 hillslope	96

Figure 5.14	Simulated cumulative free drainage fluxes on SGR2 catena elements	97
Figure 5.15	Simulated cumulative evapotranspiration fluxes on SGR3 hillslope	98
Figure 5.16	Simulated cumulative free drainage fluxes on SGR3 catena elements	99
Figure 5.17	Cumulative infiltration on SBAS3 hillslope catena elements	100
Figure 5.18	Simulated cumulative E and T on SBAS3 catena elements	101
Figure 5.19	Simulated cumulative free drainage fluxes on SBAS3 catena elements	102
Figure 5.20	Observed and simulated responses for 1 <sup>st</sup> order granite hillslope	104
Figure 5.21	Observed and simulated responses for 2 <sup>nd</sup> order granite hillslope	105
Figure 5.22	Observed and simulated responses for 3 <sup>rd</sup> order granite hillslope	106
Figure 5.23	Observed and simulated responses for 3 <sup>rd</sup> order basalt hillslope	107
Figure 5.24	Initial and updated conceptual model for 1 <sup>st</sup> order granite hillslope	110
Figure 5.25	Initial and updated conceptual model for 2 <sup>nd</sup> order granite hillslope	111
Figure 5.26	Initial and updated conceptual model for 3 <sup>rd</sup> order granite hillslope	112
Figure 5.27	Initial and updated conceptual model for 3 <sup>rd</sup> order basalt hillslope	113
Figure 9.1	Electrical resistivity for basalt 1 <sup>st</sup> order hillslope	137
Figure 9.2	Electrical resistivity for basalt 2 <sup>nd</sup> order hillslope	138
Figure 9.3	Electrical resistivity for basalt 3 <sup>rd</sup> order hillslope	139
Figure 9.4	Domain set-up with location of observation nodes for 1 <sup>st</sup> order riparian	141
Figure 9.5	Time series water balances for granite 1 <sup>st</sup> order Hillslope	142
Figure 9.6	Time series water balances for granite 2 <sup>nd</sup> order hillslope	142
Figure 9.7	Time series water balances for granite 3 <sup>rd</sup> order hillslope	143
Figure 9.8	Time series water balances for basalt 3 <sup>rd</sup> order hillslope	143
Figure 9.9	$K_{sat}$ per horizon on granite 1st order hillslope	144
Figure 9.10	$K_{sat}$ per horizon on granite 2 <sup>nd</sup> order hillslope	144
Figure 9.11	$K_{sat}$ per horizon on granite 3 <sup>rd</sup> order hillslope	145
Figure 9.12	The southern granite contour map	146
Figure 9.13	Cumulative Rainfall for the granite and basalt supersite	147

## LIST OF ABBREVIATIONS

ALARM	-	Analytical Land Atmosphere Radiometer Model
AWS	-	Automatic Weather Station
aET	-	actual Evapotranspiration
CPH	-	Capillary pressure head
DUL	-	Drained Upper Limit
ERT	-	Electrical Resistivity Tomography
ET	-	Evapotranspiration
ET <sub>H</sub>	-	Evapotranspiration simulated using Hydrus
ET <sub>SEB</sub>	-	Evapotranspiration modelled using SEBAL
GE	-	Google earth
IP	-	Induced Polarization
KNP	-	Kruger National Park
K <sub>sat</sub>	-	saturated hydraulic conductivity
K <sub>unsat</sub>	-	Unsaturated hydraulic conductivity
PUBs	-	Prediction in Ungauged Basin
pET	-	Potential evapotranspiration
SEBAL	-	Surface Energy Balance Algorithm for Land
SGR	-	Southern granite
SGR1_C	-	Southern granite 1 <sup>st</sup> order crest
SGR1_M	-	Southern granite 1 <sup>st</sup> order midslope
SGR1_R	-	Southern granite 1 <sup>st</sup> order riparian
SGR2_C	-	Southern granite 2 <sup>nd</sup> order crest
SGR2_M	-	Southern granite 2 <sup>nd</sup> order midslope
SGR2_R	-	Southern granite 2 <sup>nd</sup> order riparian
SGR3_C	-	Southern granite 3 <sup>rd</sup> order crest
SGR3_M	-	Southern granite 3 <sup>rd</sup> order midslope
SGR3_R	-	Southern granite 3 <sup>rd</sup> order riparian
SBAS	-	Southern basalt
SBAS1_C	-	Southern basalt 1 <sup>st</sup> order crest

SBAS1_M	-	Southern basalt 1 <sup>st</sup> order midslope
SBAS1_R	-	Southern basalt 1 <sup>st</sup> order riparian
SBAS2_C	-	Southern basalt 2 <sup>nd</sup> order crest
SBAS2_M	-	Southern basalt 2 <sup>nd</sup> order midslope
SBAS2_R	-	Southern basalt 2 <sup>nd</sup> order riparian
SBAS3_C	-	Southern basalt 3 <sup>rd</sup> order crest
SBAS3_M	-	Southern basalt 3 <sup>rd</sup> order midslope
SBAS3_R	-	Southern basalt 3 <sup>rd</sup> order riparian
SW	-	Signs of Wetness
TDI	-	Tension disk infiltrometer
RETC	-	Code for parameter estimation of the water retention curve and hydraulic conductivity
$\theta_r$	-	Residual soil water content
$\theta_s$	-	Saturated soil water content
$a$	-	Parameter in the soil water retention function
$n$	-	Exponent in the soil water retention function
%ED	-	Ranked percent exceedence data
2D/3D	-	2/3 Dimensional

# 1. INTRODUCTION

Semi-arid savannas are highly dynamic and complex systems that exhibit heterogeneity, at various spatial scales (Jacobs *et al.*, 2007). Savanna ecosystems are controlled by water and nutrient availability, fire and herbivory. According to, Walker *et al.* (1981), biological activity and productivity is controlled by water availability, which is the major driving force in these ecosystems. Scarcity and variable distribution of water and nutrients make these ecosystems highly sensitive to change. An understanding of the hydrological processes in such a system is crucial for the prediction of changes in the ecosystem and protection of the resource, given the worldwide water shortages mainly associated with climate change and the ever-increasing population growth (Moleele and Mainah, 2003; Wenninger *et al.*, 2004). The management of surface and groundwater resources, especially in the highly variable water regimes characteristic of semi-arid areas, requires the description and quantification of the hydrological processes for informed decisions (Uhlenbrook *et al.*, 2005; Lorentz *et al.*, 2006). This involves identifying and quantifying pathways, hydrological connectivity, the configuration of moisture residence time, the distribution of saturation patterns, quantification of flow mechanisms and thresholds of flow generation as functions that contribute to drainage in an ephemeral catchment (Haga *et al.*, 2005; Lorentz *et al.*, 2006; Wenninger *et al.*, 2008). The importance of studying hydrological processes in ephemeral systems at different scales allows for an assessment of scale-dependent processes and how they differ in the landscapes. It can also be used for a classification system that can be used to link data between sites. Knowledge of how ephemeral systems work is crucial in understanding the concomitant impacts and influence of climate, scale and geology on their hydrological response. This helps in policy-making, water resource allocation, management plans, ecosystem sustainability and prediction of responses in ungauged systems in other savanna settings.

There have been remarkable advances in the understanding of hillslope processes over the past decades through various methods and characterization techniques, such as geophysical surveys (to explore subsurface properties), hydrometric observations, isotopes (residence times of water, flow paths), sprinkling experiments, soil physics and hydrological modelling (Anderson and

Burt, 1990; Hubbard *et al.*, 1998; Uhlenbrook *et al.*, 2002; Uchida *et al.*, 2006; Troch *et al.*, 2009). Many of the findings have contributed towards the physical understanding and conceptualization of hydrological processes at different scales (Montgomery *et al.*, 1997; McGlynn *et al.*, 2002). Many processes have been explored, such as the generation of overland flow, macropore flow (Mosley, 1982), rainfall-runoff relationships and subsurface flow (van Tol *et al.*, 2011; Orchard *et al.*, 2013). Since hydrological processes vary at different scales, the estimation of how water from the hillslopes enters the stream or the groundwater store at any given site becomes problematic (Wenninger *et al.*, 2004). However, the determination of these flow pathways is fundamental for the determination of connectivity between catena elements and how this connectivity varies at different spatial and temporal scales. Some studies have revealed how characteristics, such as morphology and size of the hillslopes, affects flow paths, storage of water and residence times on hillslopes (Anderson and Burt, 1978; Spence, 2007; Tetzlaff *et al.*, 2007a; Jencso *et al.*, 2009). In small catchments, storage of water and the subsequent release during dry periods is important for ecological sustainability and ecosystem functions (Hughes, 2008). Early studies focused on ways in which rainfall (event water) moves into channels rapidly and how this affects storage e.g. Mosley (1979) and Butte (1994). With the use of isotope tracers, pre-event water stored in catchments was shown to contribute considerably to the storm flow into channels (Wenninger, 2008).

Whilst there has been tremendous interest in hillslope hydrology globally, knowledge of these processes, the interactive role of soils and how they vary in contributing areas associated with ephemeral streams has been revealed as a gap in our understanding of hillslope processes in water-limited ecosystems in southern Africa (Lorentz *et al.*, 2010). A form of classification is needed in order to link processes at different scales from various sites. Given this background, knowledge of aquatic and terrestrial systems, linkages between them and how they vary with incremental scale is now critical, bearing in mind the rate at which southern African savannas are being transformed, to cope with economic growth and for sustainable development (Pollard *et al.*, 2003; Moleele and Mainah, 2003; Venter *et al.*, 2008).

The study presented here was carried out in Kruger National Park (KNP), a protected area located within a savanna biome, which experiences seasonal, but irregular, short-lived storms

(Venter *et al.*, 2003). Many hydrological studies have been carried out in KNP, with most researchers focusing on large-scale perennial rivers (600 km long), largely ignoring the seasonal ephemeral streams (30 000 km long) that make up the major part of its drainage network (O’Keeffe and Rogers, 2003). This study focused on hydrological processes in ephemeral catchments in KNP, to bridge this knowledge gap since ephemeral systems contribute remarkably to the hydrology of savannas.

The aim of this study, therefore, was to define, characterize and quantify the differences between dominant hillslope hydrological processes (overland flow, subsurface flow and bedrock flow) in contributing areas to 1<sup>st</sup>, 2<sup>nd</sup> and 3<sup>rd</sup> order streams and between different parent materials. Hydrological processes were monitored on catena (a series of soils and vegetation linked by their topographic relationship) elements of these contributing areas. The main key question was:

How do dominant hydrological processes vary on hillslopes in contributing areas to 1<sup>st</sup>, 2<sup>nd</sup> and 3<sup>rd</sup> order streams and on a hillslope of the same order across different parent materials (basalt and granite)?

Objectives of the study were:

- To observe and characterize mechanisms of flow in the (subsurface) and along hillslopes;
- To determine hydrological soil types and classify hillslopes according to hydrology principles; and,
- To quantify catena element water budgets and compare results at the different scales

## **2. LITERATURE REVIEW**

This chapter reviews studies that have been conducted on hillslope hydrology, including the characterization, classification and numerical modelling of hydrological process dynamics in hillslopes. The review also includes the interactive role between soils and hydrology (hydropedology), the different methods and techniques that have been used in various studies to comprehend major findings, as well as the achievements and gaps in the understanding of hydrological processes at the hillslope scale, particularly in savanna settings.

### **2.1 The Savanna Ecosystem**

Savannas cover approximately 20% of the earth's surface and Africa possesses the largest of such areas (Werner *et al.*, 1991). A savanna ecosystem is characterized by sufficiently small trees and grasses that co-exist and interact, resulting in both components having a strong effect on processes, such as hydrology and nutrient cycling (Scholes and Walker, 1993). Decades of research in savannas e.g. in Australia, South America and the Serengeti Plain of Tanzania, have shown fire, herbivory, water and nutrient availability as drivers of ecosystem change. Water availability is the major driver controlling biological activity and ecological processes in these ecosystems (Maranga, 1986). Periodic rainfall events often occur as short-lived rainstorms that are irregular, with the majority of rainfall being confined to a single season. These environments are therefore, highly sensitive to change, due to the variable distribution of water and nutrients (Newman *et al.*, 2006). An understanding of the hydrological processes in such a system is therefore, crucial for the prediction of changes in the ecosystem, given the general water shortages as a result of climate change and the ever-increasing population (Lorentz *et al.*, 2010).

### **2.2 Hydrological Processes at the Hillslope Scale**

Lane *et al.* (1998) define a hillslope as a land surface from a ridge crest along the direction of water or mass flow to a defined drainage or water body, such as a stream or river. According to Cullum and Rogers (2011), the hillslope can be used for the determination of hydrological

responses resulting from varying soil assemblages, with respect to slope and position (catena effect), topography and vegetation. The hillslope is an ideal scale to use in determination of environmental forces on hydrological responses, dominant processes during low and peak flows and connectivity between catena elements (Tromp-van Meerveld and McDonnell, 2006).

Past research has shown hillslope shape and size, material type and distribution, geological features, vegetation type and density, hydraulic conductivity, macro-pores, soil depth and water retention characteristics, as factors controlling hydrological processes, responses and their distribution at the hillslope scale, both spatially and temporally (Bogaart and Troch, 2006; Western *et al.*, 2004; van Tol *et al.*, 2010). Topography is also an important factor for soil water pathway distribution and its monitoring in the subsurface has proved to be very crucial for the spatial and temporal variability of water table responses, lateral flow dynamics and run-off from the hillslopes (Freer *et al.*, 2002; Lin *et al.*, 2006; Tromp-van Meerveld and McDonnell, 2006). Morphology (e.g. geology and terrain) also influences the manner in which hillslopes respond, because it dictates the soil properties and the slope of a landscape (Woods, 1996; Sivapalan, 2003). Both the vertical and horizontal heterogeneity of soil types, soil properties and the redistribution of water along the hillslope are very important for the partitioning of water into surface and subsurface flow, which will, in turn, influence the vegetation distribution on the landscapes, depending on the quantity of nutrients and water available (Ridolfi *et al.*, 2003).

Many studies have been conducted on flow mechanisms and hydrological responses of hillslopes in different settings. Responses differ, due to a number of factors as discussed in the previous paragraph. According to Anderson and Burt (1990) the redistribution of water on hillslopes is due to the presence of saturation zones in the subsurface. Whilst Western *et al.* (1999) argues that vegetation type and spatial patterns are responsible for the redistribution and also that climatic characteristics may influence other mechanisms that initiate spatial and temporal dynamics. In a study by Graham *et al.* (2010) flow mechanisms and hydrological responses were shown to be controlled by parameters, such as bedrock permeability and bedrock topography which are difficult to measure because of the scale they operate at. This brings us back to the issue of scale which remains challenging in hydrology. Real advances in hydrological studies can

only be made once the scale issue is resolved (Bloschl, 2001). This will also make it easier for predicting behavior in ungauged systems.

Hillslope hydrological processes have, therefore, been well-documented and researched, with most researchers focusing on runoff processes and rainfall partitioning on both surface and subsurface of natural and artificial slopes (Martinez-Mena, 2001; Nicolau, 2002; Weiler and McDonnell, 2004). However, hillslope hydrology is an intricate suite of processes interacting and operating differently at varying scales because of heterogeneity at the different scales within the unsaturated zone (area between the soil surface and the phreatic zone) and the surface biotic state (Ridolfi *et al.*, 2003; Avanzi *et al.*, 2004). These include the spatial heterogeneity of soil properties and variability of the climate (Márquez *et al.*, 2005). The study of hillslope hydrology therefore, remains challenging because of the number of processes interacting at different scales, resulting in a complex system to understand (Ridolfi *et al.*, 2003).

### **2.3 Hillslope Flow Paths**

Studying flow paths and flow mechanisms on a hillslope is crucial for an understanding of water storage during wet seasons and its subsequent release during dry periods for ecosystem sustainability, predominantly in the small catchments and water-limited environments (Lin *et al.*, 2006). The major flow paths on a hillslope (Figure 2.1), comprises overland flow, subsurface saturated or unsaturated flow and bedrock flow (Ticehurst *et al.*, 2007). The various pathways are determined by the soil's physical and chemical characteristics, parent material and a network of macropores (Mosley, 1982; van Tol *et al.*, 2012). According to Lin *et al.* (2006), the rate of flow of these hydrological processes varies with lithological differences, hence the comparison of processes between two parent materials in this study. The main hillslope flow paths will be discussed in the following sub-sections.

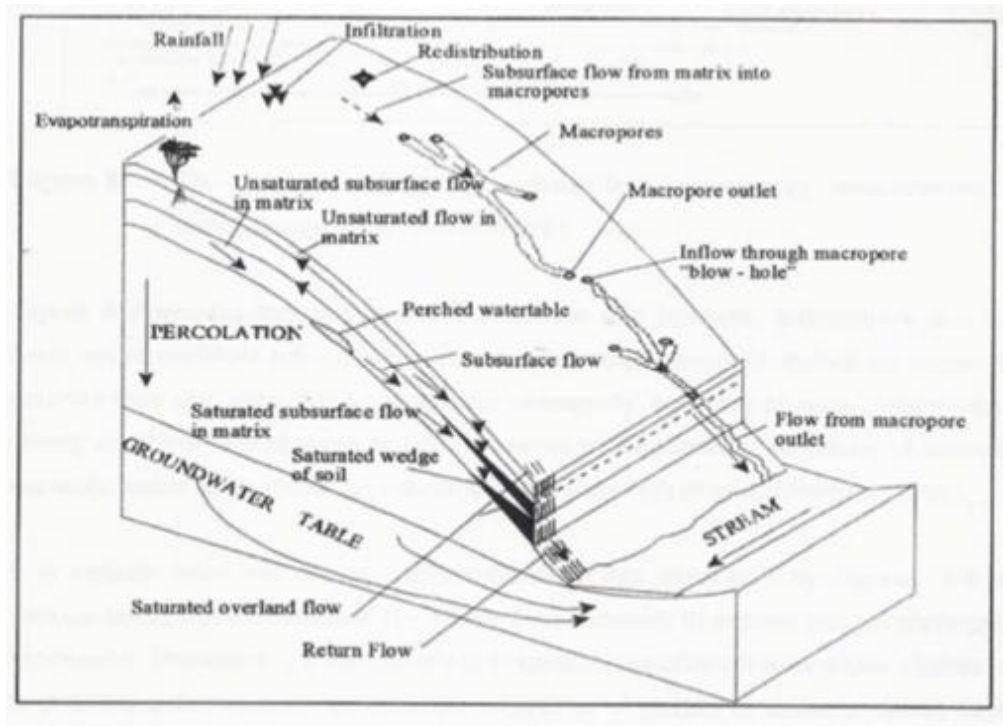


Figure 2.1 Dominant hillslope processes and flow paths (Anderson and Burt, 1990)

### 2.3.1 Overland flow

Overland flow occurs on hillslopes, either as saturation excess flow or infiltration excess flow (Hortonian). Hortonian overland flow occurs when the rainfall intensity exceeds the infiltration capacity and final infiltration rate of the soil. Saturation excess occurs when the soil and all depressions are saturated and the excess water will flow as surface runoff. On some hillslopes, the crest generates overland flow with significant erosive energy, compared to the midslope and footslope, but this is mainly governed by topography and hillslope morphology (Marsh and Kaufman, 2012). Return flow is also overland flow that can be experienced on some hillslopes depending on the slope of the area, soil properties and the soil water in the subsurface. It is lateral subsurface water that emerges on the surface as overland flow at the toe slopes. Return flow is crucial during low flow periods in arid and semi-arid environments during the dry seasons and/or dry periods during the rainy season because it sustains streamflows (Lin *et al.*, 2006).

According to Bergkamp (1998) and Cammeraat (2002) the generation of overland flow in an area is a process that is spatially and temporally variable and is not uniform. Many studies have demonstrated that runoff generation is influenced by the hillslope characteristics of topography, antecedent soil moisture, depth to the water table, the hydraulic properties of the soil and land cover (Grayson and Bloschl, 2000; McGlynn *et al.*, 2002; Hernandez *et al.*, 2007; Stieglitz *et al.*, 2003; Lin *et al.*, 2006). Numerous studies have been conducted to investigate overland flow generation, but not much has been documented on hillslopes in water-limited ecosystems. Studies conducted in other environments have shown groundcover as a factor that significantly reduces overland flow, amongst other things (Sanjari *et al.*, 2009; Podwojewski *et al.*, 2011). According to Karnoven *et al.* (1999) in addition to groundcover, soil texture influences the amount of overland flow. This is supported by Orchard *et al.* (2013) who found that overland flow on hillslopes was a function of soil clay content, soil crusting and soil surface coverage, hence the conclusion that overland flow is controlled by soil texture, surface features and has high spatial variability. Soil texture influences infiltration rate, where the generation of overland flow, particularly hortonian, depends on how fine or coarse the soil texture is.

### **2.3.2 Subsurface flow**

Subsurface flow can either occur as vertical or lateral flow. Vertical flow is basically infiltration, although in some soil types it changes flow direction, due to soil textural discontinuities and the gradient of the slope, which is when it becomes lateral flow. Subsurface lateral flow comprises of flow between soil horizons, at the soil-bedrock interface or macropore flow. The rate of flow of these processes varies with lithological differences, soil types and slope (Lin *et al.*, 2006). According to studies conducted by Puigdefabregas *et al.* (1998) and McNamara *et al.* (2005), characterizing the components of subsurface water flow is complex and challenging in hydrological process studies, especially on hillslopes, because of their dynamic nature. Other studies have shown that soil depth (Weiler and McDonnell 2004), soil horizon contacts (Mosley, 1979) and bedrock topography control and influence the generation of subsurface lateral flow. According to Anderson and Burt (1990), subsurface lateral flow is the main runoff generating mechanism in temperate regions, whilst in arid and semi-arid areas it only occurs under certain conditions, such as transient water tables, as a result of high antecedent moisture levels. As a

contributor to streamflow it, therefore, becomes crucial to understand this flow mechanisms, especially in water-limited environments.

### **2.3.3 Bedrock flow**

Water either moves on top of the bedrock (soil bedrock interface) or through cracks within the bedrock. The rate of water movement is dependent on soil type, cracks, number of pore spaces and size (i.e. the hydraulic characteristics of the medium). Water in the bedrock generally moves laterally or vertically through cracks (van Tol *et al.*, 2008). According to Ticehurst *et al.* (2007) bedrock flow is important for the recharge of groundwater levels, lower slopes and the generation of baseflow in streams. The knowledge of baseflow generation is crucial, especially in savannas for an understanding of hydrological connectivity between streams and hillslopes.

## **2.4 The Influence of Macropores and Soil Pipes on Hillslope Storage**

During intensive rainfall events, a significant amount of water moves through macropores and soil pipes as a result of plant root channels, high clay mineral contents and soil fauna (van Tol *et al.*, 2012). The presence of these pipes and macropores on a hillslope (Figure 2.2) has the potential to contribute a significant amount of water to streamflow (Uchida *et al.*, 2006). Studies have shown that flow through macropores is governed by the size, accessibility and continuity of the pores. Flow continuity is influenced by amount of soil water status and the intensity of water supply (Nieber *et al.*, 2000; Lin *et al.*, 2006). Macropores have a negative influence on water residence time and hillslope storage, since significant amounts of water are drained in a short space of time.



Figure 2.2 Macropore flow - Soil pipe outlet (photo by le Roux, 2006)

## 2.5 The Hillslope Water Budget

The water budget is important for understanding water fluxes and water storage on a hillslope. The overall forces on the hillslope water budget are the vegetation type, climate and landscape morphology of the area (Thompson *et al.*, 2011). Vegetation patterns drive the spatial evapotranspiration demand at the hillslope scale and are also signatures of water availability. The water budget is altered by vegetation at the surface through canopy cover and interception which modify infiltration rates. In the subsurface, vegetation alters the soil structure through macropore formation and root water uptake. Studies conducted in KNP have shown that although vegetation is assumed to be a control and signature of hydrological processes, the link between them varies, depending on the impact of other drivers, such as soil hydraulic properties and nutrient availability (Boisvenue and Running, 2006; Khomo and Rogers, 2009).

The quantification of water fluxes in the subsurface is a complex process, since they are compounded by both climatic forces and subsurface controls, such as morphology and soil texture, which modify the soil water dynamics. An understanding of these water fluxes and dominant flow paths helps in the quantification of the hillslope storage (McGuire and McDonnell, 2005). A comprehensive understanding of the water budget, especially in water-limited environments is important for the knowledge of the component fluxes in and out of the system. Knowing how much water can be stored in the system will help in the determination of the best land use practises for the area.

## **2.6 Hillslope Hydrological Connectivity**

Hydrologic connectivity is a quantifiable concept to describe the water-mediated transport of matter, energy and organisms within or between elements of the hydrologic cycle, such as connectivity between groundwater and surface water (Pringle *et al.*, 2007). Hydrological connectivity provides a framework that enables the study of hillslope hydrology and geomorphology, through the extraction of simplified and quantifiable characteristics that transcend an individual hillslope (Buttle *et al.*, 2004; Bracken and Croke, 2007; Freeman *et al.*, 2007). There are a range of processes that ensure connectivity at the hillslope scale, but might not always be present, such as saturated overland flow, base flow, subsurface-saturated and return flow. The dynamic behaviour of hillslope processes requires a clear understanding of the linkages between patterns and the processes, hence the need to know the connectivity between elements and components of the whole system (Tromp-van Meerveld and McDonnell, 2006). Hydrological connectivity varies due to climatic setting. In humid temperate environments, connectivity is highly dependent on connections between saturated areas, such as stream channels and hillslope hollows (Stieglitz *et al.*, 2003). However, from studies conducted in dry environments, results show that evapotranspiration meets or exceeds precipitation for much of the year, therefore, connectivity is highly temporal (Newman *et al.*, 1998; Puigdefabregas *et al.*, 1998; Gomez-Plaza *et al.*, 2001; Chamran *et al.*, 2002). Understanding connectivity in semi-arid areas is therefore, fundamental for effective water resource management, ecosystem sustainability and the general understanding of hydrological and ecosystem responses to various processes, due to the complexity and diversity of the landscape, as well as variations in geology and climate. This knowledge is also crucial in savannas, since they are important for biological diversity and humans also depend on them for their livelihoods (Falkenmark and Rostrom, 2004). Understanding hydrological connectivity at this scale is therefore, important in understanding the mechanisms of flow in and along the hillslope. Insights into this connectivity can be shown through hydrogeological interpretations of the soils.

## **2.7 Hydrogeological Soil Types and the Use Pedotransfer Functions**

Soils and hydrology have an interactive relationship. This interaction, according to le Roux *et al.* (2011) has been neglected for a long time. Due to the ever-increasing water shortages and stress

on the environment as a result of climate change and population increase, it has become important to characterize and quantify this interaction. This interaction affects various sectors of the economy and the environment, including crop production and food security (agriculture), water resources management (water use, pollution) and wetland ecosystems (le Roux *et al.*, 2011).

Integrating pedology (the study of soils in their natural environment) with hydrology enhances the faithful exploration of soil, water and landscape relationships and how these components affect one another (Lin *et al.*, 2008). Some soil properties influence hydrological processes, flow paths and the rate of water flow (i.e. structure, hydraulic conductivity and texture), whilst some can be used as indicators of the hydrological regime of soil types, such as the soil color (Lin *et al.*, 2006). In natural systems, an understanding of hydropedology is still limited, although it is crucial for the prediction of hillslope behavior and process conceptualization (le Roux *et al.*, 2011).

There are three main hydrological soil types, namely, responsive, recharge and interflow. These soil types are distinguished according to their hydrological responses (Ticehurst *et al.*, 2007; van Tol *et al.*, 2011). Recharge soils are soils that do not have a morphological indication of saturation having a vertical flow direction that can be a preferential pathway for potential groundwater recharge. Interflow (throughflow) soils are soils where subsurface lateral flow is mainly controlled by soil properties and topography. Interflow soils can thus be lateral flow between soils horizons or at the soil/bedrock interface. These soils are responsible for connectivity between catena elements and/or the whole catena and the adjacent stream. Responsive soils can be categorized into two types: shallow responsive and saturated responsive. The former becomes responsive, due to limited storage capacity (small soil water deficit), whilst the latter is due to saturation (saturation deficit = 0) (Soulsby *et al.*, 2006; van Tol *et al.*, 2012). Responsive soils are responsible for the generation of overland flow. Understanding the variability of the different soil types spatially will enhance our understanding of hillslope processes and mechanisms of flow, since soils control water storage and act as the first order control in the partitioning of flow paths (Soulsby *et al.*, 2006). An understanding of these hydrological soil types also helps in the determination of areas where there could be potential

connectivity, for example, interflow at the soil/bedrock interface in the riparian zone could mean potential connectivity between the hillslope and adjacent stream network.

The most important control on hillslope hydrological behaviour is soil (Schulze, 1995). Due to climatic regimes, especially in semi-arid regions, a large percentage of pre-event water is expected to be stored in the unsaturated zones on hillslopes, only becoming mobile due to an event-based forcing (Uhlenbrok *et al.*, 2002). An improved understanding of the fluxes can be achieved through modelling. However, in order to simulate water flow using hydrological models, surface and subsurface measurements of different parameters, such as water retention and hydraulic conductivity are needed, although they are time-consuming and some of them are expensive to measure (Ticehurst *et al.*, 2007). An alternative that other researchers have adopted is the use of pedotransfer functions. According to Bouma (2006), the use of pedotransfer functions is where the data that we have available is translated into data that we need. From data, such as soil texture and bulk density, some hydrological processes can be estimated (Pachepsky and Rawls 2002; van Tol *et al.*, 2012). Pedotransfer functions mainly emphasize the link between hydrology and pedology, using techniques that associate some soil properties with some hydrological properties (Bouma, 2006).

## **2.8 The Significance of Conducting Research at Multiple Scales**

Hydrological processes operate at different scales and they involve controls, such as landscape morphology, geology and climatic conditions in different environments (Hjalmar *et al.*, 2007). The quantification of the spatial variability of hydrological processes across multiple scales is crucial in natural resources management, ecological modelling and environmental prediction. According to Jewitt and Gorgens (1995), there are three scales in hydrological studies, namely, the observation scale, the process scale and the operation scale. The scale at which natural processes/phenomena occur is called the process scale (Blöschl and Sivapalan, 1995). According to the research objectives and aims of a study, a scale at which measurements are made is referred to as the observation scale. The operational or working scale is the one at which the main focus of the study lies (Jewitt and Gorgens 1995). According to Sivapalan (1995), the process scale and the observation scale are the two most important scales to be considered in hydrological studies.

The effect of scale on hydrological variables is one major unresolved issue in hydrological studies (Sivapalan and Kalma, 1995; Cammeraat 2002). According to Blöschl (2001) a significant effort has been put into theoretical scaling aspects, although less work has been shown in research studies. It is therefore, important to study hydrological processes at multiple spatial and temporal scales, to determine processes that are scale-dependent and to assess how processes change with incremental scales. This is still a methodological gap in the evaluation of ecosystem change since most geological and hydrological mechanisms are considered scale dependent (Lorentz *et al.*, 2010).

## **2.9 The Use of Models in Hydrological Studies**

Many hillslope behaviours can be observed, but their quantification in terms of water fluxes requires data integration and upscaling. Typically this is achieved through the integration of the numerical representation of processes in the form of a mathematical model. Reality may be represented to a certain degree, but the models have become essential tools in the integration of data and provision of insights into the hydrological functions of a catchment resulting in the better understanding of the processes (Sivapalan, 2003; Dye, 2003).

According to Mulligan and Wainwright (2004), “*models must represent the hydrological processes in the manner that is most consistent with the observations, while staying physically realistic and computationally practical*”. In physically-based modelling approaches, a field-based approach facilitates conceptualization from which the complexity of hillslope processes can be understood (Sivapalan, 2003). There have been some remarkable developments in hillslope hydrological research, but there is still need to upscale processes for varying climates, geographic areas and different geologies (Tetzlaff *et al.*, 2008).

There are numerous models that can be used to simulate flow in the unsaturated zone, such as DRAINMOD, MODFLOW, HYDRUS and FEFLOW. A review of literature shows HYDRUS to have more simulation capabilities over other models, because it can simulate flow in partially saturated, saturated and unsaturated areas and also under heterogeneous conditions (Smethurst *et*

*al.*, 2009). HYDRUS can model evaporation using an extraction function that is based on Darcy's Law and a sink term is used for the calculation of transpiration, depending on the root zone water potential of the surrounding soil. HYDRUS relates subsurface water partitioning processes to measured soil hydraulic properties, root distribution and water uptake. It therefore, allows a close examination of the effects of soil and vegetation on water partitioning into different fluxes (Guan *et al.*, 2010).

## **2.10 Model Sensitivity Analysis**

Distributed hydrological models are fundamental for the simulation and upscaling or downscaling of processes and they play a key role in hydrology and water resources studies. They have become important tools in research studies for investigation of issues relating to the planning and management of water resources (Muleta and Nicklow 2005). In order for model predictions to be reliable, the structure of the model must be well parameterized and defined. This helps in efficient use and application of the model. However, it is a difficult task to estimate model parameters, due to uncertainty that results from the determination of parameter values that cannot be measured easily in the field (Liu *et al.*, 2005). This is where model sensitivity analysis comes in. Sensitivity analysis is a technique that can be used to assess parameters used as input variables with respect to their contribution to output variability (Hamby, 1994). Focusing on the sensitive model parameters helps in better understanding and estimation of parameter values, hence reducing uncertainty in model output (Leinhart *et al.*, 2002). Future characterization would therefore, be required for data which the model was most sensitive to so that results can be reliable and credible (Jakeman *et al.*, 2006) and for successful model application and proper planning for future research (Sieber and Uhlenbrok 2005).

## **2.11 Evapotranspiration: Conventional/Remote Sensing Techniques**

In order to manage catchments, water supply systems and other ecosystems, an understanding of the spatial and temporal distribution of soil water depletion through evapotranspiration is essential. There is potential and actual evapotranspiration, where the former refers to an estimate of the amount of water that can be extracted through evaporation from the soil surface and

transpiration from plants, assuming that there is no control on water supply. The latter refers to the actual measure of water lost to the atmosphere through the two processes. Since natural landscapes in particular are heterogeneous, the determination of ET becomes complex. Although it is complex, the accurate determination of ET reduces some water balance uncertainties in catchments (Cleugh *et al.*, 2007).

There are conventional methods that are based on climate data that can be used to calculate evapotranspiration for a reference crop i.e. alfalfa (Wright and Jensen, 1972) and short uniform grass (Doorenbos and Pruitt, 1977; cited by Allen *et al.* 1998). A crop coefficient is used that is specific to each area under study and crop water requirements are determined for the different stages of crop growth. Since the crop water requirement is often from literature, the crop factors might not be accurate, due to the different growth stages. Estimates are localized; therefore, the spatial variation at larger scales becomes impossible. ET estimates are nevertheless crucial for an indication of climatic aspects that are linked to the water balance, plant productivity and energy supply, especially in hydro-ecological studies (O'Brien, 2006). There is high species diversity in savannas, therefore, soil water demand is high, especially during the dry season when plant water stress will be high for shallow-rooted plants species (Scholes and archer, 1997). Actual ET can be calculated, using remote sensing techniques (Bastiaanssen *et al.*, 2002). Actual ET can be computed at a range of a single pixel to a raster image. This makes it easier for the acquisition of soil water data in terms of what is lost through evaporation from the soil surface and transpiration from plants (Ahmad *et al.*, 2005). Different remote sensing techniques that can be used will be discussed in detail in the following section.

## **2.12 Review of Methods used in this study**

There have been many advances in hillslope hydrology globally and researchers have used various methods and techniques to characterize hydrological responses (Freer *et al.*, 1997; Asano *et al.*, 2002; Wainwright and Mulligan, 2004). These include qualitative assumptions, geophysical surveys, tracer-based observations and quantitative hydrometric data of the soil water dynamics and responses to evaporation and rainfall (Uhlenbrook *et al.*, 2002; Lorentz *et al.*, 2003).

Measurement of the hydraulic conductivity and infiltration rate of soil has been conducted, using a number of different instruments. The double ring infiltrometer is one such instrument that measures the saturated soil hydraulic conductivity *in situ*. It can be used on the soil surface or at different depths in pits. Although, simple to use this technique, it cannot be applied where the test surface is below the water table or where there is some resistance to ring penetration because that will disturb the soil, hence introducing a bias in the results (Johnson, 1991). Alternatively, field  $K_{sat}$  (saturated hydraulic conductivity) can be measured using the mobile permeameter or the Guelph permeameter. These two instruments operate more or less the same way where the steady-state rate of infiltration is recorded, whilst maintaining a constant head of water in an augered hole where the permeameter is submerged. These instruments are easy to use and they allow for the measurement of soil permeability of different horizons in the subsurface (Amoozegar, 2008). The TDI (Tension Disk Infiltrometer) is used to measure the  $K_{unsat}$  (unsaturated hydraulic conductivity) of the soil. This instrument has the advantage of allowing the measurement of the steady-state infiltration rate of water into the porous medium at different tensions. However, the TDI is not suitable for surfaces that have cracking (characteristic of heavy clays) or coarse soils otherwise the results become unreliable (Ankeny *et al.*, 1991).

The measurement of soil water helps to get feedback that can assist in water management decisions. Subsurface soil water dynamics can be measured by a wide range of instruments. Some of the instruments give output data in water contents, whilst some give soil water tension. In the past, tensiometers and soil moisture sensors were used for the characterization of soil potentials, but there have been advances with the introduction of instruments such as Time Domain Reflectometry, which is now used in conjunction with the other instruments (Uhlenbrook *et al.*, 2002; McDonnell *et al.*, 2003; van Tol *et al.*, 2013). The neutron probe is an instrument that measures water content. It is accurate and measurements can be repeated. It also samples large areas, but it is relatively expensive to use, whilst the Time Domain Reflectometry is less expensive and easy to log, but only samples small areas. Tensiometers can be used to measure soil water tension. They are less expensive, but they require high maintenance. A granular matrix sensor (watermark<sup>TM</sup>) can also be used to measure soil water tension. This instrument is very cheap, easy to use, does not require high maintenance, but has highly variable output data (Uhlenbrook *et al.*, 2002).

To explore subsurface material distribution, geophysical techniques such as the Induced Polarization (IP) and Electrical Resistivity Tomography (ERT) have been used. They measure the earth's mineral capacitance and subsurface resistivity distribution, respectively. This has proved very helpful over the years in the provision of accurate bedrock measurements and lithographic distributions. A time series analysis through ERT also helps in the assessment of soil water dynamics and for wetting and drying phases in the subsurface (Rodriguez-Iturbe *et al.*, 2000; Rodriguez-Iturbe and Porporato, 2004).

Soil and hydrology have an interactive relationship. Soil characterization helps to improve the understanding of the hydrological processes. Soils can be classified, using the taxonomical classification of South Africa by the 1991 working group. This classification gives the diagnostic horizons and the soil form. To pin soils and hydrology together, soils can be classified hydropedologically (van Tol *et al.*, 2013) according to their hydrological response, using the hydrological soil types, namely, recharge, interflow and responsive (le Roux *et al.*, 2011). This hydropedological classification of soils is still in its infancy, but nonetheless forms a basis for the integration of data at the hillslope scale.

An important aspect in hillslope hydrological studies is the hillslope water budget. In order to calculate the water budget it is fundamental to know how much is being lost from the vadose zone through ET. As discussed earlier, this can be achieved through conventional methods or through remote sensing techniques. The estimation of actual evapotranspiration has mostly been done, using satellite remote sensing (Bastiaanssen *et al.*, 2002). Actual ET can be computed at a range of a pixel to a raster. This makes it easier for the acquisition of soil water data (Ahmad *et al.*, 2005). The Surface Energy Balance Algorithm for Land SEBAL (Bastiaanssen *et al.*, 1998) is one example of a satellite remote sensing technique that can be used to compute actual ET, using visible thermal and near infrared bands. Through the latent heat of vaporization flux, actual ET can be estimated directly. Quite a number of satellite remote sensing models are available besides SEBAL. These include METRIC (Allen *et al.*, 2007), Analytical Land Atmosphere Radiometer Model (ALARM; Suleiman *et al.*, 2009) and ReSET (Elhaddad and Garcia, 2008). The majority of them use the surface energy balance equation:

$$Rn = LE + G + H \quad (2.1)$$

Where:

- $Rn$  - Net radiation ( $Wm^{-2}$ )
- $LE$  - Latent heat flux ( $Wm^{-2}$ )
- $G$  - Soil heat flux ( $Wm^{-2}$ )
- $H$  - Sensible heat flux. ( $Wm^{-2}$ )

According to Tasumi *et al.* (2003), SEBAL is a widely accepted method that has been tested and proved to have a high degree of accuracy. SEBAL was applied worldwide in more than thirty countries and results show that its accuracy on annual aET is 96% and 85% on daily ET for a wide variety of plant assemblages and different soil water indices. SEBAL can be used for ET estimation, irrespective of the availability of crop and soil information (Bastiaanssen *et al.*, 2005).

### 2.13 Conclusion

There have been many advances in hillslope hydrological studies globally and there have been numerous achievements, but scale issues and the classification of processes remain a problem. Various studies have shown how hillslope hydrology allows the determination of different environmental forces on hydrological processes and the connectivity of different systems, through the study of flow paths. However, hillslope hydrology has been shown as an intricate suite of processes that operate differently at different scales, due to heterogeneity in the unsaturated zone.

This review has also shown how important soils are in the study of hydrological processes, since soils control hydrological properties and also serve as indicators of hydrological regimes. A hydro-pedological classification can therefore, serve as a basis for data integration and hydrological modelling through pedotransfer functions. Modelling in turn, helps in the calculation of hillslope water budgets, to understand storage and water fluxes in and out of the system. All these data will then assist in the development of an abiotic template of hydrological processes in an ephemeral catchment.

The function of ephemeral catchments in a water-limited (Savanna) environment has been shown as a knowledge gap in our understanding of processes in the KNP region therefore, the review of literature led to the development of the key questions and objectives in the following section.

## 2.14 Key Questions, Hypothesis Development and Study Objectives

Key Questions formulated through the review of relevant literature.

- How do dominant hydrological processes vary on hillslopes areas contributing to 1<sup>st</sup>, 2<sup>nd</sup> and 3<sup>rd</sup> order streams and on hillslopes of the same order across different parent materials (basalt and granite)?;
- How does soil water potential vary temporally at catena element scale, with increasing depth?; and
- Are there contributions from upslope catena elements to downslope elements or potential aquifer recharge?

The following hypotheses were also drawn, based on the literature review:

- Vertical subsurface flow was anticipated on the granite crest catena elements because they are characterized by sandy soils (high hydraulic conductivity), since most clay particles would have been washed downslope through eluviation processes. This will be tested using soil surveys, hydrogeology principles and conductivity data;
- Lateral contributions to downslope catena elements were anticipated, due to the slope in the granites, hence there will be hydrological connectivity between elements. This was tested through hydrogeology principles and conductivity data;
- $K_{sat}$  and  $K_{unsat}$  was expected to be high on the granites, due to the sandy soils characteristic of granite derived soils, compared to basalt soils that have a high clay percentage;
- Basalt hillslope was expected to be characterized by vertical subsurface flow and no lateral contributions from interfluvies to downslope elements (disconnected elements),

due to the low gradient topography. This was verified through hydropedology principles and hydrological modelling.

- Soil water potential would be more negative in the basalts because clay soils have higher water retention capacity compared to sandy soils characteristic of the granites.

Study Objectives were:

- To observe and characterize mechanisms of flow in (subsurface) and along hillslopes;
- To determine hydrological soil types and classify hillslopes according to hydropedology principles; and,
- To quantify catena element water budgets and to compare results at the different scales.

## **3 STUDY SITES AND METHODOLOGY**

### **3.1 Location: Kruger National Park (KNP)**

The KNP is located in the Lowveld, in the north-eastern part of South Africa, bordering on Mozambique. According to Kokwaro and Gillet (1980), it occupies an area of about 18 998 km<sup>2</sup> (approximately 1 900 000 ha) between latitudes 22° 25' to 25° 32' to the South and longitudes 30° 50' to 32° 02' to the East.

### **3.2 Climate**

The Kruger National Park has a semi-arid climate. Conditions vary from hot and humid summers to mild and dry winter months. According to Tyson and Dyer (1978), cited by Kokwaro and Gillet (1980), the southern part of the park receives an annual rainfall of  $\pm 750$  mm, whilst the north receives  $\pm 350$  mm. The rainfall also decreases in a westerly to easterly direction in the South, and vice versa in the North (Figure 3.1). In summer, temperatures may rise to as high as 44°C.

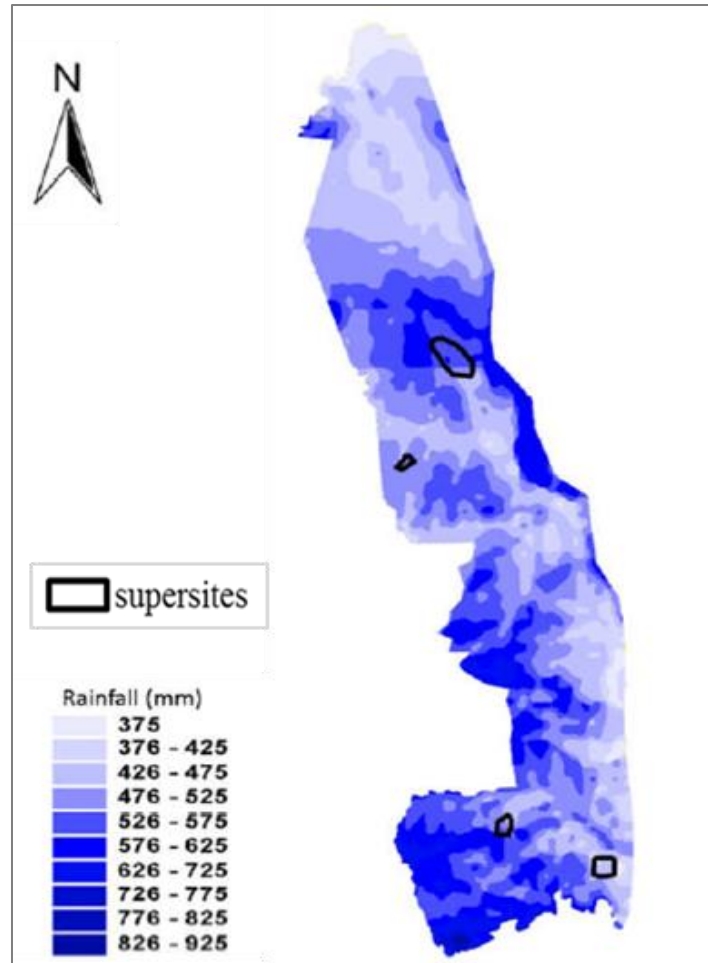


Figure 3.1 Rainfall distributions in KNP and location of sites (Riddell *et al.*, 2011).

### 3.3 KNP Geology and Soils

According to Venter (1990), the geology of KNP comprises sedimentary, metamorphic and igneous rocks. Longitudinally, the geology follows a north-south orientation, with granites in the west and basalts in the east (Figure 3.2). Due to parent material diversity, a variety of soil and plant communities are found in the Park. Soils range from coarse grained sands to fine loams in the granites, whilst the basalts comprise fine clays (Venter, 1990).

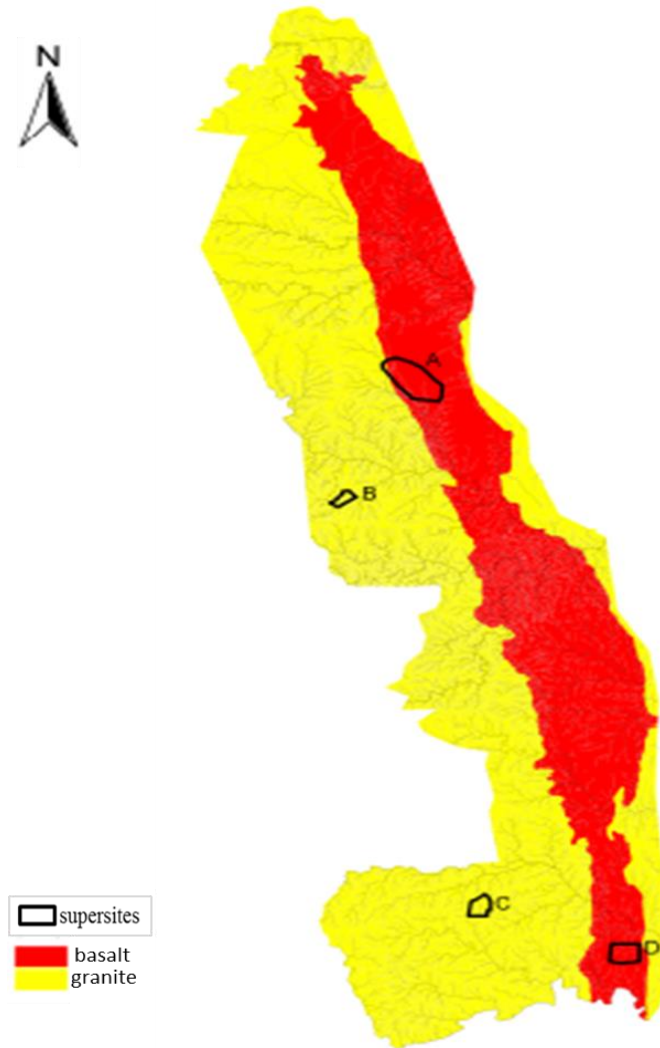


Figure 3.2 Geology of KNP and location of supersites within the land systems (after Riddell *et al.*, 2011).

### 3.4 Drainage

According to Venter (1990) KNP is drained by seven major rivers, namely, the Crocodile, Letaba, Olifants, Sabie, Luvuvhu, Shingwedzi and Limpopo Rivers. Some of the rivers originate in the Northern Drakensberg and then flow eastwards. The small streams and tributaries of these rivers form dendritic patterns in the granites (high stream density), compared to the rectangular pattern in the basalts.

### 3.5 Vegetation

According to Venter (1990), there are more than 1 900 different plant species in the KNP. The southern granite areas comprise dense woodland, compared to the basalts. Crests in the granites are mainly characterized by sandy soils that support *Combretum apiculatum*, *Combretum zeyheri*, and *Terminalia sericea*. Riparian zones and valley bottoms comprise *Euclea divinorum*, *Dichrostachys cinerea* and *Acacia nigrescens*, whilst the midslopes comprise some *Dichrostachys cinerea* and *Acacia nilotica*. The basalts have sparsely populated vegetation, dominated by *Acacia nigrescens* and *Sclerocarya birrea* in the south (Venter, 1990).

### 3.6 Overview: Supersites

In KNP, researchers have focused on manipulated sites, such as the existing burn plots and exclosures, when applying controlled treatments. However, some researchers preferred to do research in non-manipulated or near pristine sites, which they conducted haphazardly throughout the park, making it difficult or almost impossible to integrate and link datasets from the different projects (Smit *et al.*, 2013). Due to the absence of such data rich, long-term monitoring sites on near pristine areas, research sites colloquially termed “Supersites”, were then selected as being representative of catchment characteristics of the various landscape systems within the park. Each site has at least three different stream orders (Figure 3.3), for the description and measurement of processes at different scales. Each site contains hillslope soils and vegetation patterns (catena sequence) that are common throughout the land system.

This research was conducted on the two southern sites C and D (Figure 3.2). These are the Southern Granites and the Southern Basalts popularly known as Stevenson-Hamilton and Nhlowa respectively. The Stevenson-Hamilton supersite falls under the Skukuza land system according to Venter’s classification (Venter, 1990). It is within the Renosterkoppies land type, which is finely dissected, resulting in a high stream density (Smit *et al.*, 2013). Crests on the southern granite supersite are dominated by *terminalia sericea* and *combretum spp*, whilst the *acacia niloticas* are on the midslopes and valley bottoms dominated by *Euclia divinorium*. The Nhlowa supersite lies in the Satara land system (Venter, 1990). It is characterized by *sclerocarya*

*birrea* and *acacia nigresens* (open savanna), with a dense grass cover, a result of the nutrient rich basalt soils. The basalts have a low gradient topography comprising very large interfluves and a riparian zone, whilst the granites hillslopes can be subdivided into four or five elements distinguished by the organization of soils and vegetation on the slopes (catena sequence).

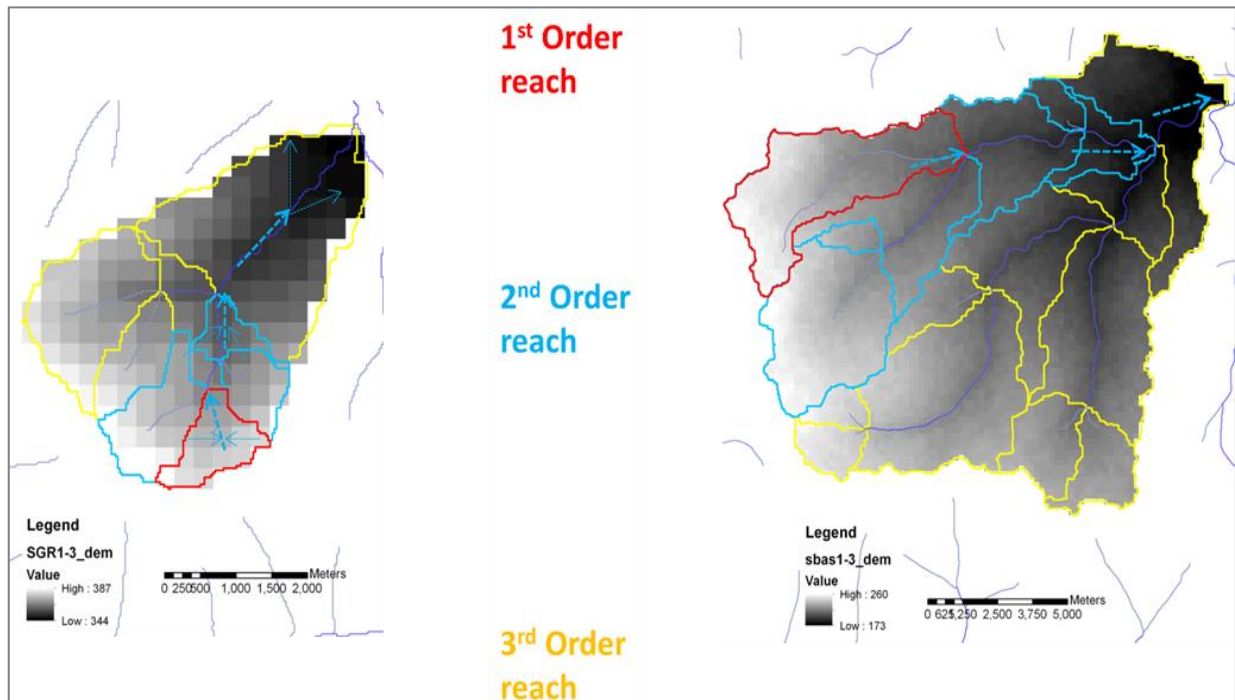


Figure 3.3 The southern granite supersite and southern basalt supersite showing the boundaries for the different stream orders.

### 3.7 Methodology Roadmap

To accomplish the study objectives, the methods used will be outlined (Figure 3.4) and discussed in this chapter. The determination and quantification of hillslope processes and flow mechanisms, such as interflow and overland flow in contributing areas of 1<sup>st</sup> to 3<sup>rd</sup> order streams was achieved using a number of characterization techniques including, geophysical surveys (ERT), soil surveys, hydrometry and physically-based numerical modelling. This chapter outlines these techniques in detail, showing maps with locations of the instrumentation (Figures 3.5 and 3.6). Monitoring and data collection on the KNP Supersites commenced in July 2011 however, data that specifically contributes to this study is presented from October 2012 to April 2013

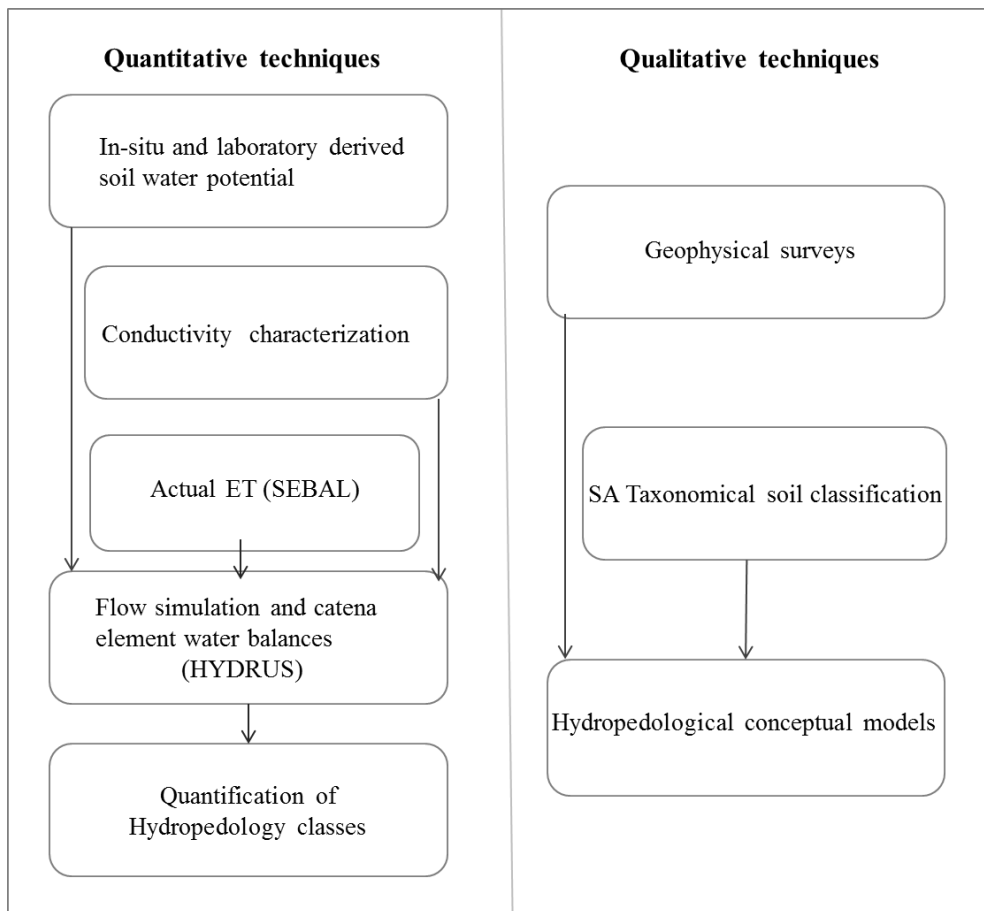


Figure 3.4 Methodology roadmap

### 3.8 Instrumentation Network

The instrumentation network comprises three transects on each supersite (Figures 3.5 and 3.6). These transects run parallel with the slope of the catena, from the crest to the toeslope. This is where measurements were concentrated i.e. geophysics ERT and the monitoring stations for soil water sensors were also nested along these transects. Due to logistical constraints, ERT and saturated hydraulic conductivity was not conducted at the basalt supersite.

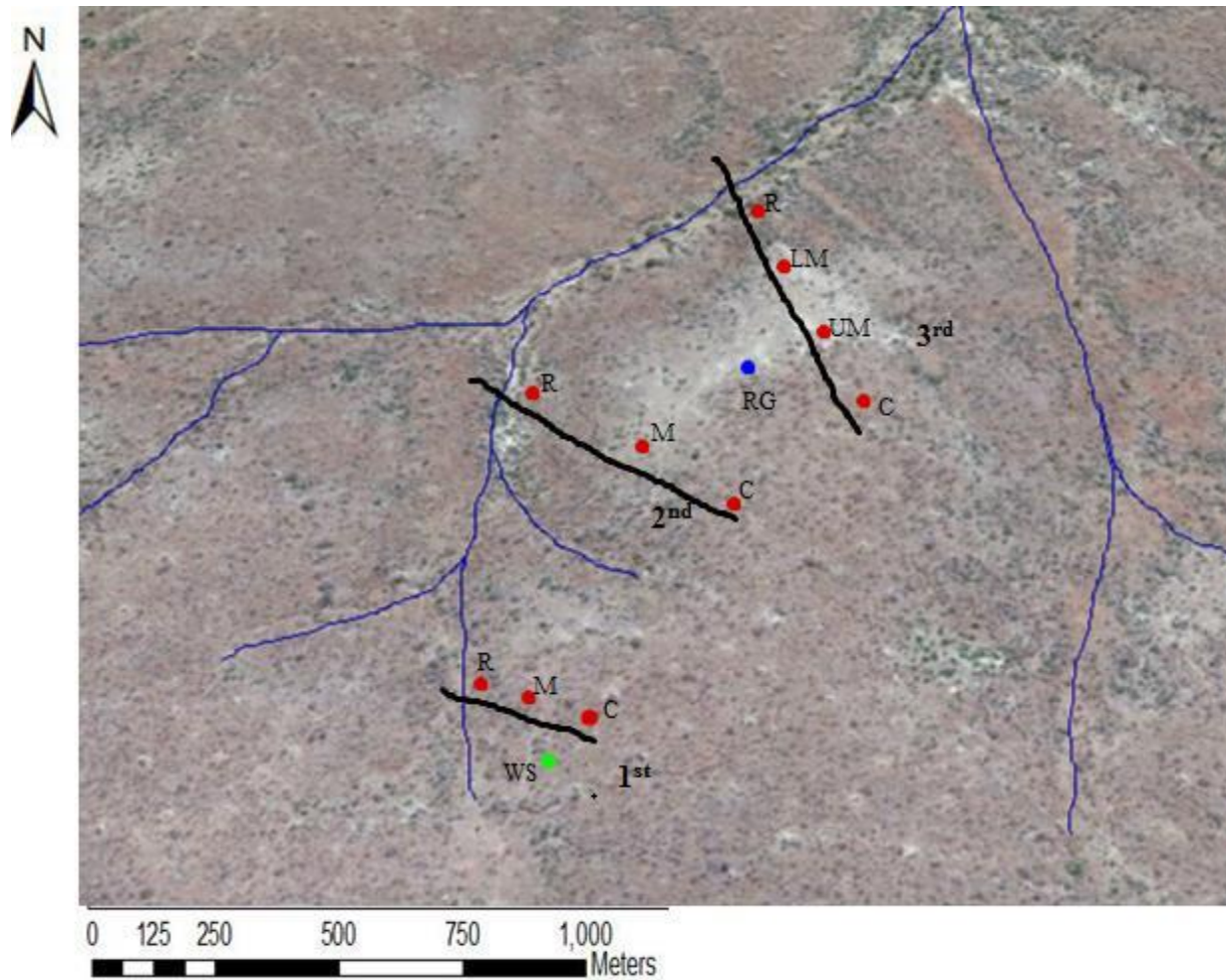


Figure 3.5 Monitoring stations and geophysics transects on granite supersite, respectively. Green = weather station, Red = soil moisture sensors station, Blue = rain gauge, C = Crest, M = Midslope, R = Riparian, black line = geophysics transect

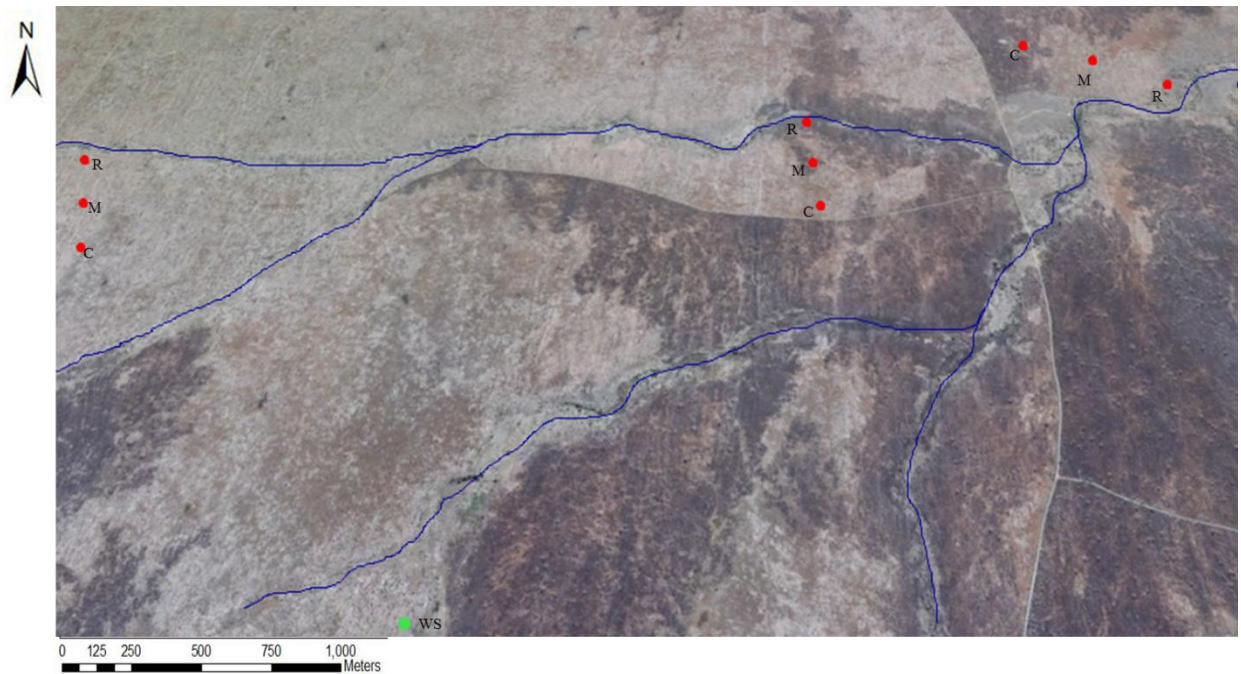


Figure 3.6 Monitoring stations and geophysics transects on basalt supersite, respectively. C = Crest, M = Midslope, R = Riparian, black line = geophysics transect and Red = soil moisture sensors station, Green = weather station

The two sites differ in topography. The granites have steeper slopes than the basalts. Slopes at the granites are 2.3 % on the 1<sup>st</sup> order hillslope and 3.2 % for the 2<sup>nd</sup> and 3<sup>rd</sup> order hillslopes (refer to Figure 9.12 for a contour map). The basalts have a low gradient topography with slopes of 1.4% on all the hillslope transects.

### 3.8.1 Meteorological station

Tipping bucket rain gauges (Texas™ and Davis™) were installed on the granite and basalt supersites, respectively, for the measurement of event-based rainfall. Tipping bucket rain gauges were used because they can measure the rainfall intensity. They were calibrated to 0.1 mm (granites) and 0.2 mm (basalts). Temperature (°C), solar radiation ( $Wm^2$ ), wind direction and wind speed (m/s) were also recorded and these sensors were connected through a console, which would then be used to download the recorded data, using Weather link software™.

### 3.9 Characterization of Soil Hydraulic Properties

Hydraulic conductivity measurements were conducted on the hillslope transects of each catena element close to the soil water monitoring stations at the two supersites.

#### 3.9.1 Field measurement of unsaturated hydraulic conductivity ( $k_{\text{unsat}}$ )

The Tension Disc Infiltrometer, TDI (Figure 3.7) was used to determine the soil  $K_{\text{unsat}}$ . Measurements were made at each soil horizon interface in the profile. The steady-state infiltration of water was recorded, whilst a suction/tension was maintained in the water supply pipe. Four tensions were used (5 mm, 60 mm, 90 mm and 120 mm) on the same surface, to determine the steady-state infiltration rate of water at the different tensions. The  $K_{\text{unsat}}$  of the soils calculated from the TDI was determined according to the method of Ankeny *et al.* (1991). TDI data is useful for quantification of effects of macropores on infiltration rates of different soil textures. It can also be used for quantification of preferential paths and the evaluation of saturated hydraulic conductivity (van Genuchten and Šimůnek, 1996)

$$A = \frac{Q_{tA} - Q_{tB}}{Q_{tA} + Q_{tB}} \times \frac{2}{tB - tA} \quad (3.1)$$

- $A$  - Parameter for  $K_{\text{unsat}}$  equation [ $\text{mm}^{-1}$ ],  
 $Q$  - Steady-state infiltration rate [ $\text{mm}^3 \cdot \text{min}^{-1}$ ],  
 $tA$  - 1<sup>st</sup> tension in [mm]  
 $tB$  - 2<sup>nd</sup> tension in [mm].

Calculation of  $K_{\text{unsat}}$ :

$$K_{\text{unsat}} = \frac{AQ_{t6}}{(A\pi r^2) + 4r} \quad (3.2)$$

Where

- $K_{\text{unsat}}$  - Unsaturated Hydraulic conductivity [ $\text{mm} \cdot \text{min}^{-1}$ ], and  
 $r$  - Infiltration radius [mm].

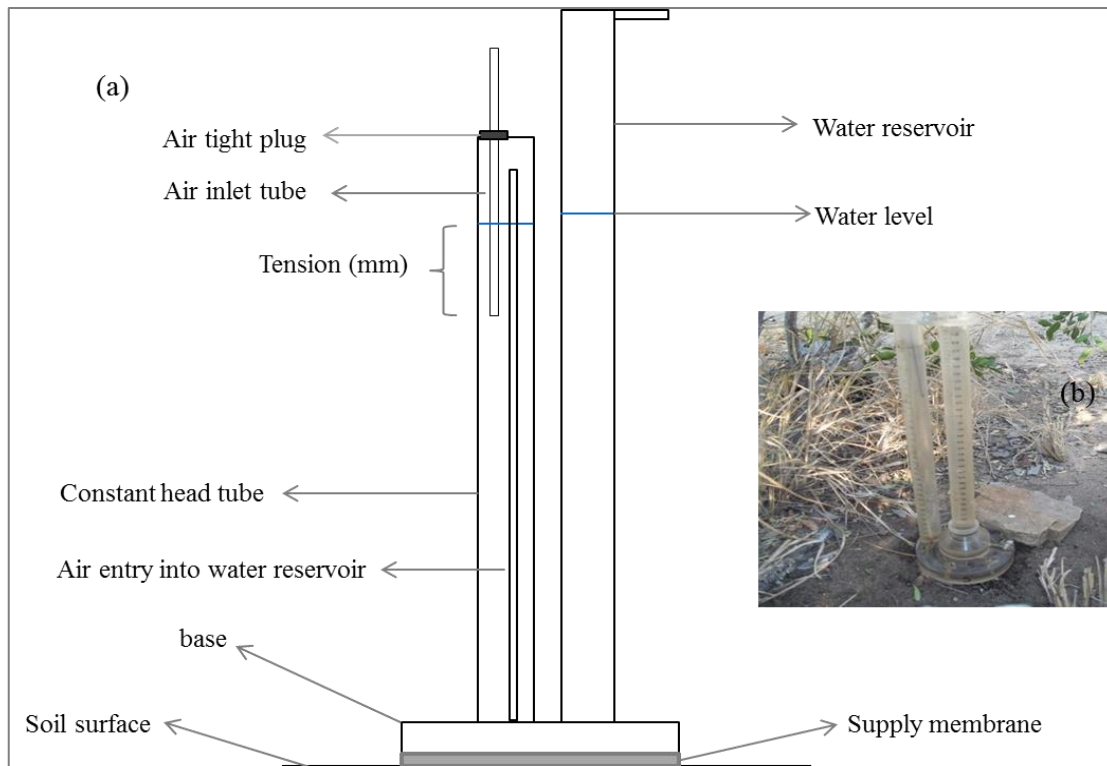


Figure 3.7 (a) Schematic of a tension disk infiltrometer, (b) infiltrometer set-up in the field.

### 3.9.2 Field measurement of saturated hydraulic conductivity ( $k_{sat}$ )

The double ring infiltrometer and mobile permeameter were used to measure  $K_{sat}$  on the southern granite supersite (Figure 3.8). The double ring was used at the same spot where the  $K_{unsat}$  was measured and also in the B-horizons.  $K_{sat}$  was also measured in the subsurface using the mobile permeameter where holes were augured to the desired depths and the steady-state rate of inflow of water was recorded. Due to the nature of soils in the basalt,  $K_{sat}$  could not be measured because of the time it would take to conduct the measurements.



Figure 3.8 Field measurement of  $K_{sat}$  using the double ring infiltrometer and permeameter, respectively.

### 3.9.3 The double ring infiltrometer

Using the measurements from the field, the following equation was used to calculate the field saturated hydraulic conductivity of the soils.

$$V_{IR} = \Delta V_{IR} / (A_{IR} * \Delta t) \quad (3.3)$$

Where:  $V_{IR}$  = Inner ring incremental velocity mm/hr

$\Delta V_{IR}$  = Volume of liquid used to maintain a constant head in the inner ring ( $\text{mm}^3$ )

$A_{IR}$  = Area of internal inner ring ( $\text{mm}^2$ )

$\Delta t$  = Time interval in hours

Space between rings:

$$V_A = \Delta V_A / (A_A * \Delta t) \quad (3.4)$$

$V_A$  = Incremental velocity in annual space mm/hr

$\Delta V_A$  = Volume of liquid used to maintain constant head in outer ring in ( $\text{mm}^3$ )

$A_A$  = Area of space between rings in ( $\text{mm}^2$ )

### 3.9.4 The mobile permeameter

The steady-state infiltration of water into the soil was determined in an augered cylindrical hole, where a constant head of water was maintained in the hole, whilst water infiltrates from a 20-litre container with two permeameters connected on one pipe. This method allowed for measurements to be performed in subsurface soil horizons in a profile (Figure 3.9). The 3-D water flow is governed by the Glover equation below (Amoozegar, 2008):

$$K_{\text{sat}} = CQ \quad (3.5)$$

Where:

$K_{\text{sat}}$  = Saturated hydraulic conductivity (mm/ hr)

$Q$  = Steady-state rate of water flow (mm<sup>3</sup> hr)

$C$  = Constant

Where:

$$C = \left[ \sinh^{-1} \left( \frac{H}{r} \right) - \left( \frac{1+r^2}{H^2} \right)^{0.5} + \left( \frac{r}{H} \right) \right] / (2\pi H^2) \quad (3.6)$$

And where:

$H$  = Height of water in the reservoir (mm)

$r$  = Radius of the cylindrical augered hole (mm)

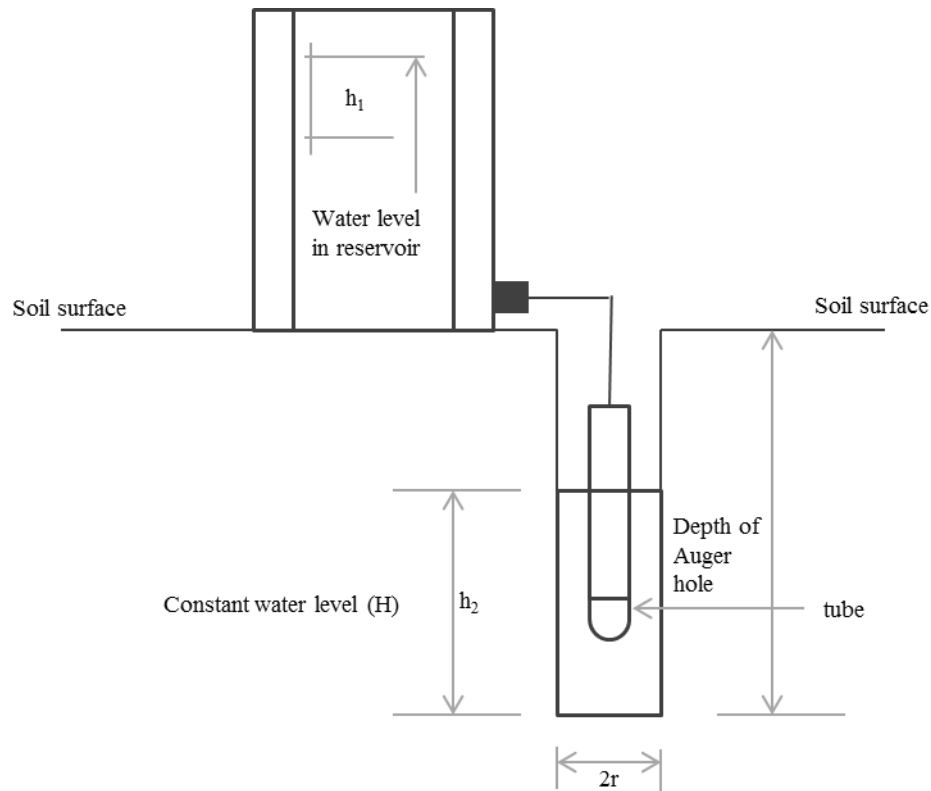


Figure 3.9 Schematic of the measurement of  $K_{sat}$  using the mobile permeameter

There is a distinction between saturated and unsaturated hydraulic conductivity. Saturated hydraulic conductivity is measured in saturated soils where matric potential for the soil is zero. The resistance to movement in saturated soils is determined by the size and arrangement of pores amongst other factors such as soil structure and soil grain size. Unsaturated hydraulic conductivity is a measure of the soil's ability to transmit water under unsaturated conditions. It is important to measure the saturated and unsaturated hydraulic conductivity of a soil for the evaluation of movement of nutrients, the development of unsaturated zone models and monitoring systems. The measurement of unsaturated hydraulic conductivity at different tensions allows for the estimation of the role played by macropores in water movement in the soil (Amoozegar, 2008).

### 3.10 Soil Classification

Soil properties, such as morphology, can serve as indicators of the hydrological regime. Soils have a governing influence on a number of hydrological processes therefore, soils were surveyed and classified. Holes were augured and pits were dug from the soil surface down to saprolite on each catena element (Figure 3.10). Soil samples were collected at each diagnostic horizon for the determination of particle size distribution in the lab. Diagnostic horizons were identified and classified according to the taxonomical soil classification system of South Africa (Soil Classification Working Group, 1991).



Figure 3.10 Taxonomical soil classifications on catena elements showing Sterkspruit soil form at 3<sup>rd</sup> order midslope (a) and Pinedene form at 2<sup>nd</sup> order crest (b) respectively.

During surveys, soil structure, texture and visible hydrological features (i.e. the presence of mottles) were recorded for hydro pedological classification. This classification was performed according to le Roux *et al.* (2013) and van Tol *et al.*'s (2013) principles and the hydrological soil types (Figure 3.11).

Hydrological soil type	Description	Symbol
Recharge	Soils without any morphological indication of saturation. Vertical flow through and out of the profile into the underlying bedrock is the dominant flow direction. These soils can either be shallow on fractured rock with limited contribution to evapotranspiration or deep freely drained soils with significant contribution to evapotranspiration.	
Interflow (A/B)	Duplex soils where the textural discontinuity facilitates buildup of water in the topsoil. Duration of drainable water depends on rate of ET, position in the hillslope (lateral addition/release), and slope (discharge in a predominantly lateral direction).	
Interflow (soil/bedrock)	Soils overlying relatively impermeable bedrock. Hydromorphic properties signify temporal build of water on the soil/bedrock interface and slow discharge in a predominantly lateral direction.	
Responsive (shallow)	Shallow soils overlying relatively impermeable bedrock. Limited storage capacity results in the generation of overland flow after rain events.	
Responsive (saturated)	Soils with morphological evidence of long periods of saturation. These soils are close to saturation during rainy seasons and promote the generation of overland flow due to saturation excess.	

Figure 3.11 Hydrological soil types (after van Tol *et al.*, 2013)

The whole hillslope was classified according to their soil types and hydrological regimes, using the dominant processes defined by the soil types of the catena elements. The classification system is still in its infancy but, was nevertheless used in this study because it forms the basis on which data can be linked, compared and integrated at the hillslope scale for the conceptualization of processes. The hillslope classes are summarized in Table (3.1).

Table 3.1 Hydropedological Soil Types (after van Tol *et al.*, 2013)

CLASS	NAME OF CLASS
1	Interflow (Soil/Bedrock Interface)
2	Shallow Responsive
3	Recharge to Groundwater (Not Connected)
4	Recharge to Wetland
5	Recharge to Midslope
6	Quick Interflow

### 3.11 Monitoring of Subsurface Soil Water Dynamics

Soil moisture sensors (WaterMarks<sup>TM</sup>) were used to determine characteristic subsurface soil-water dynamics within typical catena soils at the hillslope scale (Figure 3.12). WaterMark<sup>TM</sup> sensors measure electrical resistance of porous medium in kilo-ohms (k $\Omega$ ). They have a gypsum block type of sensor to measure the resistance. The material around the gypsum-type sensor is water-permeable in which the electrodes are embedded. Therefore, the resistance between the electrodes is influenced by the moisture content. Where there is low water content, a high resistance is recorded and vice-versa. In order to convert the millivolt readings to capillary pressure head, a calibration function for three channels is applied, using Equation (3.7). Each sensor is calibrated and the temperature readings are corrected, allowing for the conversion to soil water potential (derived from Lorentz and Pretorius, 2008). The sensors are then connected to a HOBO 4-channel data logger (three soil moisture sensors and one temperature sensor as channel four). The sensitivity range for the sensors is from zero to approximately 15 000 mm of pressure. This was the range that measurements were considered realistic. At each station, two or three sensors were installed in a single profile in different diagnostic horizons that were identified during the soil surveys.

$$\varphi_h = 0 \quad \text{Where } mV < E \quad (3.7a)$$

$$\varphi_h = \frac{A(BmV)}{1-(CmV-[DT])} \quad \text{Where } E < mV < F \quad (3.7b)$$

$$\varphi_h = GmVH \quad \text{Where } mV < F \quad (3.7c)$$

Where:

- $\varphi_h$  - CPH (Capillary Pressure Head in mm), a tension which is a positive equivalent of matric potential
- $mV$  - millivolts
- $T$  - Temperature ( $^{\circ}C$ )
- $A - G$  - Empirical constants for logger channels (Table 3.2)

Table 3.2 Derived constants for parameter A-G (derived by Lorentz and Pretorius, 2008)

Parameter	Channel 1	Channel 2	Channel 3
A	-380	-760	-680
B	1900	1900	1700
C	0.37	0.357	0.357
D	0.01205	0.01205	0.01205
E	0.2	0.4	0.4
F	1.85	1.85	1.85
G	2543511.5	2543511.5	2543511.5
H	-4485496	-4633564	-4633563

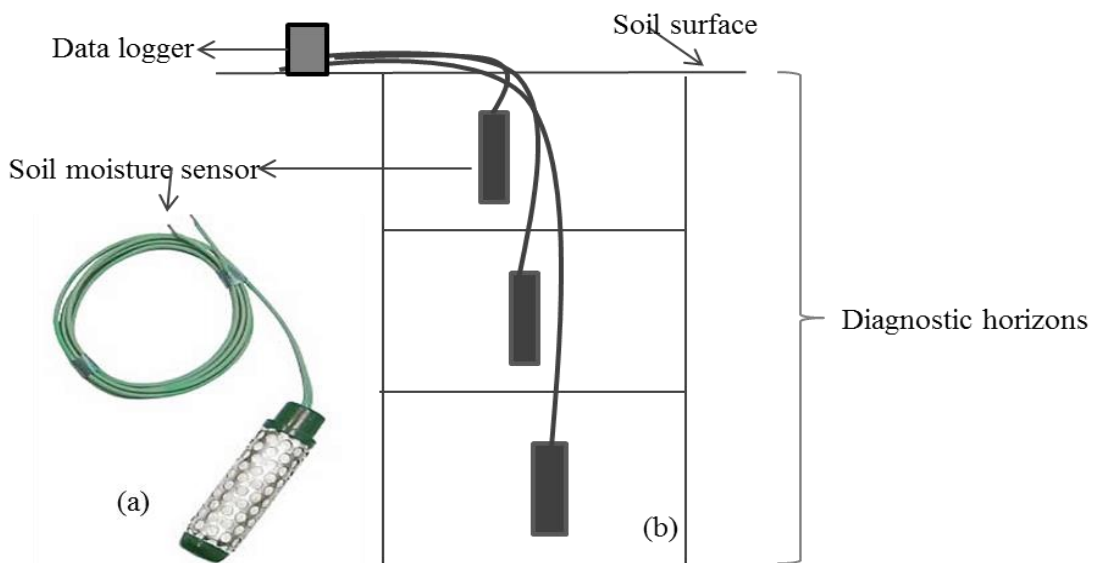


Figure 3.12 (a), soil moisture sensor (Cal Africa, 1978) and (b) schematic of installed sensors in soil a profile

### **3.11.1 Laboratory-derived soil water potential**

The PotentiaMeter (Model WP4, Decagon) was used to measure the water potential of the soil. Soil samples from the two 3<sup>rd</sup> order hillslopes (granites and basalts) were collected in order to make a qualitative comparison of gravimetric water content and water potential of the soils between the two geologies. The PotentiaMeter (Figure 3.13), can measure the water potential of a soil sample between -40 and zero MPa (air dry to saturated) with an accuracy of 0.1 MPa.

The PotentiaMeter measures the effect of both the osmotic and matric potential of the soil dependent on the amount of dissolved materials in the sample. It uses a chilled mirror inside that determines the matric potential. At dew point temperature, the vapor pressure is calculated in the headspace above the equilibrated sample in the sample chamber (Petry and Byrant, 1993). Wet range readings are approximately equal to tensiometer readings, whilst the dry range sensors respond to atmospheric humidity changes, thereby making this a reliable and convenient method to use.

The soil samples were oven-dried at 105 degrees Celsius for 24 hours. Samples were transferred to measuring cups and weighed to get the mass of the dry sample. A known volume of deionized water was added daily (between 0.1-0.2 g) and samples were left for the next 24 hours, so that they could equilibrate. This was repeated on a daily basis, until the soils were fully saturated. Water was added, so that the gravimetric water content could be calculated at which the matric and osmotic potential was measured. Daily results were then calculated to give a graph of water content against water potential for the different soils. Since oven-dried samples were used, the volumetric water content was also calculated from water that was added to the samples and measured each day.



Figure 3.13 WPA Dewpoint Potentiometer to measure soil water potential

### 3.12 Geophysical Surveys

Electrical resistivity (ERT) is a geophysics technique that can be used to determine subsurface resistivity distribution, using the instruments shown in Figure (3.14). It has mainly been used in hydrogeology, but has recently been adopted to solve hydrological problems as well (Berthold *et al.*, 2004).



Figure 3.14 ERT instrumentation ABEM Terrameter (ABEM [2005]: Instruction Manual)

The theory behind (ERT) is that the ground resistivity is related to a number of geological parameters, such as the dissolved ions in soil water, porosity, fluid content, minerals and degree of water saturation in the rock (ABEM, 2005). Different rocks and sediments have different resistivity values (Figure 3.15).

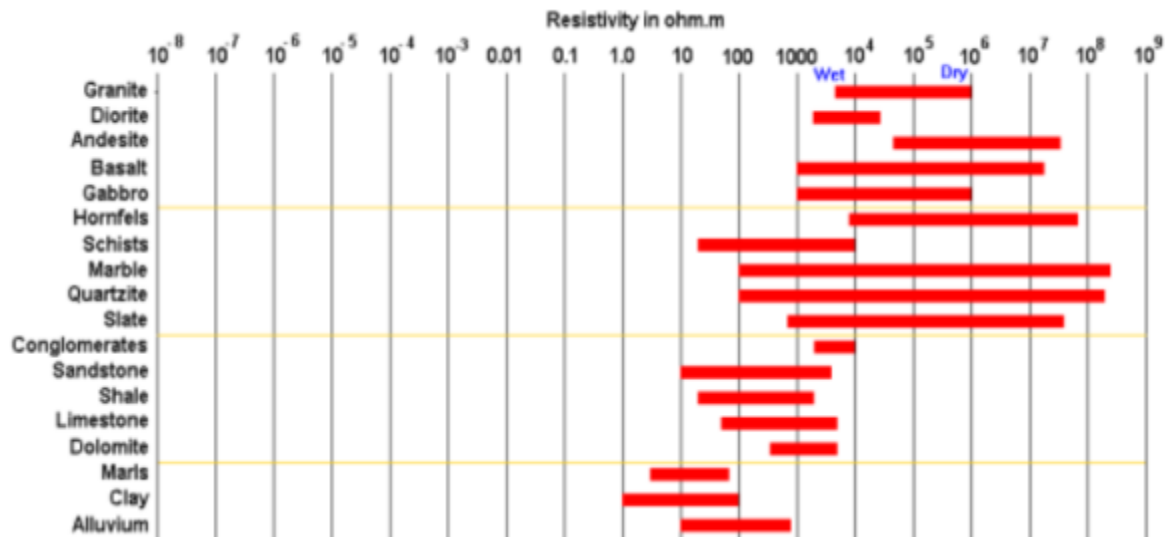


Figure 3.15 Resistivity ranges of various sediments and rock types (after Loke, 2004)

To measure the subsurface resistance, a current was injected into the ground using two electrodes (see Figure 3.16b). A resultant voltage between the two electrodes was used to derive the apparent resistance. There are a variety of arrays that can be used to measure the subsurface resistivity, such as, Wenner Alpha and Wener Beta, Wenner-Schlumberger and Dipole-dipole (Loke, 1999). According to Loke (2004), they have different geometric factors, therefore, they have different properties in the depths they can read (shallow or deep) and the resolution in which they can operate (vertical or horizontal). The apparent resistivity of the subsurface was governed by the equations:

$$pa = k V/I \tag{3.8}$$

$$pa = kR \tag{3.9}$$

Where:

$pa$  - Apparent resistivity ( $\Omega$ )

- $k$  - The geometric factor
- $V$  - Velocity (m/s)
- $I$  - Current (Amps)
- $R$  - Resistance ( $\Omega$ )

This gives an apparent resistivity not the true resistivity of the subsurface. True resistivity was derived from Jacobian matrix calculations in the inversion modelling software RES2DINV (Loke, 2004).

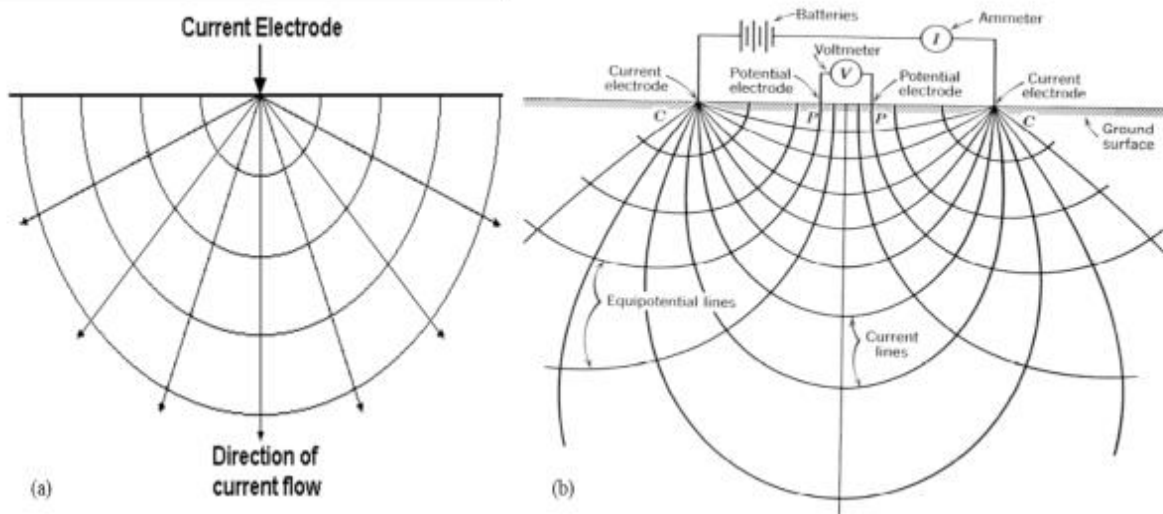


Figure 3.16 Basic electrical resistivity circuits from (a) one (b) two electrodes (after Todd 1980)

ERT, if applied as a time series analysis can be used in conjunction with hydrometric observations for a clear understanding of subsurface structure and composition, since hydrometric observations are mainly localised, making it difficult to interpret soil water fluxes. These time series surveys were conducted on the southern granite supersite to compare the wet and dry season's subsurface moisture dynamics and distribution of hillslope water. The probes were left on site at fixed positions because subsurface material remains fixed, but moisture content changes over time. Measurements were repeated at different times in a season to observe the change in moisture distribution over time. The first measurements were conducted on site in 2011 and the results were used as the dry season signature of the subsurface resistivity (Riddell

*et al.*, 2011). The repeated measurements were conducted in January 2013 after a high intensity rainfall event (e. g. 28 mm/hr.) and again in March 2013, towards the end of the wet season. Since the hillslopes are long, a roll-along was done, using half of the electrodes at the other end of the transect when one run was complete. This enabled the resistivity survey of the several hundred meter hillslopes to be possible. An inverse modelling technique (RES2DINV) was used for the inversions.

### 3.13 Simulation of Flow and Catena Element Water Balances using HYDRUS 1D

HYDRUS-1D (Šimůnek *et al.*, 2013) was used to simulate flow and calculate model catena element soil water budgets. This was the model of choice, since the review of literature showed that it has the most simulating capabilities, compared to other models. HYDRUS can simulate water flow, solute and heat transport in saturated, unsaturated and partially saturated porous media and even on non-uniform soils, which was crucial in this study, considering the non-homogenous soils on the study sites. HYDRUS 1D numerically solves the Richards equation for variably-saturated water flow (Equation 3.11). There is a sink term that accounts for root water uptake by plants and also different types of flow, such as macropore flow and/or matrix flow. The user specifies the type of domain, boundary conditions, initial conditions and the distribution of materials in the soil profile (Figure 3.17). Simulated results from the model were then used to calculate water balances, using the Equation (3.10) by Zhang *et al.* (2002).

$$\Delta S = P - ET - R - FD \quad (3.10)$$

Where:

- $\Delta S$  - Change in water storage (mm)
- $P$  - Precipitation (mm)
- $ET$  - Evapotranspiration
- $R$  - Surface runoff (mm)
- $FD$  - Free drainage or groundwater recharge (mm).

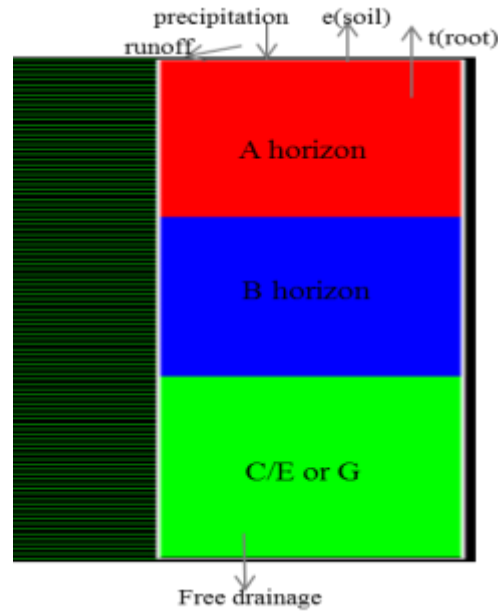


Figure 3.17 A schematic illustration of diagnostic horizons and boundary conditions in HYDRUS 1D. e (soil)=evaporation from surface, t (root)= root water uptake

### 3.13.1 Water flow simulation and its governing equations

Water flow through the unsaturated porous medium is highly variable and is controlled by a number of soil physical properties, such as texture and pore configuration. Antecedent moisture conditions in the soil also play a part in controlling water movement through the medium. A modified form of the Richard's Equation (3.11) is used to describe the one-dimensional water movement in porous media. An assumption is made that the air phase is insignificant in the water flow process and that thermal gradients can be ignored (Šimůnek *et al.*, 2013).

$$\frac{\partial \theta}{\partial t} = \frac{\partial}{\partial x} \left[ K \left( \frac{\partial h}{\partial x} + \cos \alpha \right) \right] - S \quad (3.11)$$

Where

$h$  - Water pressure head (L)

$\theta$  - Volumetric water content ( $L^3L^{-3}$ )

$t$  - Time (T)

$x$  - Spatial coordinate (L)

$S$  - Sink term ( $L^3L^{-3}T^1$ )

$\alpha$  - angle between flow direction and axis (vertical)

$K$  - Unsaturated hydraulic conductivity function ( $LT^{-1}$ ) which is given by the following equation:

$$K(h, x) = K_s(x)K_r(h, x) \quad (3.11b)$$

Where:

$K_r$  - Relative hydraulic conductivity (-)

$K_s$  - saturated hydraulic conductivity ( $LT^{-1}$ )

### 3.13.2 Simulation period

The modelling period was from the 3<sup>rd</sup> of October 2012 to the 30<sup>th</sup> of April 2013 (wet season), giving it a total of 210 days. The model was run in hourly time steps, therefore, there were a total of 5 040 hours and the print times (model output) were after every 24 hours, giving 210 print times.

### 3.13.3 Location, domain set-up and boundary conditions

The domain set-up was for each catena element. The domain was designed according to depths that were measured during the soil surveys and material distribution from soil textural classes for each element. At the surface, the atmospheric boundary condition with surface runoff was used and a free drainage boundary at the bottom. The iteration criterion was set (Figure 3.18). Initial conditions for the run were set in pressure heads, according to the observed values from the soil moisture sensors. From the data, it was shown that the soils got very dry before the beginning of the rainy season, therefore, a CPH of -15 000 mm was used as the minimum. At the granite site, upslope contributions as surface runoff were added to the precipitation on the adjacent downslope catena element (Table 5.3).

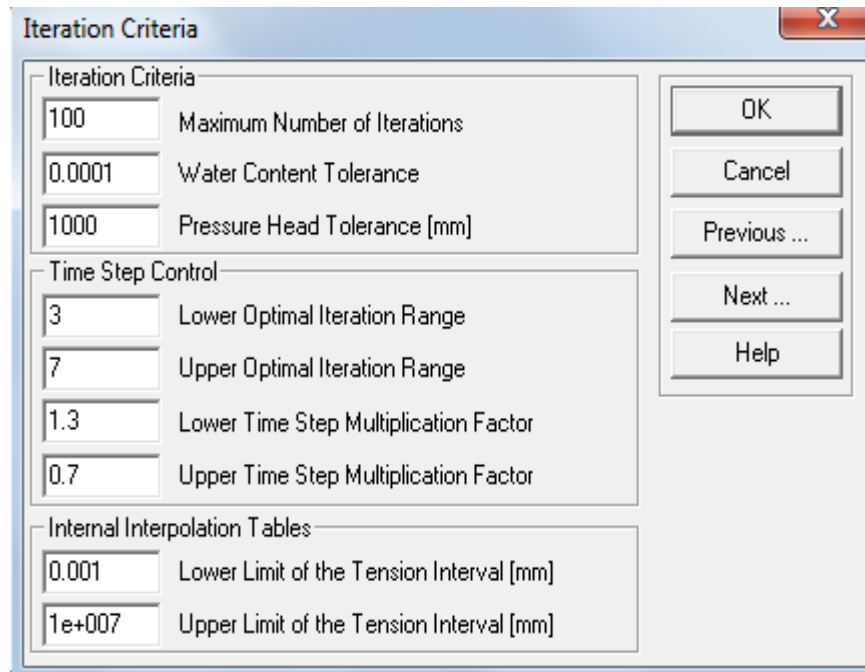


Figure 3.18 Iteration criteria on HYDRUS 1D

### 3.13.4 The Residual and Saturated Soil Water Content

HYDRUS-1D default values for  $\theta_r$  (residual soil water content) and  $\theta_s$  (saturated soil water content) were set for the different soil textures. The  $\alpha$  (parameter in the soil water retention function) and  $n$  (exponent in the soil water retention function) values were obtained using RETC, which is a computer program that can be used to describe the hydraulic properties of unsaturated soils. Several models can be fitted to the observed hydraulic conductivity and water retention data. Using our measured  $K_{\text{unsat}}$  data, the accompanying RETC program (van Genuchten *et al.*, 1991) was used to fit  $\alpha$  and  $n$  values.

Precipitation measured onsite from the rain gauge at the weather station was used as a driving input parameter at the atmosphere boundary layer along with the derived aET derived from the SEBAL Penman-Montieth disaggregation. Initial conditions ascribed to the model domain were applied in terms of CPH as determined from the representative soil water data for a particular horizon.

### 3.14 Actual Evapotranspiration from Satellite Imagery

Actual ET data was acquired from available SEBAL (Surface Energy Balance Algorithm for Land) satellite imagery (rasters). SEBAL computes the energy balance and radiation, together with resistance for water vapor flux and heat for each pixel, based on infrared reflectance (Tasumi *et al.*, 2003). The actual evapotranspiration was determined, using residuals from the surface energy budget equation (Farah, 2001):

$$\lambda ET = R_n - G - H \quad (3.12)$$

Where:

$\lambda ET$  - Flux for latent heat of vaporisation (W/m<sup>2</sup>)

$R_n$  - Flux for net radiation at the surface (W/m<sup>2</sup>)

$G$  - Soil heat flux (W/m<sup>2</sup>)

$H$  - Sensible heat flux (W/m<sup>2</sup>)

The evapotranspiration data was used as an input parameter to run the HYDRUS model for catena element water balances. All water fluxes were in millimeters per hour, therefore, the SEBAL data, which was at a weekly time interval, had to be disaggregated to hourly time steps.

The SEBAL data set was obtained at a 30 m pixel resolution, courtesy of eLeaf via the Inkomati Catchment Management Agency. Google Earth (GE) was used to create boundaries (polygons) of catena elements, using the distinct vegetation guilds visible from the GE imagery of the hillslopes (Figure 3.19a). Using Arc Map, the rasters were then clipped (Figure 3.19b). The data from the clipped rasters was then aggregated to get weekly values per catena element. The crest and midslope rasters on the basalt supersite were combined and treated as one interfluvium on the hillslopes due to the low gradient topography.

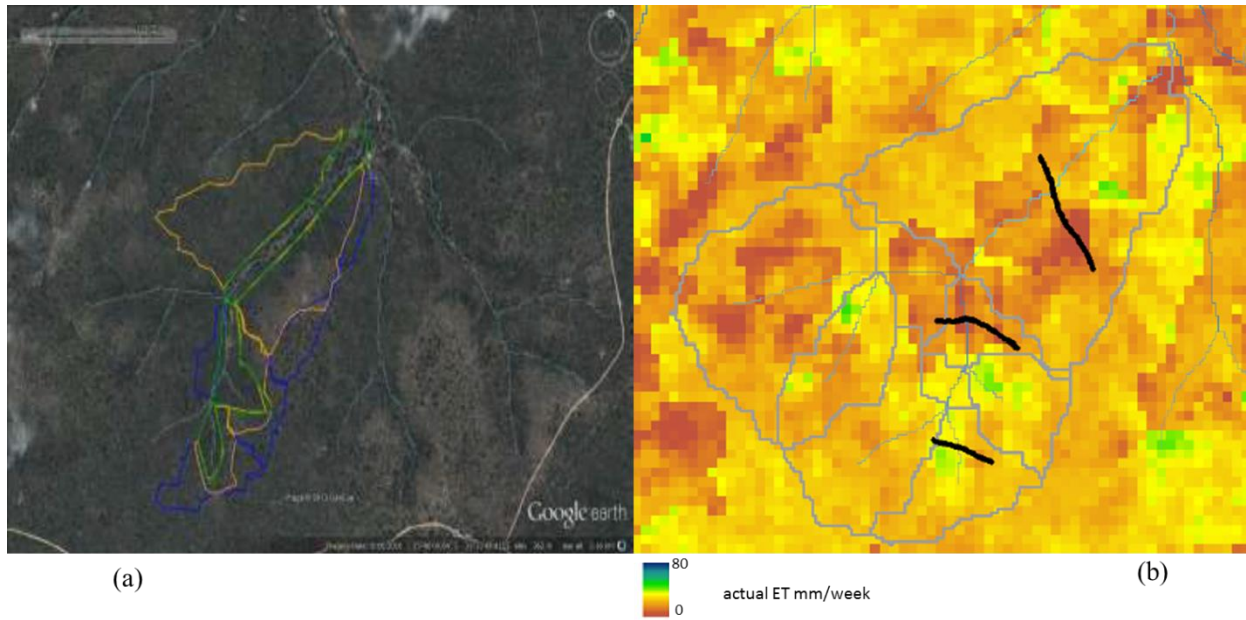


Figure 3.19 (a) Boundaries of catena elements demarcated on Google Earth (b) example of SEBAL actual ET for the sub-catchments on the Southern Granite Supersite.

In order to use the SEBAL data as an input, the weekly values were disaggregated to hourly time steps, by fitting them to a relationship derived from the Penman Monteith Equation (3.13).

$$\frac{aET}{hr} = \frac{pET(hr)}{Total\ pET(week)} \times Total\ aET\ (week) \quad (3.13)$$

Where:

$aET$  - Actual ET

$pET$  - Potential ET.

### 3.14.1 Partition of evapotranspiration into soil and vegetation root components

The model runs with evaporation and transpiration as separate entities, therefore, the actual evapotranspiration was partitioned into two components. In order to achieve this, a simple dimensionless partitioning model was used in the form of the equation overleaf (Smithers and Schulze, 1995):

$$ft = \frac{\lambda(t)-0.2}{0.8} \quad (3.14)$$

Where:

$t$  - Time (days)

$\lambda$  - Site-specific crop factor

To partition the evapotranspiration, ( $ft$ ) is then used as follows:

$$pT = p ET_0 ft \quad (3.14)$$

And

$$p E_{soil} = p ET_0 - p T \quad (3.15)$$

A value of  $\lambda=1$  means 5% of  $p ET_0$  will be for evaporation from the soil. When  $\lambda$  is greater than one, evaporation from the soil becomes zero.

### 3.15 Model Validation (Sensitivity Analysis)

There are many ways to perform sensitivity analysis which include differential analysis, sensitivity index, subjective analysis and one time sensitivity measures. The one time sensitivity measure was used to test for sensitivity in model parameters for HYDRUS 1D which was used to simulate flow and quantify fluxes in this study. According to Hamby (1994), different values are used repeatedly for one parameter whilst all the others are fixed when using one at a time sensitivity analysis. The parameters tested include rainfall, soil properties and evapotranspiration. The choice for these three was based on the fact that the model was being used for quantification of fluxes and water balances. Soil properties, rainfall and ET are known to affect hydrological responses in a system. A 50% increase and decrease in rainfall and ET was tested. A relative increase (>80 mm) and decrease (<10 mm) in soil hydraulic properties ( $K_{sat}$ ) was also tested. The percent change in model output from original is then calculated using the following equation:

$$Change\ from\ original\ (\%) = \frac{Output\ value\ after\ change - original\ output\ value}{Original\ output\ value} * 100 \quad (3.16)$$

The total percent change was calculated by adding all percent output variables of the water balance (all as positive values to get total percentage change) using the following equation.

$$Total (\%)change = \% \Delta FD + \% \Delta R + \% \Delta ET + \% \Delta S + \% \Delta P \quad (3.17)$$

When calculating the total percent change, if it was for ET, then the change in ET was omitted since it was the value that has been manipulated and the same applies for the calculation of the other parameters under analysis. The difference between the maximum and minimum values of the total change was then calculated to see which parameter the model was most sensitive to.

### Summary

Revisiting the objectives to show how the above-mentioned methods and characterization techniques will be used to achieve them.

- To observe and characterize mechanisms of flow in (subsurface) and along hillslopes;
- To classify soils hydro pedologically for conceptualization of hydrological processes; and
- To quantify catena element water budgets and to compare results at the different scales.

Mechanisms of flow in and along the hillslopes were determined, using hydrometry (Watermarks<sup>TM</sup>) and time series geophysical analysis. Soil classification was conducted, using the taxonomical classification and hydro pedological classification. The former helps in the identification of diagnostic horizons, whilst the latter helps in the identification of the hydrological responses of different soil types. The hydro pedological classification was used as a basis for process conceptualization and output data from HYDRUS 1D model was used for the calculation of catena element water budgets.

## 4.0 HILLSLOPE PROCESS CHARACTERIZATION RESULTS AND DISCUSSION

The results presented in this chapter pertain to both the southern granites and southern basalt supersites and cover the characterization of hillslope processes at the two sites (refer to roadmap in Figure 4.1 below).

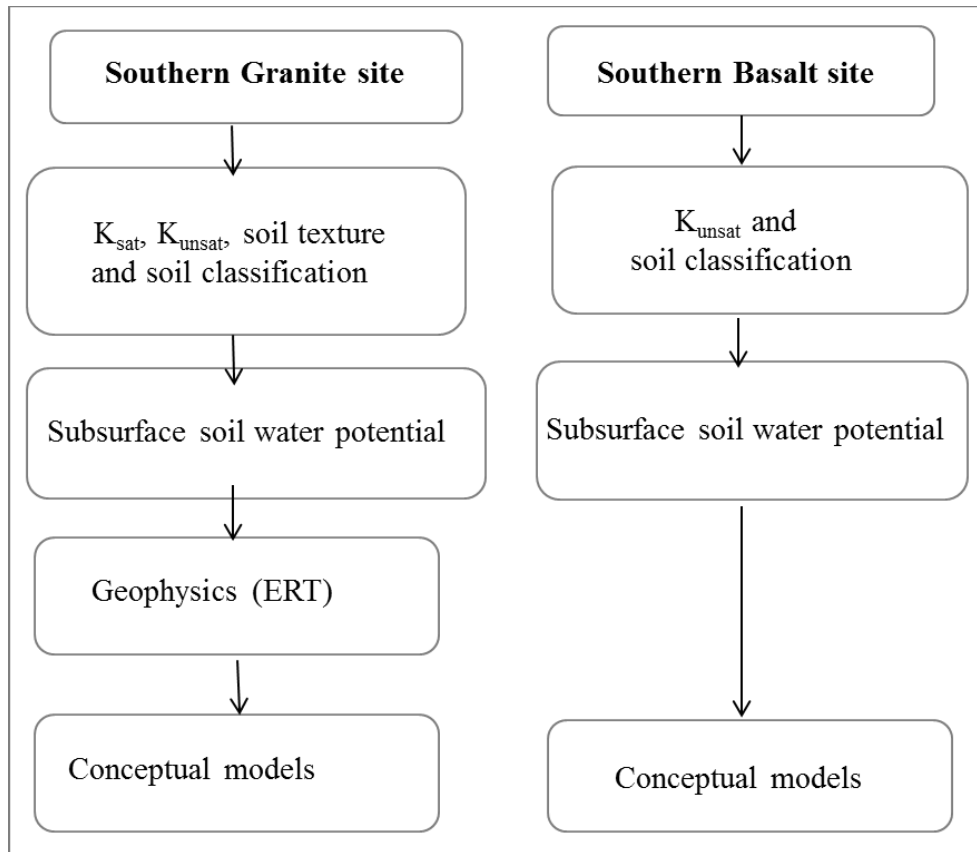


Figure 4.1 The characterization chapter roadmap

### 4.1 Southern Granite Hydraulic Characterization

#### 4.1.1 1<sup>st</sup> order hillslope

Results for soil texture,  $K_{unsat}$  and  $K_{sat}$  measured on the 1<sup>st</sup> order hillslope are represented on Figure (4.2 a, c and d) respectively.  $K_{sat}$  measurements were replicated (Figures 9.9-9.11). This

hillslope comprises crest soils with high  $K_{\text{unsat}}$  at low pressure head (34 mm/hr at  $\phi=5$  mm) on the surface compared to the lower slopes (midslope and riparian catena elements). This element comprises sandy loams (Figure 4.2a) therefore, high  $K_{\text{unsat}}$  was anticipated. The midslope and riparian catena elements show low  $K_{\text{unsat}}$  on the surface especially at high pressure heads (0.4 mm/hr and 0.7 mm/hr at  $\phi =120$  mm, respectively). This was attributed to the clay loams encountered at both these catena elements (Figure 4.2a). Clay particles are washed downslope through colluviation, hence the low  $K_{\text{unsat}}$  measurements on these catena elements. The crest element also has high  $K_{\text{sat}}$  compared to the catena elements down slope (Figure 4.2d). The midslope has the lowest  $K_{\text{sat}}$  on this hillslope (0.89 mm/hr), due to the clay loams encountered on this catena element throughout the whole profile (Figure 4.2a).

The 1<sup>st</sup> order crest was classified as a Cartref soil form (Table 4.1). The presence of an illuviated E horizon over a lithocutanic B horizon in this soil form implies the possibility of a perched water table forming (van Tol, 2008). This was supported by the low  $K_{\text{sat}}$  on the B horizon (28 mm/hr) underlying the E horizon on this element (Figure 4.2d). This implied interflow at the AE/B interface. Therefore, lateral contributions to downslope elements are expected and thus potential hydrological connectivity through lateral subsurface flow between the crest and the midslope.

The midslope and riparian catena elements are classified as a Bonheim soil forms (Table 4.1) and they both show low  $K_{\text{sat}}$  (0.9 mm/hr – 3.9mm/hr) on the B and C horizons. They both have the same hydrological soil type (interflow soils), based on hydropedological field surveys (this does not necessarily mean all Bonheim soils are interflow soils). The presence of interflow soils from the crest down to the riparian zone implies potential connectivity between catena elements through subsurface lateral flow. Potential connectivity was therefore, anticipated between the hillslope and the stream network.

Table 4.1 Soil classification per catena element on granite 1<sup>st</sup> order hillslope

Catena Element	Taxonomical class	Diagnostic Horizons	Depth of horizons	Hydrological soil type
SGR1_Crest	Cartref	Orthic A	0-250	Interflow
		E	250-500	
		Lithocutanic B	500+	
SGR1_Mid	Bonheim	Melanic A	0-200	Interflow
		Pedocutanic B	200-550	
		Unspecified	550+	
SGR1_Rip	Bonheim	Melanic A	0-200	Interflow
		Pedocutanic B	200-600	
		Unspecified	600+	

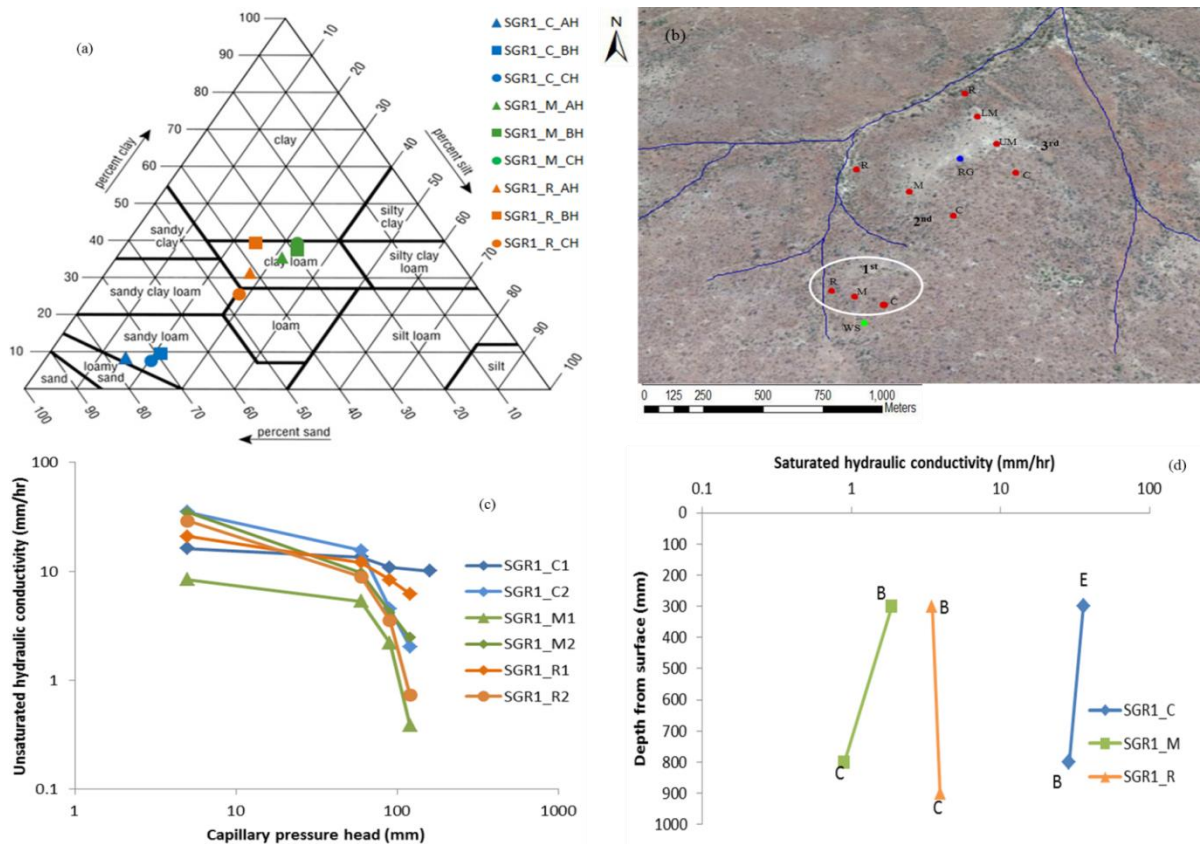


Figure 4.2 (a) Soil texture triangle (b) site map (c)  $K_{unsat}$  at soil surface (d)  $K_{sat}$  per soil horizon on granite 1<sup>st</sup> order hillslope

### 4.1.2 2<sup>nd</sup> order hillslope

The 2<sup>nd</sup> order hillslope shows high  $K_{\text{unsat}}$  at the crest at low capillary pressure head (41 mm/hr at  $\phi = 5$  mm) on the surface (Figure 4.3c). Sandy loams were characteristic of this catena element (Figure 4.3a). Although values were low, the crest also showed high  $K_{\text{sat}}$  down the profile compared to the midslope catena element (Figure 4.3d). The crest of the 2<sup>nd</sup> order comprised a Pinedene soil form (Table 4.2). The  $K_{\text{sat}}$  data (Figure 4.3d) for the crest showed that the B horizon had a higher  $K_{\text{sat}}$  than the underlying unspecified horizon (with signs of wetness). Since  $K_{\text{sat}}$  was lower at the unspecified horizon this implied restricted flow on that horizon hence, interflow in the overlying A and B horizons was anticipated.

The midslope catena element showed the lowest  $K_{\text{unsat}}$  (0.02 mm/hr at  $\phi = 5$  mm) compared to other catena elements. The 2<sup>nd</sup> replicate for the midslope showed values more or less similar to those for the crest element. This large variation in  $K_{\text{unsat}}$  at the midslope was likely to be evidence of soil heterogeneity in the form of macro-porosity and soil pipes. Meanwhile,  $K_{\text{sat}}$  in the subsurface on this catena element was low especially at the C horizon (2.5 mm/hr). This meant that flow was generally restricted in this region. This 2<sup>nd</sup> order midslope comprised a duplex Sterkspruit soil form (Table 4.2) where clays particles are washed downslope through colluviation from the crest and accumulate at the midslope. Thus when water is moving from the crest downslope, a seepage line develops between the crest and midslope, due to textural discontinuities when the water infiltrates and get to the clay layer. Interflow and/or overland flow was anticipated on this soil form, since the prismatic B horizon (clay variant) limits water movement. This means during rainfall events there is interflow at the A/B interface and/or infiltration excess flow (shallow responsive) at the soil surface, depending on rainfall amount. Since lateral contributions are expected from the crest, this implies potential hydrological connectivity through to the riparian zone.

The riparian catena element at the 2<sup>nd</sup> order was classified as a Cartref soil form (Table 4.2); interflow at the AE/B interface was therefore, anticipated. Since the  $K_{\text{unsat}}$  was lower than that at the crest element (6 mm/hr at  $\phi = 5$  mm), flow was expected to be slow. Subsurface connectivity through lateral flow on this 2<sup>nd</sup> order hillslope was expected but could be highly temporal and intensity-driven.

Table 4.2 Soil classification per catena element on granite 2<sup>nd</sup> order hillslope

Catena Element	Taxonomical class	Diagnostic Horizons	Depth of horizons (mm)	Hydropedological soil type
SGR2_Crest	Pinedene	Orthic A	0-200	Interflow
		Yellow Brown Apedal B	200-400	
		Unspecified with signs of wetness	400+	
SGR2_Mid	Sterkspruit	Orthic A	0-200	Responsive
		prismacutanic B	200-400	
		-		
SGR2_Rip	Cartref	Orthic A	0-50	Interflow
		E	50-200	
		Lithocutanic B	200+	

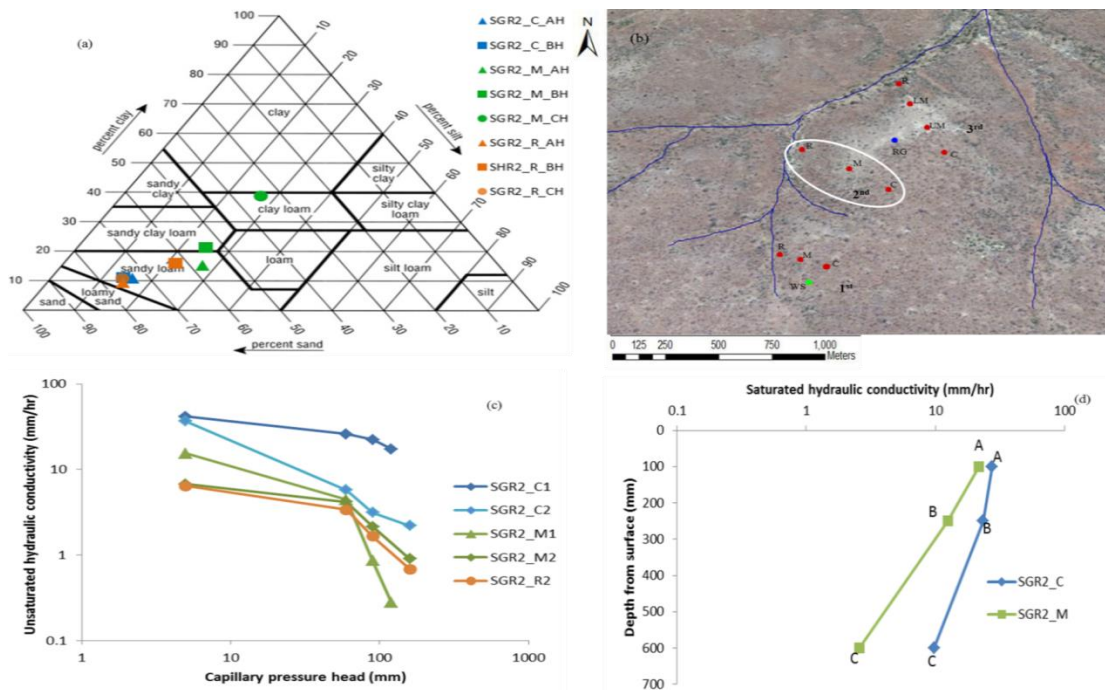


Figure 4.3 (a) Soil texture triangle (b) site map (c)  $K_{unsat}$  at soil surface (d)  $K_{sat}$  per soil horizon on granite 2<sup>nd</sup> order hillslope

### 4.1.3 3<sup>rd</sup> order hillslope

The 3<sup>rd</sup> order crest catena element (Figure 4.4c), showed high  $K_{\text{unsat}}$  on the surface (26 mm/hr and 76 mm/hr at  $\phi = 5$  mm). Values were expected to be low due to the clay loams close to the surface at this location (Figure 4.4a)  $K_{\text{sat}}$  on the A horizon was also expected to be lower (clay loams), then high in the B horizon where there are sandy loams. Nevertheless, interflow was expected on this catena element since  $K_{\text{sat}}$  in the A horizon was higher than the underlying horizons which was also expected for a Pinedene soil form characteristic of this catena element. This suggested potential subsurface lateral connectivity with the downslope elements.

The 3<sup>rd</sup> order midslope (Figure 4.4c) showed low  $K_{\text{unsat}}$  especially at low pressure heads (0.14 mm/hr - 1.7 mm/hr at  $\phi = 5$  mm). This was also the case with the  $K_{\text{sat}}$  data (Figure 4.4d) where it had the lowest conductivity on the whole hillslope (0.7 mm/hr - 0.9 mm/hr), attributed to the clay loams (Figure 4.4a). Since there was not much variation in the very low  $K_{\text{sat}}$  values this would be a potential responsive soil. Similar to the 2<sup>nd</sup> order, a seepage line was also anticipated to develop between the crest and midslope due to textural discontinuities.

The riparian catena element soils showed intermediate  $K_{\text{unsat}}$  and  $K_{\text{sat}}$  compared to the crest and midslope catena element soils (Figure 4.4c and 4.4d, respectively).  $K_{\text{sat}}$  data for this element was showing a decrease with depth. This means rate of water movement was high in the A horizon but gradually decreasing with an increase in depth augmenting the hydrogeological classification (Table 4.3) of slow potential recharge (Figure 4.4a).

Similar to the 2<sup>nd</sup> order hillslope, hydrological connectivity between catena elements on this hillslope could be highly temporal and intensity-driven. Since there was a potential recharge soil at the riparian zone, this hillslope was expected to be disconnected from the adjacent 3<sup>rd</sup> order stream network.

Table 4.3 Soil classification per catena element on granite 3<sup>rd</sup> order hillslope

Catena element	Taxonomical class	Diagnostic Horizons	Depth of horizons	Hydropedological soil type
SGR3_Crest	Pinedene	Orthic A	0-250	Interflow
		Yellow Brown Apedal B	250-500	
		Unspecified with signs of wetness	500+	
SGR3_Mid	Sterkspruit	Orthic A	0-100	Responsive(shallow)
		prismacutanic B	100-400	
		-		
SGR3_Rip	Bonheim	Melanic A	0-300	Slow Recharge
		Pedocutanic B	300-500	
		Unspecified	500+	

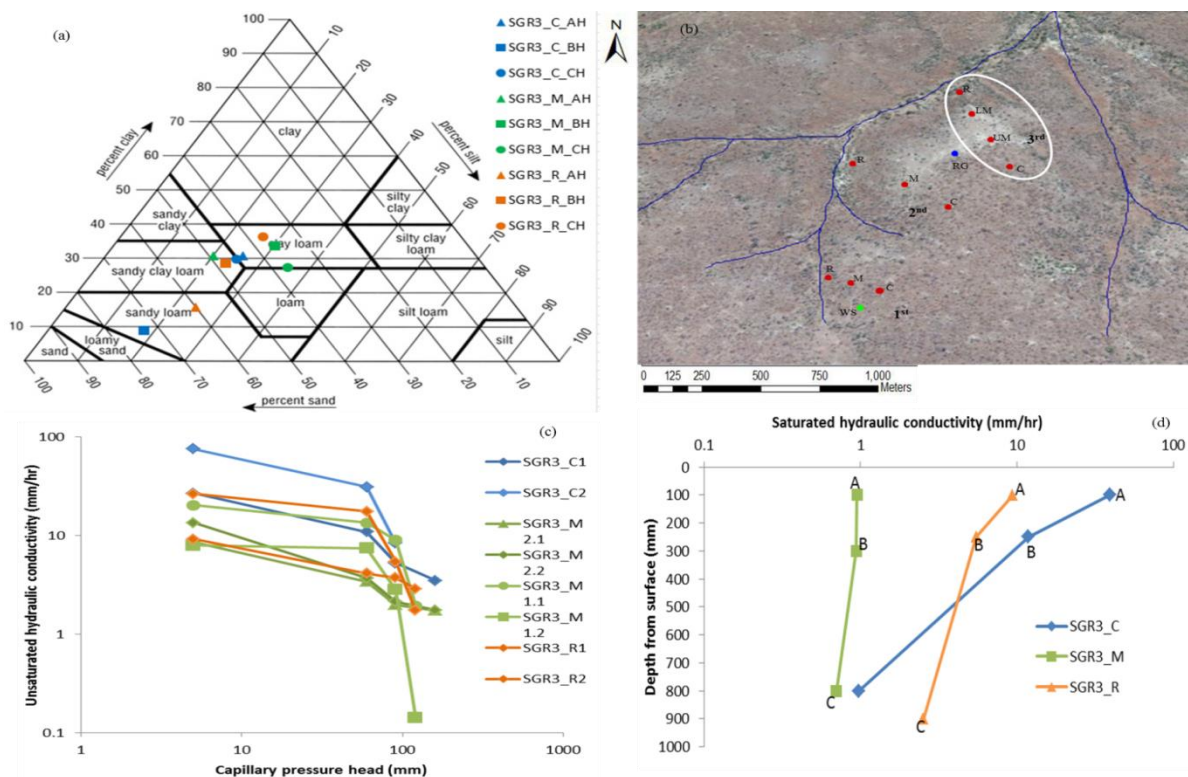


Figure 4.4 (a) Soil texture triangle (b) site map (c)  $K_{unsat}$  at soil surface (d)  $K_{sat}$  per soil horizon on granite 3<sup>rd</sup> order hillslope

## 4.2 Subsurface Soil Moisture Dynamics on Southern Granite Supersite

From the graphs presented in this section, the blue, red and green lines represent the shallow, intermediate and deepest soils, respectively. From the data presented, the higher the matric potential ( $>1\ 000\ \text{mm}$ ), the drier the soil and vice versa. The figures also display the ranked percentage exceedence curves (%ED) derived from the soil moisture data (Watermarks<sup>TM</sup>). This allows the determination of the proportional amount of time each profile maintains a certain level of saturation, in this case during the wetter part of the hydrological season (September 2012 – April 2013). This was crucial for determination of sites that are relatively drier or wetter than others. It also helped in delineation of regions that are relatively wet in a single profile.

### 4.2.1 1<sup>st</sup> order hillslope

The 1<sup>st</sup> order crest profile responded to all the rainfall events (Figure 4.5). Responses in all horizons show a more or less similar trend throughout the season showing fewer differences in wetting and drying cycles. The profile was below DUL ( $<1\ 000\ \text{mm}$ ) as a result of most of the rainfall events, although the % ED data showed that these soils were dry ( $>1\ 000\ \text{mm}$ ) for more than 60% of the time. Important to note is that there was no sensor in the C horizon. These quick responses shown at this catena element implied vertical subsurface flow but hydrogeology and  $K_{\text{sat}}$  data show some flow restriction in the C horizon, therefore, interflow was anticipated.

The midslope profile responded to the first rains (September 2012). The deep soil layers (depth= 450 mm) and the shallow soils (100 mm) showed a quicker drying cycle. The intermediate layer (depth= 300 mm) dried out last for most of the events and this was due to the presence of fine textured soils (Figure 4.2a). The shallow soils dried out for the greater part of November and March probably due to a high evaporative demand from the soil surface during those periods whilst the other soil layers retained some moisture. % ED shows that for about 50% of the time, this profile remained relatively below DUL (at  $<1\ 000\ \text{mm}$ ). From field observations, whilst these data are suggesting moisture storage for approximately 50% of the time on the crest and midslope, the absence of ponded conditions suggested subsurface flow. These responses therefore, showed that it was quick interflow and this supported the hydrogeological classification (Table 4.1) for this hillslope.

The riparian catena element on this first order hillslope showed a response to the early rains from the shallow and intermediate soils (rapid wetting cycle) whilst the deeper soil layers in the C horizon (depth=1 000 mm) showed a lag of two months then finally responded at the beginning of December season. This was due to either soils having low hydraulic conductivity deep in the profile, which is evident on Figure (4.2d) and/or the water being lost to ET before it could percolate deep into the profile. Overall, the riparian catena element retained moisture (<1 000 mm) for about 40% of the entire season mostly in the shallow and intermediate layers whilst the deep layers were relatively dry (>1 000 mm) for the greater part of the season. This therefore, showed that the upper horizons are wet areas compared to the deep soil layers.

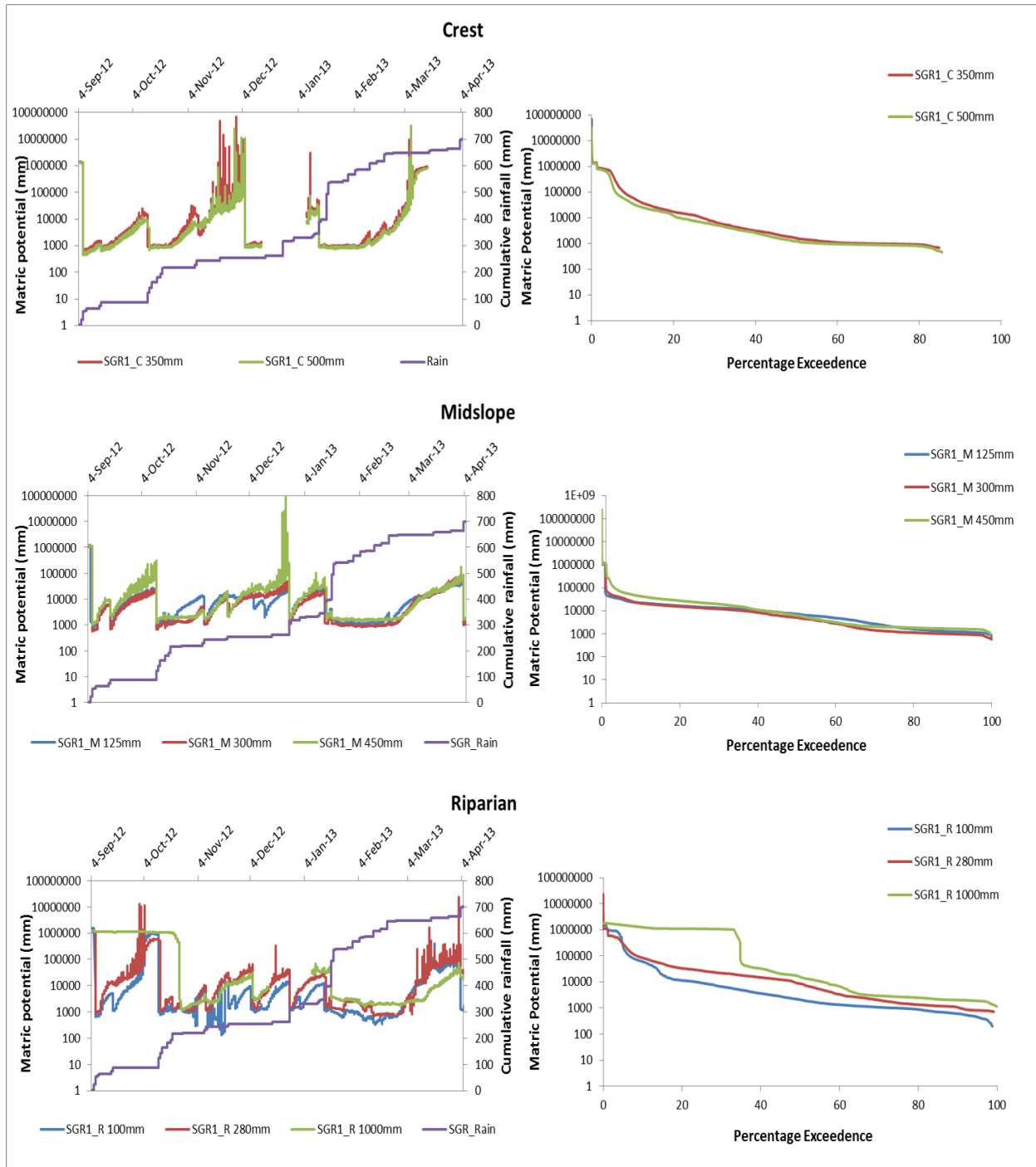


Figure 4.5 Soil moisture responses and Percentage exceedence curves for granite 1<sup>st</sup> order hillslope

#### 4.2.2 2<sup>nd</sup> order hillslope

The 2<sup>nd</sup> order hillslope (Figure 4.6), between September 2012 and April 2013 showed that the shallow soils (depth=100 mm on A horizon) had quicker drying cycles compared to the B-horizon soils (depth= 250 mm on B horizon). They both seemed to follow a similar wetting and drying pattern only that the intermediate soils showed a slight lag when drying. Since this was a Pinedene soil form, interflow was still anticipated between the B horizon and the unspecified (with signs of wetness) region. Although this crest had quick wetting and drying cycles, %ED showed that this was generally a dry area showing high potentials (>1 000 mm) for the greater part of the season.

The midslope showed a quick full profile response to the first rainfall events with soils getting below DUL (<1 000 mm). Whilst the shallow and intermediate soils dried out, the deeper soil retained moisture for the greater part of the wet season (Taking note that the first two sensors are in the diagnostic orthic A-horizon of the duplex Sterkspruit form). The B horizon was a prismaeutanic horizon (clay variant); it was therefore, characterized by soils with low hydraulic conductivity (Figure 4.3d). The clay particles in that horizon helped to retain moisture, hence the low potentials. Potential movement of water on this catena element was interflow (A/B interface) but infiltration excess flow was anticipated during high intensity rainfall events (i.e some of the October 2012 and January 2013 events). This was generally a dry region (>1 000 mm) as illustrated by the %ED data which showed the intermediate and deeper soils getting below DUL (<1 000 mm) only about 35-40% of the time.

The riparian zone soils also showed a full profile response to the first rains (sensors only in A and B horizon). The intermediate sensor (depth=250 mm) was faulty at some point so the data was not consistent but nevertheless it showed that the soils were responding to some but not all of the events. The intermediate soil layers showed a slow drying cycle compared to the overlying soils. Since there was a Catrtref soil form at this element (Table 4.2), the E horizon was an indication of a potential perched water table therefore, some flow restriction in the underlying lithocutanic B horizon, hence the low potential on the intermediate soils for a considerable amount of time (Figure 4.6). %ED data shows that this was a relatively dry area (values > 1 000

mm) suggesting temporal or no connectivity with upslope catena elements through lateral or overland flow. Due to the impeding layer (B horizon), infiltration excess was anticipated during high intensity rainfall events.

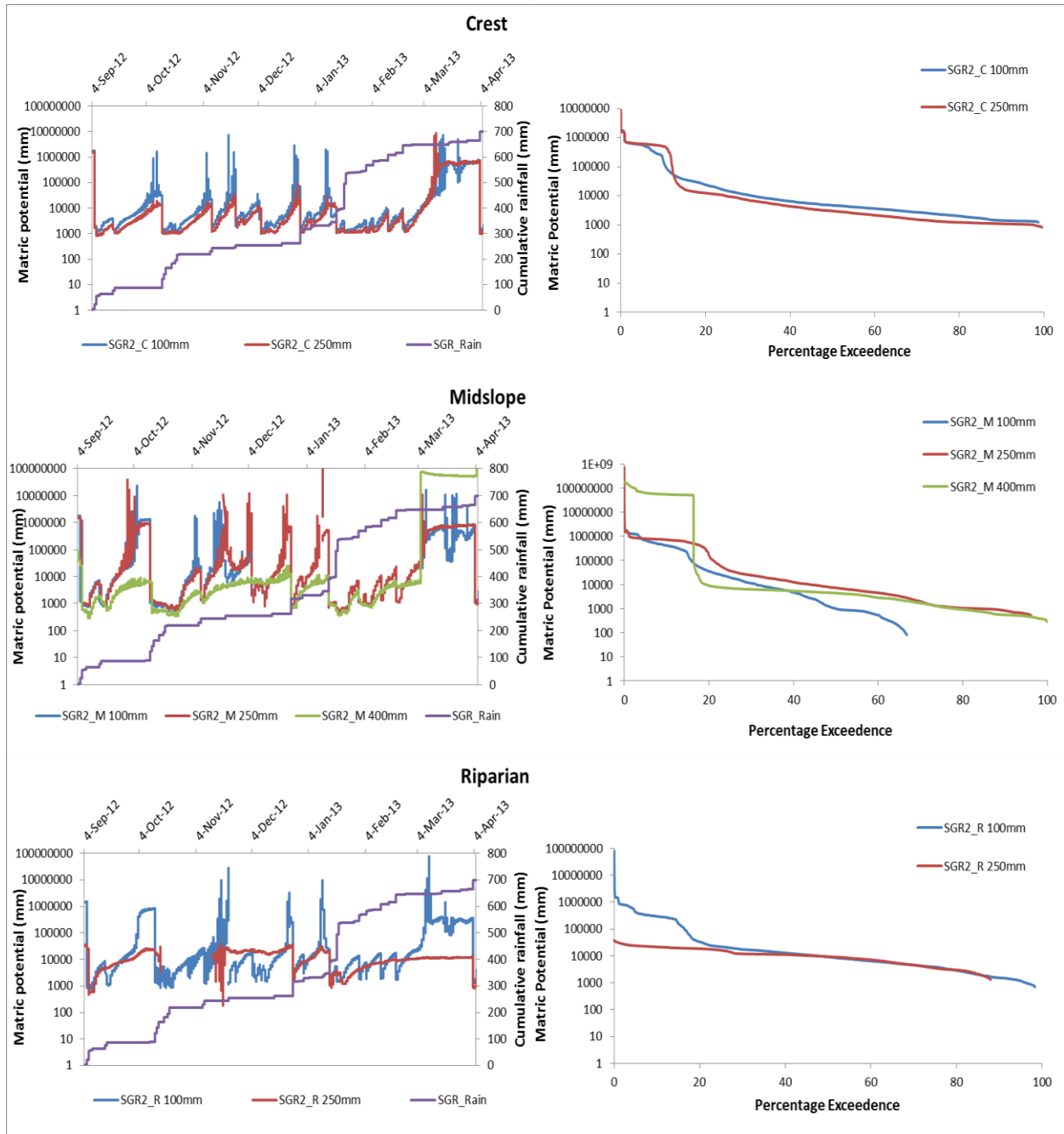


Figure 4.6 Soil moisture responses and percentage exceedence curves for granite 2<sup>nd</sup> order hillslope

### 4.2.3 3<sup>rd</sup> order hillslope

The 3<sup>rd</sup> order crest (Figure 4.7) showed low potentials for both shallow and intermediate soils but showed quick wetting-drying cycles for most of the rainfall events similar to crest soils in the lower orders (the deepest sensor at 350 mm was faulty therefore, data was omitted). The shallow and intermediate soils got below DUL for most of the events (<1 000 mm). Water was retained ~40% of the time which was a contribution mainly from the large January-February rains. Depending on the amount and intensity of rainfall received, contributions to the lower slopes were anticipated since these are interflow soils due to flow restriction in the unspecified region of the Pinedene soil form.

The 3<sup>rd</sup> order upper midslope (Figure 4.7) showed relatively low potentials for the shallow soils and intermediate soils whilst the deeper layers (depth=>300 mm) showed a lag of more than one month before they responded to rainfall events. They only get below DUL in response to the January event and at the beginning of March but for more than 90% of the time, they remained relatively dry (> 1 000 mm). Important to note is that even after the exceptional event in January 2013 a piezometer at this location remained dry. This suggested absence or limited subsurface flow therefore, infiltration excess (shallow responsive) was anticipated during exceptional events and this is typical of duplex soils characteristic of this catena element. Importantly, this catena element showed a reasonably prolonged saturation of shallow and intermediate soils (~50%). Hydrologically, this catena element was disconnected from the downslope elements and connectivity was expected to be temporal following high intensity rainfall events (e.g. some of the October 2012 and January 2013 events) through infiltration excess flow.

The lower midslope (Figure 4.7) showed a full profile response to the early rains (September 2012). The shallow soils had a quick drying cycle compared to soils in the underlying horizons. Similar to the upper midslope, due to the presence of duplex soils, water retention was expected to be high in the underlying horizons where there were finer soil particles. On this catena element is how the intermediate soils (depth=300 mm) retained moisture for the greater part of the season whilst the deep and shallow soils dried out. A possible interpretation is that the soils

are in a region less affected by both evaporation from the soil surface and transpiration from the deep root zone. Since the upper midslope catena element was showing a disconnection with this lower midslope, this meant water retained on this site was probably due to direct infiltration or to a lesser extent, contributions through overland flow from upslope catena elements after high intensity events.

The riparian zone (Figure 4.7) showed full profile responses to most rainfall events for the greater part of the season. The responses showed more or less similar wetting and drying cycles. The rapid drying cycles were an indication of high evapotranspiration and/or free drainage. %ED data was similar for the full profile implying a well-drained profile but a relatively dry one (>1 000 mm) for more than 90% of the time. This catena element may be connected to the lower midslope element but these data suggests a disconnection from the adjacent 3<sup>rd</sup> order stream network. This augmented the hydrogeological classification for this profile which suggested recharge (potential).

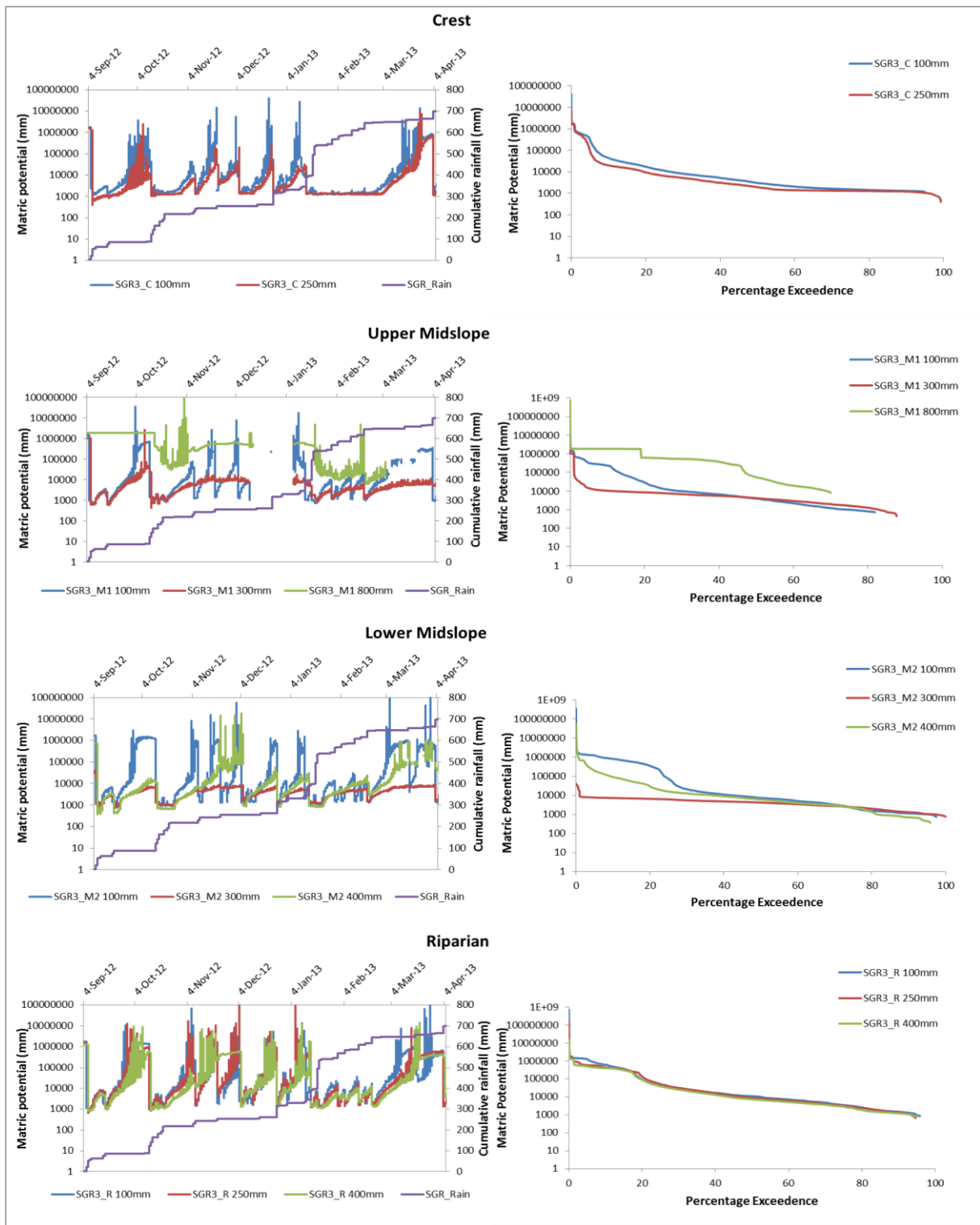


Figure 4.7 Soil moisture responses and percentage exceedence curves for granite 3<sup>rd</sup> order hillslope

### 4.3 Soil Water Potential (Lab Results)

Soil samples from the 3<sup>rd</sup> order hillslopes from both sites were collected and their water potential was measured. According Buckingham (1907), water movement in the soil is driven by gradients in soil water potential. From the results obtained (Figure 4.8) soil water is able to move freely in granite soils compared to the basalts where it is held more tightly in the soil hence the smaller potential to move freely especially at low water contents. This therefore, suggests high water retention at the basalts than at the granites considering the high clay percent in basalt derived soils.

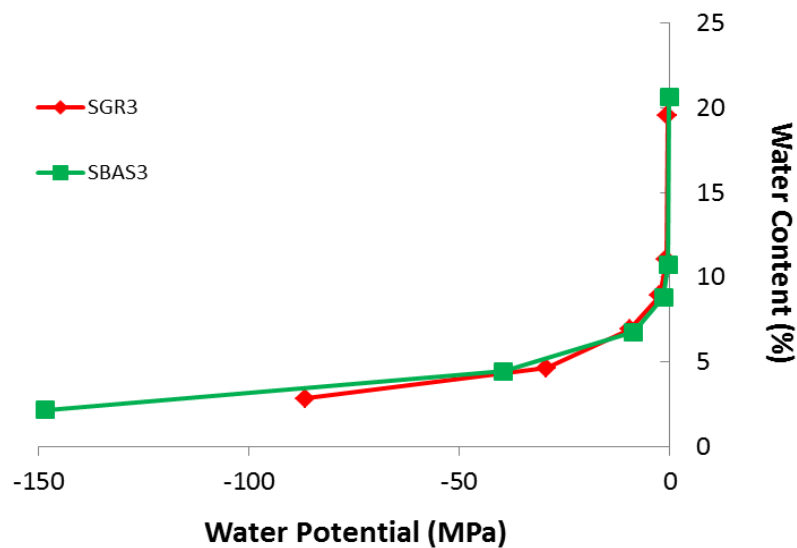


Figure 4.8 A comparison of water potential against water content between the 3<sup>rd</sup> order hillslopes

### 4.4 Results from Geophysical Surveys (ERT) on Granite Supersite

#### 4.4.1 1<sup>st</sup> order hillslope ERT

The pseudosections presented show results from the time series analysis conducted during the 2013 wet season. The 2011 dry season surveys (Riddell *et al.*, 2011) are presented for comparison purposes. The 1<sup>st</sup> order hillslope (Figure 4.9) shows very high resistivity values

(Figure 4.9a  $\Omega \sim 641$ ) at the crest implying the presence of a shallow rock between the crest and the midslope, thereby resulting in shallow soils on the crest. On the 2011 pseudosection (at 64m) shows some low values possibly moisture and or lower porosity material (4.9b). On the 2013 January (4.9c) and March (4.9d) results suggest water percolating to deeper horizons after some high intensity rainfall events in January 2013. In March 2013, it shows that this water had percolated all the way down into the profile implying slow matrix flow in this region (comparison of Figure 4.9c and d), due to reduction in resistivity. This interpretation was also supported by the soil moisture data which shows the deeper soils in the horizon retaining some moisture for longer periods during the same period (Figure 4.5) at the riparian zone.

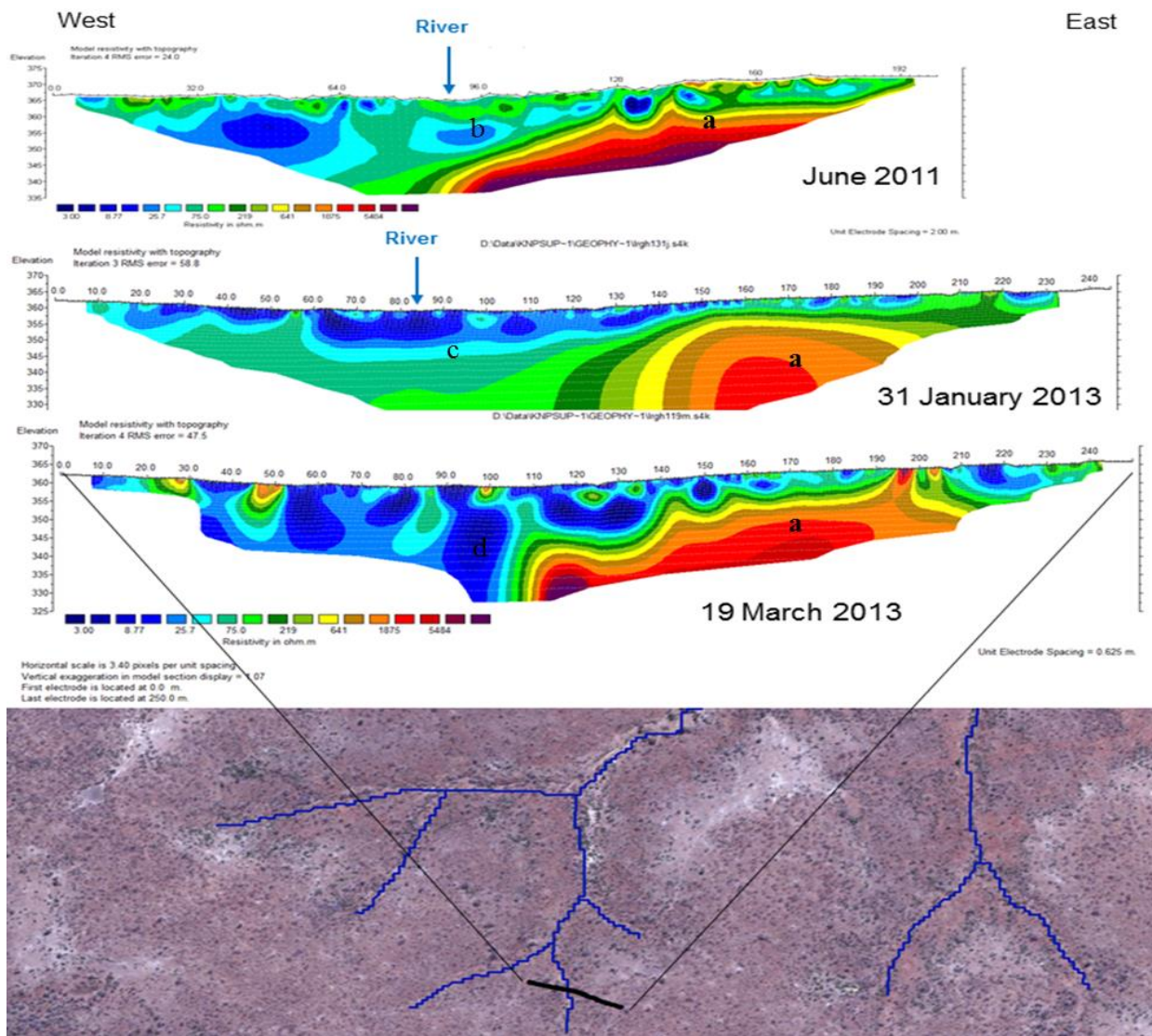


Figure 4.9 Time series ERT for granite 1<sup>st</sup> order hillslope

#### 4.4.2 2<sup>nd</sup> order hillslope ERT

The 2<sup>nd</sup> order hillslope (Figure 4.10) showed possible geological controls ( $\Omega \sim 1800$ ) on both the crest and the valley bottom extending to the stream bed (Figure 4.10e and f). It also showed that the low resistivity values were not extending deeper into the profile so the water here was probably flowing laterally and or as surface runoff.

A comparison of the February and March survey showed no clear evidence of deep percolation or matrix flow into deeper layers therefore, this implied that water on this hillslope was lost through evapotranspiration and limited drainage out of the system as free drainage.

From the hydrogeological classification, this hillslope's hydrological processes are mainly controlled by the underlying rock shown below (Figure 4.10f). Lateral flow (whole catena) and infiltration excess (midslope and riparian) was therefore, anticipated and the development of seep lines (at 200 m and at 340 m) due to textural discontinuities.

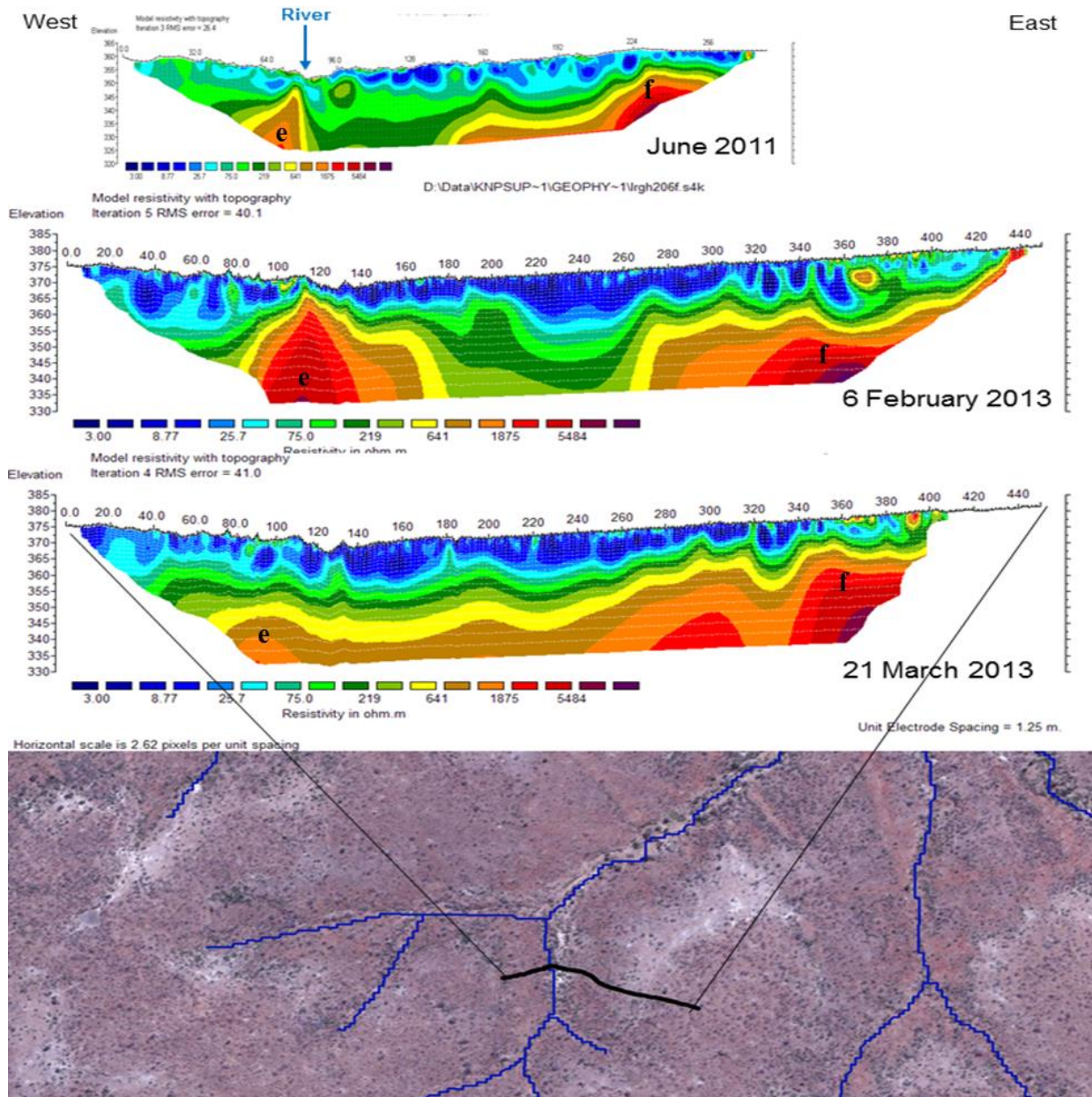


Figure 4.10 Time series ERT for granite 2<sup>nd</sup> order hillslope

#### 4.4.3 3<sup>rd</sup> order hillslope ERT

The 3<sup>rd</sup> order hillslope had high resistivity values ( $\Omega \sim 5400$ ) at the crest (Figure 4.11h). This high resistant material implied shallow rock and hence shallow soils with low storage. At the midslope (Figure 4.11g) on all the pseudosections it showed low resistivity values ( $\Omega < 641$ ) which might be the presence of fine textured material on the midslope and/or moisture. The

February results showed a wet profile compared to the March results implying no matrix flow or deep percolation but rather water lost either to evaporation and/or transpiration.

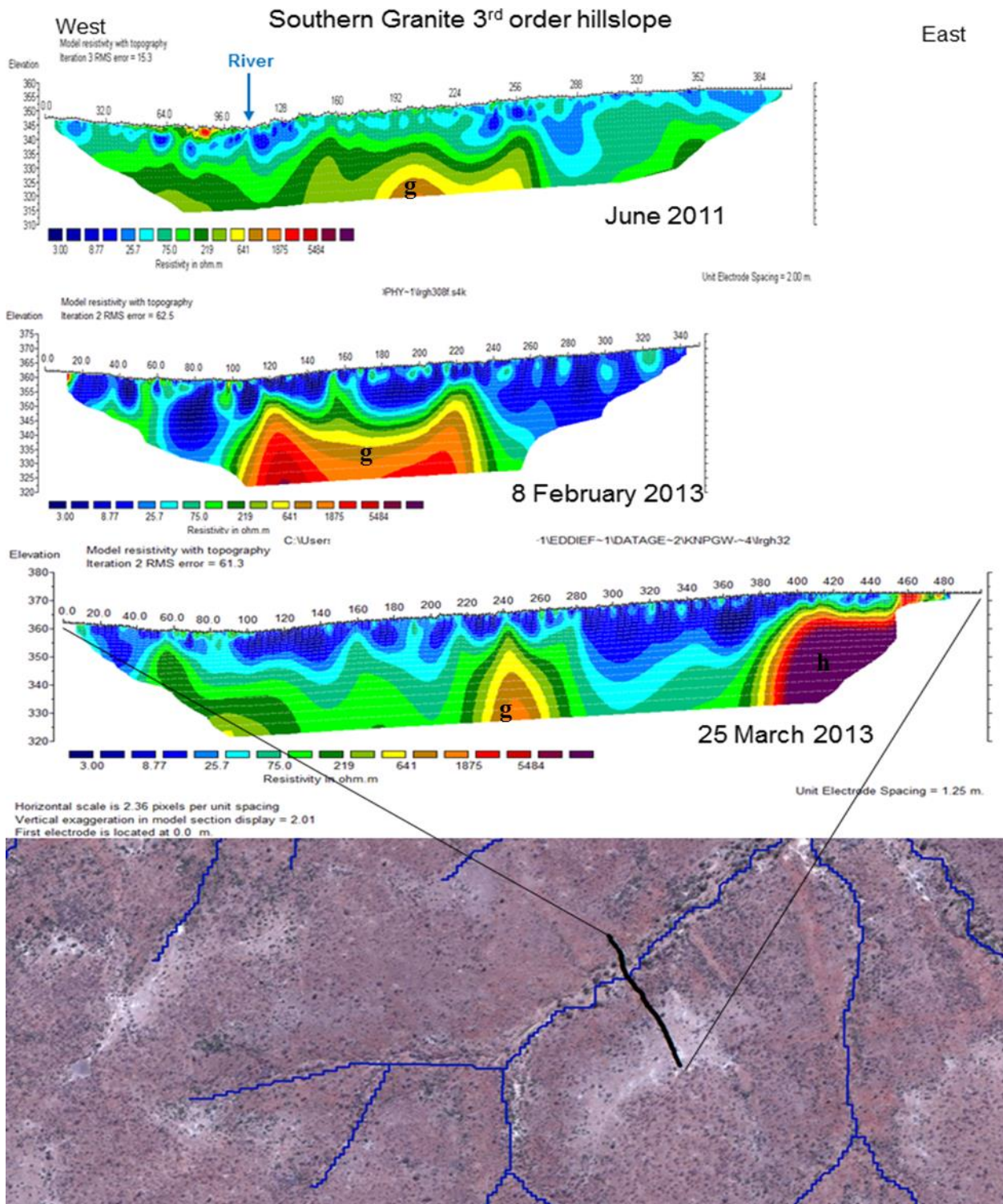


Figure 4.11 Time series ERT for granite 3<sup>rd</sup> order hillslope

#### 4.5 Hydropedological Hillslope Interpretations on Southern Granite Supersite

Conceptual models of hillslope processes were developed to show soil moisture distribution patterns and water flow paths on the hillslope based on the hydrological soil types (Figure 4.12) of the three catena elements on each hillslope. This conceptualization, utilizing van Tol *et al.* (2013) hillslope classification helped to improve the understanding of flow mechanisms on these hillslopes.

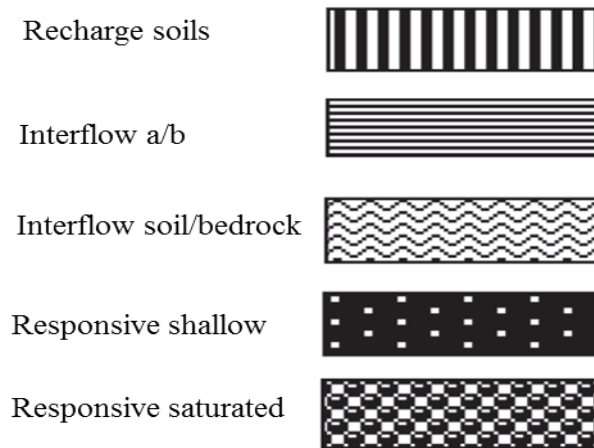


Figure 4.12 Hydrological soil types (after van Tol *et al.*, 2013)

##### 4.5.1 1<sup>st</sup> order hillslope conceptual model

*Hillslope Class 6: Quick Interflow*

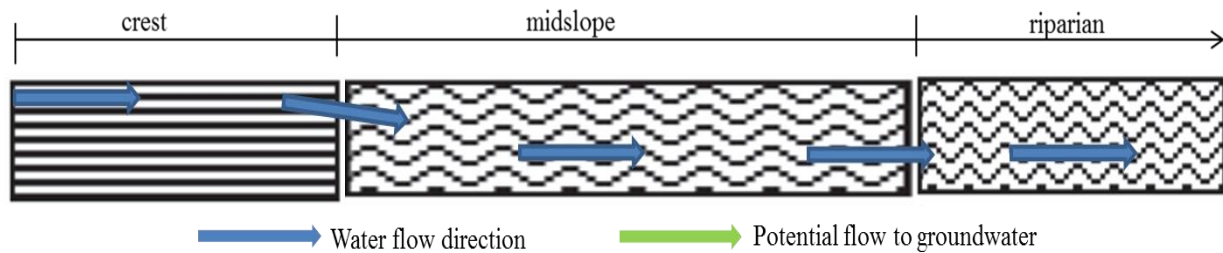


Figure 4.13 Hydrological soil types and conceptual flow paths for granite 1<sup>st</sup> order hillslope

This hillslope was characterized by quick interflow soils (Figure 4.13). The majority of soils on the catena elements that make up this hillslope showed indications of lateral flow at the A/B interface i.e. at the crest, the absence of ponding water suggested infiltration of water into the subsurface but flow was restricted in the lithocutanic B horizon underlain by an E horizon (Table

4.1) therefore, resulting in interflow at the A/B interface. As this water moved downslope into the midslope, it continued to flow laterally but as deep interflow. Judging from field observations, the riparian zone soils sometimes become responsive due to infiltration excess from direct precipitation but only after exceptional events. According the van Tol *et al* (2013), the rate of lateral flow mainly depends on the gradient of the slope and this means therefore; this 1<sup>st</sup> order hillslope had quick interflow compared to the 2<sup>nd</sup> and 3<sup>rd</sup> order hillslopes since it had a steeper slope than the higher orders. There was a high probability of lateral subsurface connectivity with the adjacent stream network but less hillslope storage was expected due to the quick interflow.

#### **4.5.2 2<sup>nd</sup> order hillslope conceptual model**

##### *Hillslope Class 2: Shallow responsive*

Perceptual flow paths of the 2<sup>nd</sup> order hillslope are represented on Figure (4.14). There was deep interflow at the crest and a seepage line between the crest and the midslope due to textural discontinuities (Pinedene soil form at the crest and Sterkspruit form characterized by duplex soils at the midslope). Some of the water continued to flow laterally into the midslope. The prismatic B horizon (clay variant) at this catena element impeded the vertical subsurface flow of water, thereby resulting in overland flow and some possibility of lateral flow. According van Tol *et al.* (2013), in drier climates characteristic of savannas, gypsum, lime and salt precipitates maybe washed downslope and the impermeable underlying rock in the riparian zone promotes limited contributions to the stream because of ET. Contributions to the stream may have been from infiltration excess only after high intensity and or exceptional events. In terms of storage, this hillslope was expected to have limited storage due to the presence of impeding layers and low conducting material mostly in the B horizons of the catena elements; hence water could be lost through ET and/or overland flow.

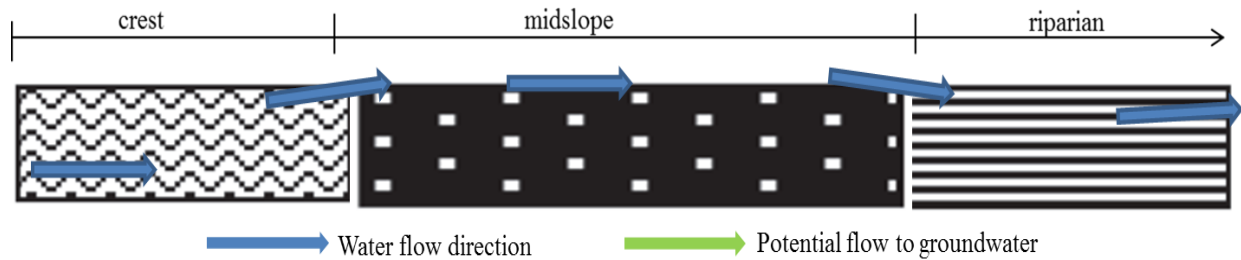


Figure 4.14 Hydrological soil types and flow paths for granite 2<sup>nd</sup> order hillslope

### 4.5.3 3<sup>rd</sup> order hillslope conceptual model

#### *Hillslope Class 2: Shallow Responsive*

The 3<sup>rd</sup> order hillslope (Figure 4.15) was dominated by shallow responsive soils. This hillslope had a large highly developed grassy midslope that comprises a duplex Sterkspruit soil form on both the upper and the lower midslope. This therefore, implied responsive soils at this catena element. Meanwhile, lateral contributions from the crest resulted in the development of a seep line due to discontinuities in soil texture between the crest and the midslope. On the other hand, the riparian zone had a potential recharge soil therefore, whilst there might have been temporal connectivity through overland flow, the free draining soils at this element disconnected this hillslope from the adjacent 3<sup>rd</sup> order stream network. In terms of storage, this hillslope was expected to also have less storage because the crest and midslope had shallow soils due to underlying shallow rocks. The riparian zone had deep soils, hence more storage was anticipated but due to its free draining natural water loss was anticipated through ET and free drainage.

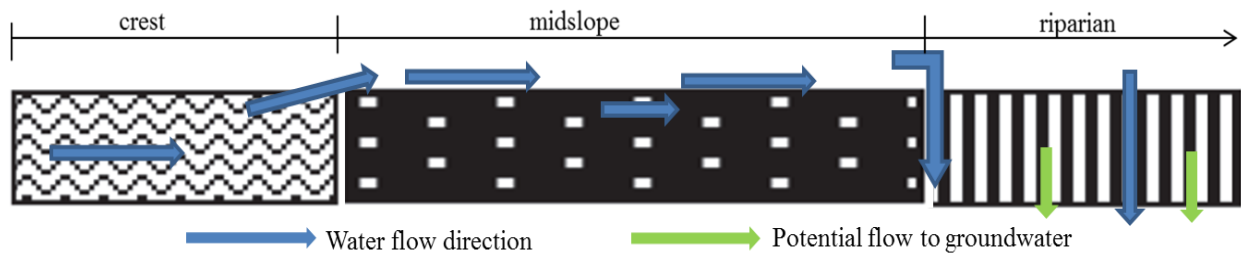


Figure 4.15 Hydrological soil types and flow paths for granite 3<sup>rd</sup> order hillslope

## 4.6 Southern Basalt Characterization Results

Characterization at the southern basalt supersite was conducted through  $K_{\text{unsat}}$  measurements and soil classification.  $K_{\text{unsat}}$  was measured at the surface at each catena element close to the soil water monitoring stations. Due to time and logistical constraints,  $K_{\text{sat}}$  measurements and time series geophysical surveys were not conducted.

### 4.6.1 1<sup>st</sup> order hillslope

High  $K_{\text{unsat}}$  (12 mm at  $\phi = 5$  mm) was shown at the crest on this 1<sup>st</sup> order hillslope (Figure 4.16). Values decreased moving downslope with the riparian zone having the least (0.4 mm at  $\phi = 5$  mm). This was attributed to the presence of more clay particles on the riparian catena element that had been gradually washed downslope over the years possibly through wind or water and possibility with some contributions from river alluvium. The whole hillslope was characterized by Shortlands soil form (Table 4.4) and the red structured B horizon characteristic of this soil form was a potential recharge soil (le Roux *et al.*, 2013). This therefore, suggested the possibility of an absence of lateral flows on the entire hillslope implying a hydrological disconnection between catena elements and also between the entire hillslope and the adjacent stream network.

Table 4.4 Soil classification per catena element on basalt 1<sup>st</sup> order hillslope

Catena Element	Taxonomical soil class	Diagnostic Horizons	Depth of horizons	Hydropedological soil type
SBAS1_Crest	Shortlands	Orthic A	0-200	Recharge
		Red Structured B	200-600	
		-		
SBAS1_Mid	Shortlands	Orthic A	0-200	Recharge
		Red Structured B	200-700	
		-		
SBAS1-Rip	Shortlands	Orthic A	0-200	Recharge
		Red Structured B	200-700	
		-		

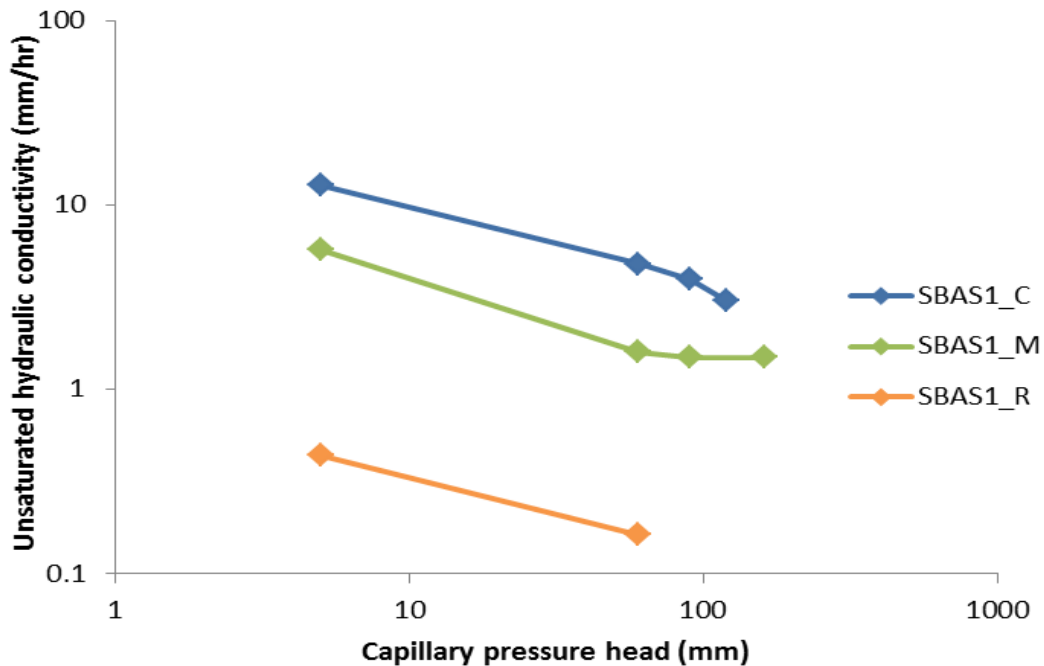


Figure 4.16 Unsaturated hydraulic conductivity of the A-horizon on 1<sup>st</sup> order hillslope

#### 4.6.2 2<sup>nd</sup> order hillslope

Measured  $K_{unsat}$  on the 2<sup>nd</sup> order hillslope (Figure 4.17) showed the riparian zone to have the highest conductivity at lower capillary pressure head and vice versa (37 mm/hr at  $\phi = 5$  mm). This suggested high clay content since clay soils sometimes tend to have high  $K_{unsat}$  at low pressure heads (Artiola *et al.*, 2004). This also depends on the bulk density of the soil. The crest showed low  $K_{unsat}$  at low capillary pressure head compared to the midslope and riparian zones. Hydropedological classification showed variability in the distribution of soils on this hillslope (Table 4.5). Due to the lack of any morphological indication of saturation within the diagnostic horizons throughout soil profiles, all the catena elements at this hillslope were classified as potential recharge soils implying no hydrological connectivity between elements and also suggesting a hydrological disconnection from the stream network.

Table 4.5 Soil classification per catena element on basalt 2<sup>nd</sup> order hillslope

Catena Element	Taxonomical soil class	Diagnostic Horizons	Depth of horizons	Hydropedological soil type
SBAS2_Crest	Glenrosa	Orthic A	0-200	Recharge
		Lithocutanic	200-400	
		-		
SBAS2_Mid	Mayo	Melanic A	0-250	Recharge
		Lithocutanic	250-300	
SBAS2_Rip	Swartland	Orthic A	0-200	Recharge
		Pedocutanic B	200-420	
		Saprolite	400+	

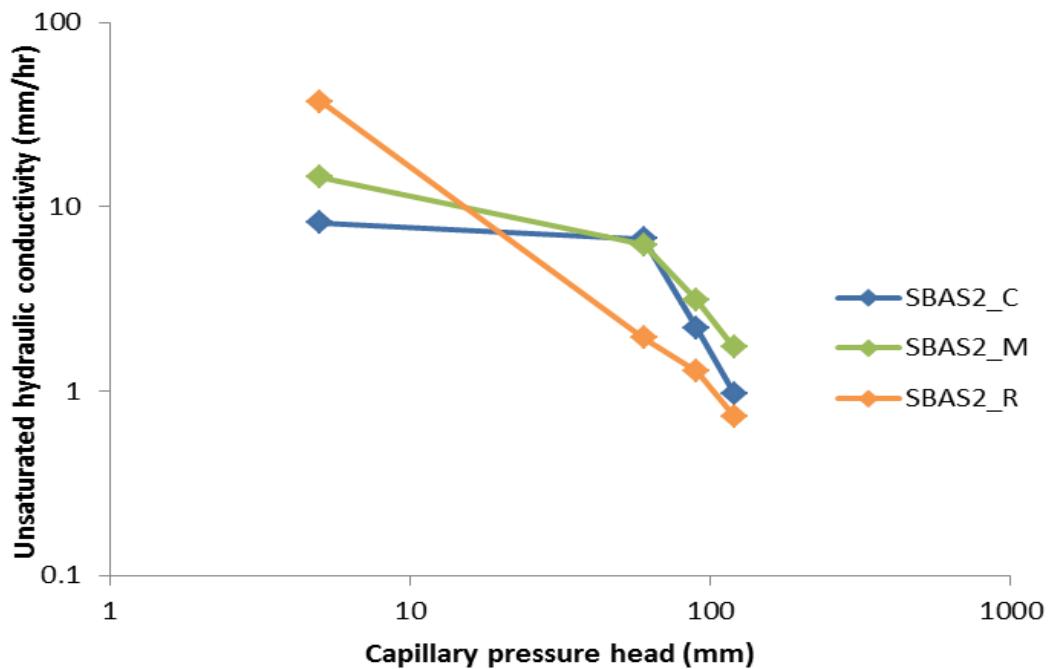


Figure 4.17 Unsaturated hydraulic conductivity of the A-horizon on 2<sup>nd</sup> order hillslope

### 4.6.3 3<sup>rd</sup> order hillslope

Results for the 3<sup>rd</sup> order hillslope (Figure 4.18) showed soils with low  $K_{\text{unsat}}$  at both low and high pressure heads on the crest (0.4 mm/hr – 0.7 mm/hr) whilst on the contrary; the riparian zone showed high conductivity at both low and high pressure heads.  $K_{\text{unsat}}$  was expected to be low at the riparian zone due to clays being washed downslope and/or contributions through river alluvium but due to the low gradient topography on this site, it probably meant there were still more clays at the crest than at the riparian zone. Hydropedological classification on this hillslope showed the Mispah soil forms (Table 4.6) which are typically responsive soils due to shallow soil depth. This hillslope was therefore, anticipated to have limited storage. Similar to the 1<sup>st</sup> and 2<sup>nd</sup> order hillslopes, this 3<sup>rd</sup> order shows no connectivity between catena elements or the adjacent stream.

Table 4.6 oil classification per catena element on basalt 3<sup>rd</sup> order hillslope

Catena Element	Taxonomical soil class	Diagnostic Horizons	Depth of horizons	Hydropedological soil type
SBAS3_Crest	Mispah	Orthic A	0-300	Recharge
		Hard Rock	300+	
		-		
SBAS3_Mid	Mispah	Orthic A	0-250	Recharge
		Hard Rock	250-500	
		-		
SBAS3_Rip	Mispah	Orthic A	0-250	Recharge
		Hard Rock	250-500	
		-		

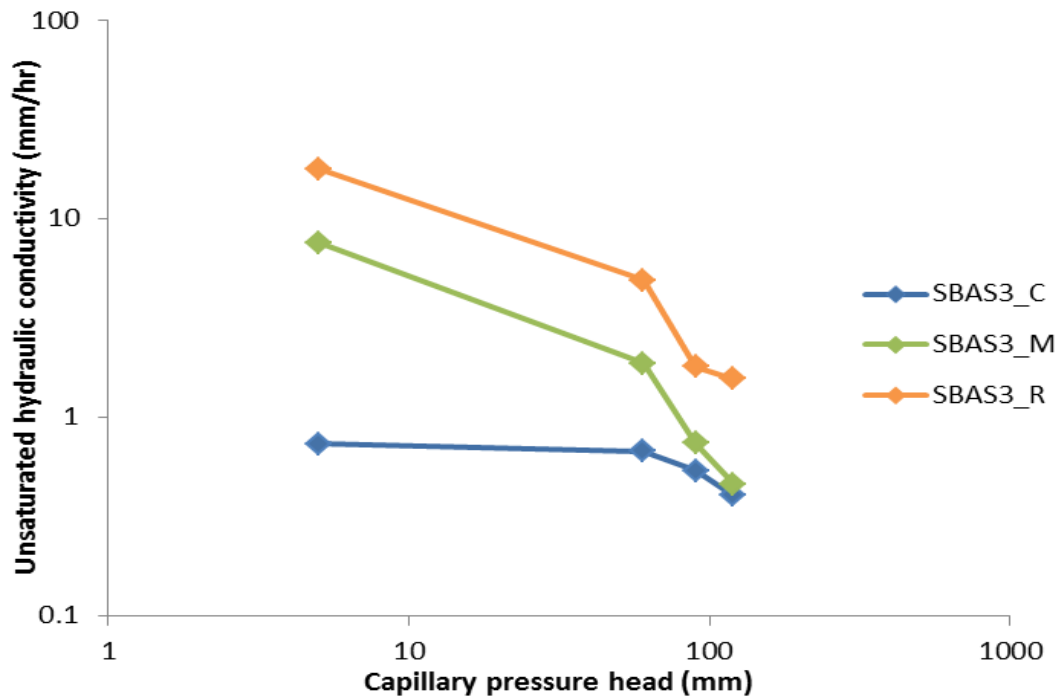


Figure 4.18 Unsaturated hydraulic conductivity of the A-horizon on 3<sup>rd</sup> order hillslope

In conclusion, the basalt hillslopes have all shown an absence of hydrological connectivity between catena elements on each hillslope, as well as between the hillslopes and their adjacent stream networks. Soil depth on these hillslopes decreased with an increase in hillslope orders therefore, the 1<sup>st</sup> order hillslopes had deeper soils, hence more storage was anticipated whilst the 3<sup>rd</sup> order hillslopes have the shallowest depths. There was a possibility of colluvial processes acting in the low order hillslopes compared to the higher orders as shown by low  $K_{unsat}$  at the riparian regions of the low order hillslopes

## 4.7 Subsurface Soil Moisture Dynamics of Catena Elements on the Southern Basalt Supersite

### 4.7.1 1<sup>st</sup> order hillslope

Soil moisture responses on the 1<sup>st</sup> order hillslope (Figure 4.19), showed low soil water matric potential for shallow soils on the crest in response to the first rainfall events (September 2012).

The B-horizon soils showed a lag of about two weeks after the first rains whilst the deeper soil layers had a 6 week lag only to respond mid October which was when some exceptional high intensity rainfall events occurred. The deep soils responded to high intensity events only (i.e some of the October 2012 and January 2013 events). Since these were Shortlands soils, the red structured B horizon was a potential recharge soil implying free draining soils. Since the deeper soils did not respond to most of the events this suggested a high ET demand therefore, moisture was being taken up by plant roots and evaporation from the soil surface before percolating deep into the profile. This catena element was generally a dry area as illustrated by the % ED data which showed that they were dry (>1 000 mm) for more than 80 % of the time.

The midslope also followed a similar pattern to the crest where the shallow soils responded to the first rainfall event and the intermediate soils responded after a two week lag. They did not saturate but remained relatively dry (>1 000 mm) for ~85% of the time. The deeper layers showed no response to the first 18 weeks of the wet season only responded to the high intensity event in mid January 2013 before drying up. This supported the presence of interflow from the hydrogeological classification. This midslope was drier than the crest as illustrated by the %ED curves showing they were dry for almost 90% of the time.

Data for the 1<sup>st</sup> order riparian catena element was omitted because the soil moisture sensors failed.

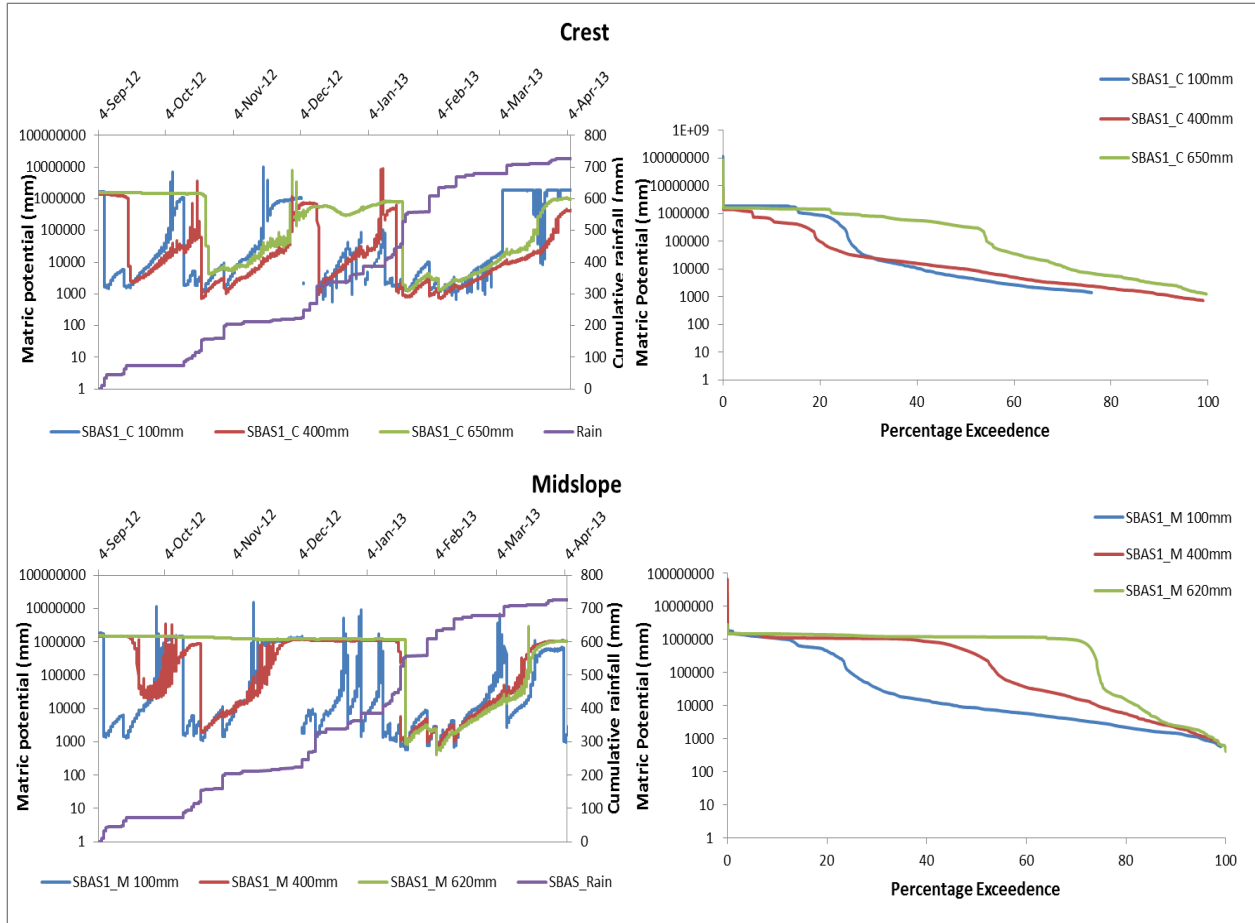


Figure 4.19 Soil moisture responses and percentage exceedence curves for 1<sup>st</sup> order hillslope

#### 4.7.2 2<sup>nd</sup> order hillslope

The data presented for the 2<sup>nd</sup> order hillslope (Figure 4.20) is for the crest and riparian catena elements, no data will be presented for the midslope since sensors were pulled out by wild animals. At the crest, shallow and intermediate soils showed low matric potential in response to the first September rains then the deeper layers responded after a two week lag. Unfortunately the deepest sensor was pulled out just after the January events therefore, only data from September to January is presented for the deep soils at this element. The shallow and intermediate soils showed more or less similar wetting and drying cycles. Soils got below DUL (<1 000 mm) for almost 40% of the time as illustrated by the %ED curves. Soils here were classified as recharge and these data suggest that water does not easily infiltrate to deeper layers due to root water uptake and evaporation from the surface.

The riparian zone showed low potentials for both shallow and intermediate soils in response to the early September rains whilst the deep soils showed a 6 week lag to the rains only to respond to the October high intensity events. The deeper soils only responded to high intensity events ((i.e some of the October 2012 and January 2013 events)) but %ED curves showed that this element was dry for more than 65% of the time. The similar wetting and drying cycles of the shallow soils implied some vertical subsurface flow (potential recharge) augmenting the hydrogeological classification (Table 4.5) but the lag in response by the deep soils suggested water loss through ET therefore, water would not percolate deep into the profile. Since the riparian soils are described as potential recharge, this means they were largely disconnected from the stream network.

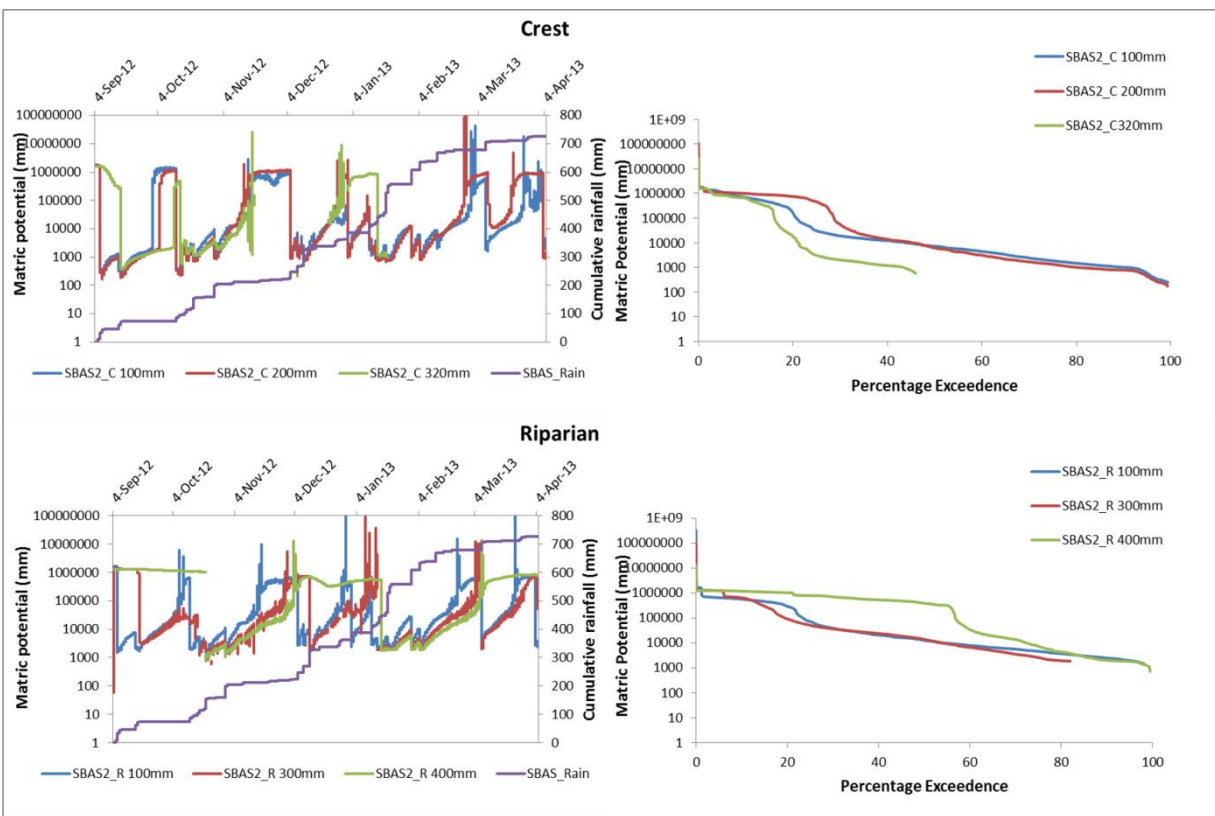


Figure 4.20 Soil moisture responses and percentage exceedence curves for 2<sup>nd</sup> order hillslope

### 4.7.3 3<sup>rd</sup> order hillslope

Sensors on this 3<sup>rd</sup> order hillslope were installed a month later after the onset of rains so data presented here is from October to April. The crest (Figure 4.21), showed quicker responses from the shallow and intermediate soils after the first rains then the deep soil layers (depth=490 mm) responded after a week's lag. The whole profile started drying out and the first two horizons responded to some of the events again (December) but deeper soils remained dry only to respond to the January events. This showed that the deep soil layers were only responding to high intensity events which could be attributed to a high rate of evapotranspiration where water was lost to the atmosphere before it percolated deep into the soil. This catena element was generally a dry area as illustrated by %ED curves showing only the intermediate soils retaining moisture for about 40% of the time whilst the other layers were relatively dry (>1 000 mm). These responses showed free drainage in the shallow and intermediate soils but since deep soils were showing infrequent responses this meant water was lost through ET, thereby implying a disconnection of this element to downslope elements on this hillslope.

Low matric potential was shown for the midslope shallow soils in response to the early rains and intermediate soils responded a few days after then they all showed a similar trend of responses until mid-November, the intermediate sensor then became faulty. Nonetheless, it showed that the soils in this region responded to some of the events but not all compared to the shallow soil responses which were also able to maintain moisture for almost 40% of the time as illustrated by %ED curves. If the shallow soils were able to retain moisture for almost 40% of the time, this means, there was a possibility of water retention in the deep horizons once water percolated from the upper horizon. Low soil water potentials were shown for the full profile at the riparian zone in response to the high intensity October rainfall events. The wetting and drying cycles for this catena element were similar throughout the season except on a few occasions in December and October where shallow soils got very below DUL (<500 mm). This catena element was therefore, able to retain moisture for longer periods (more than 50% of the time) as illustrated by the %ED curves. These responses augmented the  $K_{\text{unsat}}$  data that was presented earlier (Figure 4.18) where the riparian zone was shown to have high conductivity than the other catena elements.

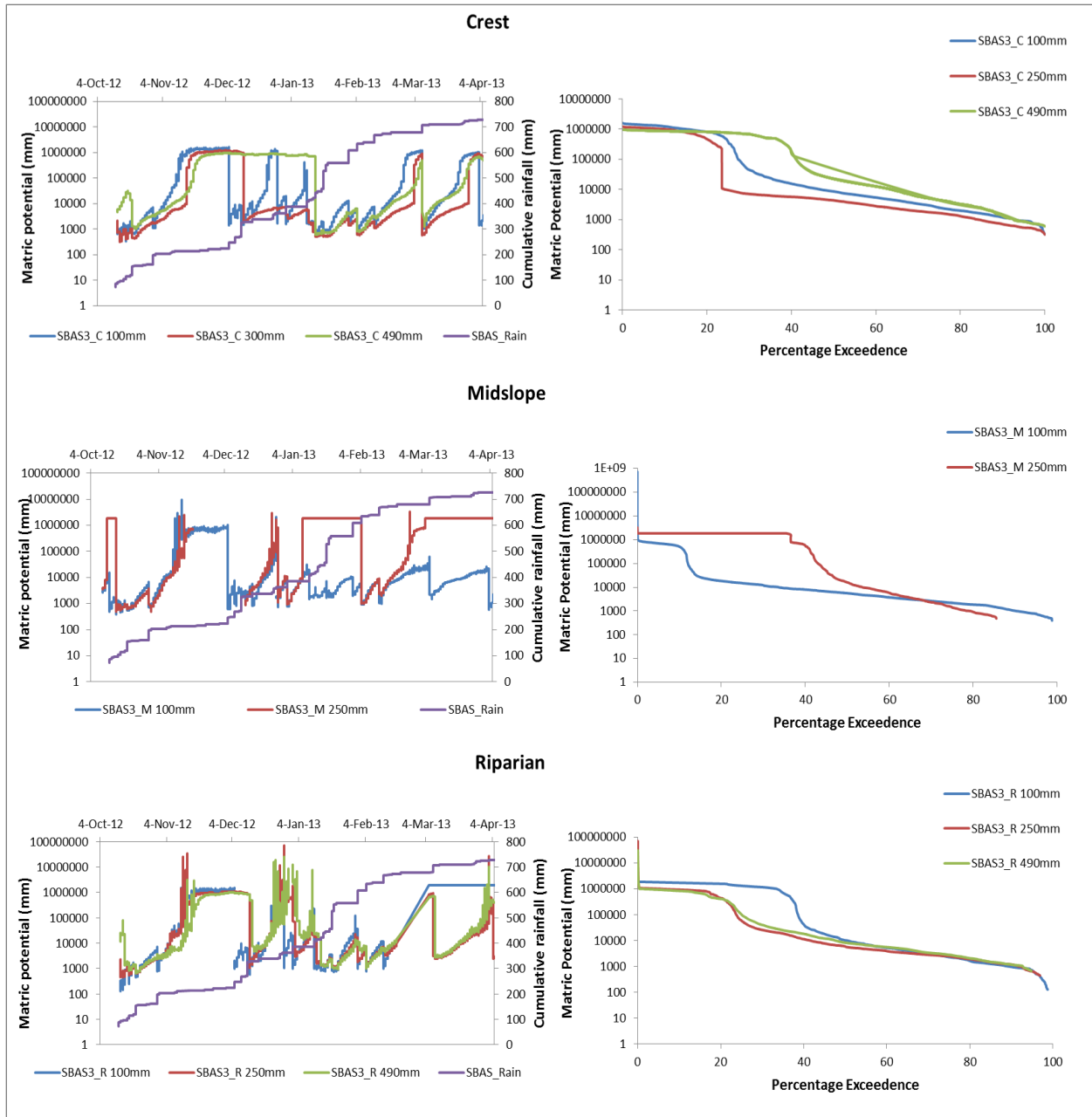


Figure 4.21 Soil moisture responses and percentage exceedence curves for 3<sup>rd</sup> order hillslope

In conclusion, the basalt hillslopes are characterized by recharge soils (potential) but from the majority of responses shown, most of the water does not percolate into the deeper layers of the soil profiles. This has been attributed to water lost through ET before percolating to these deep layers. This shows that these soils require a certain threshold in the amount and intensity of rainfall received so that they can be replenished after the dry winter seasons. The absence or

limited possibility of lateral subsurface flow in these soils due to low gradient topography suggests a hydrological disconnection of the catena elements from one another.

#### 4.8 Conceptual Models Derived from Hydropedological Interpretations on Southern Basalt supersite

The 1<sup>st</sup>, 2<sup>nd</sup> and 3<sup>rd</sup> order basalt hillslopes comprises different soil forms including Mispah, Mayo and Shortands, respectively (Tables 4.4, 4.5 and 4.6). From the soil surveys, the majority of the profiles had no morphological indications of saturation therefore all the soils were classified as potential recharge soils (Figure 4.22). Due to the low gradient topography on these sites (Colgan *et al.*, 2012), this term only refers to the vertical subsurface movement of water but not necessarily recharging to groundwater and since the water had a limited possibility of flowing laterally, it was therefore, lost through evapotranspiration. Overland flow was only anticipated after exceptionally large events and this was the only time when the possibility of hydrological connectivity between catena elements on the hillslopes was anticipated.

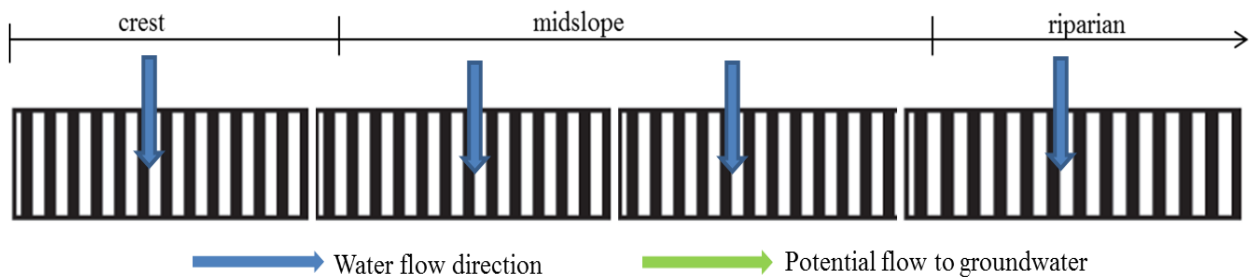


Figure 4.22 Hydrological soil types and flow paths for basalts 1<sup>st</sup>, 2<sup>nd</sup> and 3<sup>rd</sup> order hillslopes

In this chapter, the aim of the research to define and characterize the differences in hydrological responses at different scales and parent material was achieved through conductivity characterization data, water potential, ERT and hydropedology. Processes such as hydrological connectivity are shown to be scale-dependent and highly driven by rainfall intensity.

## 5.0 QUANTIFICATION RESULTS AND DISCUSSION

HYDRUS 1D was used to simulate flow and determine water budgets for all granite catena elements (1<sup>st</sup>, 2<sup>nd</sup> and 3<sup>rd</sup> order hillslopes) and the basalt 3<sup>rd</sup> order hillslope catena elements. This improved the understanding of characterized processes at the two sites. Actual ET was modelled using SEBAL between 01 October 2012 and 30 April 2013 (refer to chapter 3 sub-section 3.14 for more information). Results will be presented as shown on the roadmap (Figure 5.1).

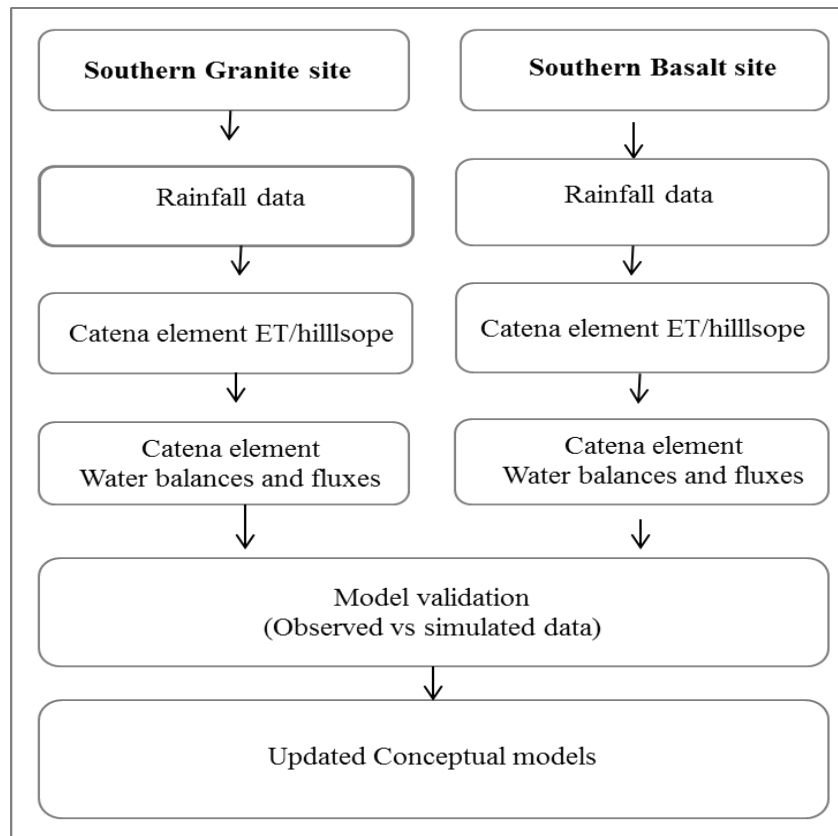


Figure 5.1 Roadmap for results presentation

### 5.1 Rainfall Distribution on the Granite Site

Rainfall on the southern granite supersite (Figure 5.2) showed much variability during the modelled period of October 2012 to April 2013. High intensity events were sometimes experienced where more than 20 mm of rainfall was received in one hour (Figure 5.2). These

events were experienced more frequently in January and to a lesser extent in December and February. The October events (intensities  $>6$  mm/hr) also had some notable effects on hydrological processes as discussed in the previous chapter. Dry spells were experienced in October, November, March and April (Figure 5.2) by the absence of rainfall for weeks during the season.

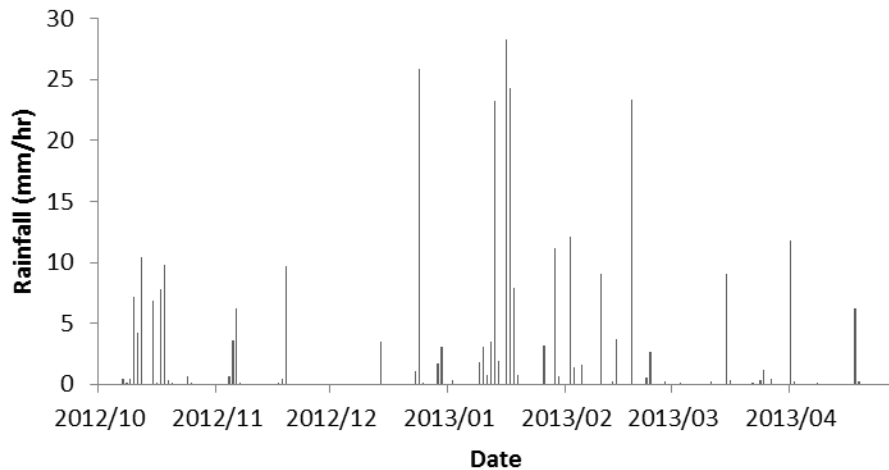


Figure 5.2 SGR rainfall intensities over the modelling period

## 5.2 Modelled Actual ET at the Supersites

The 1<sup>st</sup> order hillslope (Figure 5.3) showed an increase in actual  $ET_{SEB}$  from the crest moving downslope. There were distinct differences on water use between the three catena elements with highest demand at the riparian zone (809 mm) whilst the crest and midslope had 765 mm and 784 mm, respectively. The riparian zone on this hillslope was characterized by more vegetation than at the crest therefore, these results were deemed realistic. At the beginning of the season between the 10<sup>th</sup> of October and 10<sup>th</sup> of November, it showed that the midslope and the riparian zones did not have much variation in water use compared to the crest which had low water use from the onset. Since the crest vegetation had broad leaved vegetation, more water was expected to be lost there.

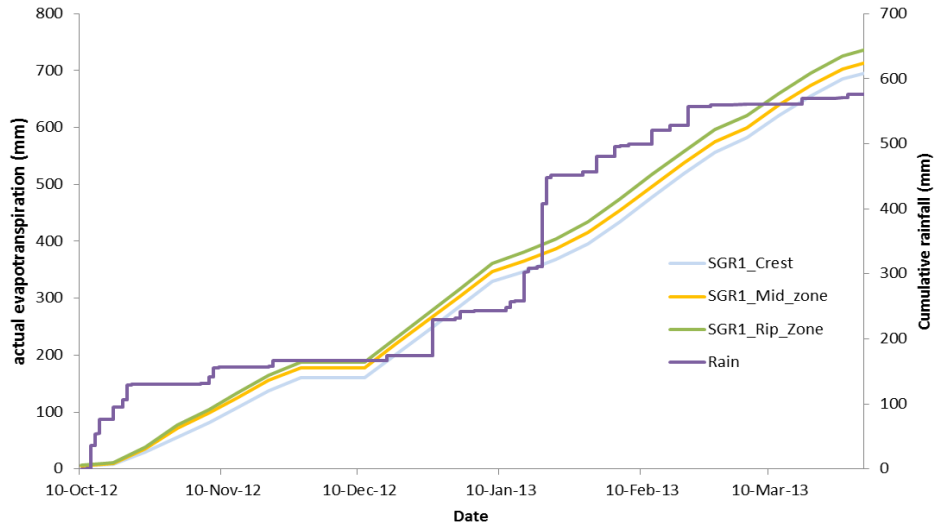


Figure 5.3 actual  $ET_{SEB}$  per catena element for granite 1<sup>st</sup> order hillslope

The 2<sup>nd</sup> order hillslope (Figure 5.4) did not show much variation in water use between the 10<sup>th</sup> of October and the 10<sup>th</sup> of December. However, from December to the end of the dataset, the crest and riparian zone continued showing no great difference having 782.5 mm and 779 mm, respectively. Meanwhile, the midslope had a lower water use compared to the other two elements (755 mm). From field observations, the midslope on this hillslope was characterized by sparse woody vegetation compared to the crest and the riparian zone. This therefore, implied that less mass was lost through transpiration compared to the crest and riparian zones. High potential storage was therefore, anticipated at this catena element since water use was minimal.

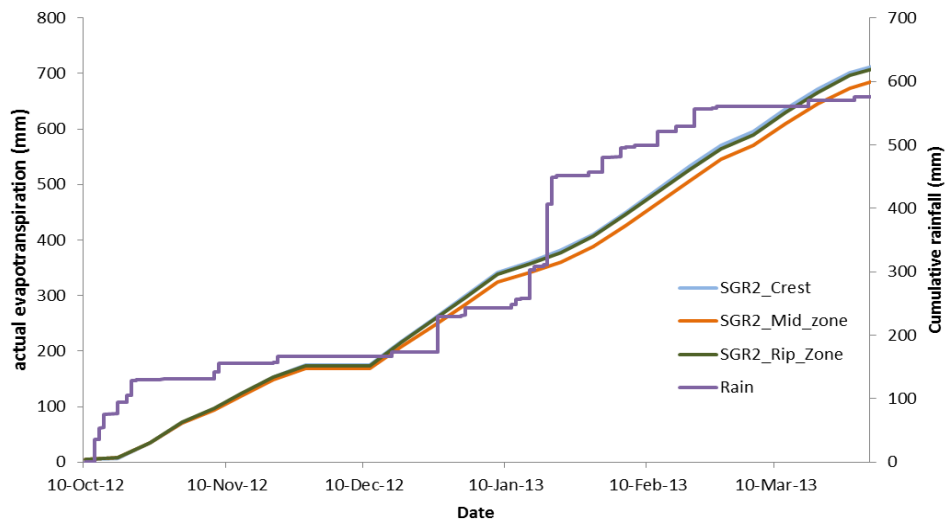


Figure 5.4 actual  $ET_{SEB}$  per catena element for granite 2<sup>nd</sup> order hillslope

The 3<sup>rd</sup> order hillslope (Figure 5.5), showed no notable differences in water use between catena elements. The crest had the highest water use (767 mm) followed by the riparian zone (765 mm) then the midslope (762 mm) with slight differences of 2 mm and 3 mm between them, respectively. Due to a large highly developed grassy area on the midslope of this catena, characterized by many bare patches and a very sparse woody cover, actual ET was anticipated to be lower than the crest and riparian zones that has a much dense woody cover. This showed that the evaporative demand was high at this element; therefore, more water was lost from the surface than through transpiration.

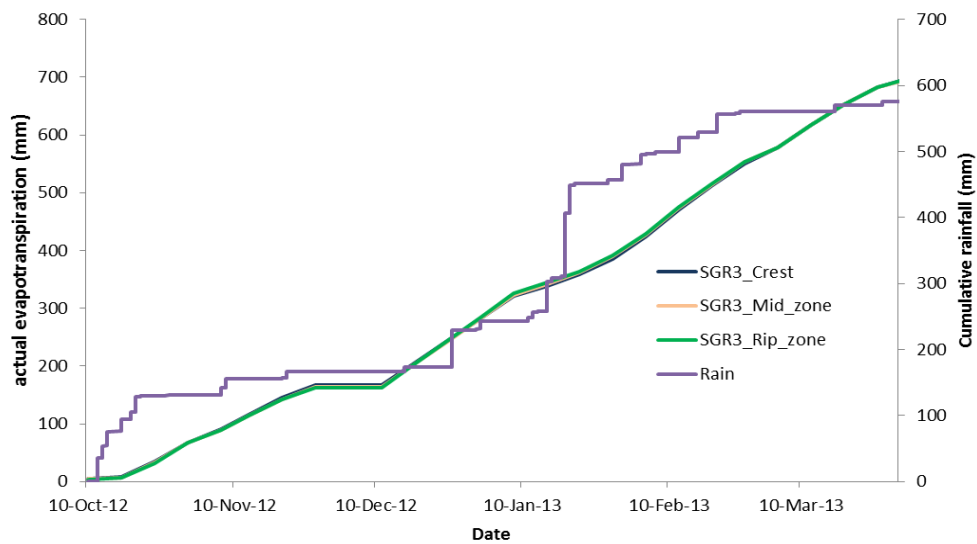


Figure 5.5 actual ET<sub>SEB</sub> per catena element for granite 3<sup>rd</sup> order hillslope

### 5.3 Rainfall Distribution on the Basalt (Nhlowa) Site

Similar to the rainfall distribution on the granite site, the basalt rainfall (Figure 5.6), shows much variability during the modelled period (October 2012- April 2013). There was a higher frequency of high intensity events (>10 mm/hr) on this site compared to the granite site (Figure 5.2) but similar to the granite site, only the October and January events were shown to have impacts on processes and hydrological responses at this site. A few dry spells were experienced compared to the granites (February and March). In terms of overall cumulative rainfall over the modelled period, the basalt supersite received more rainfall compared to the granite supersite (Figure 9.13).

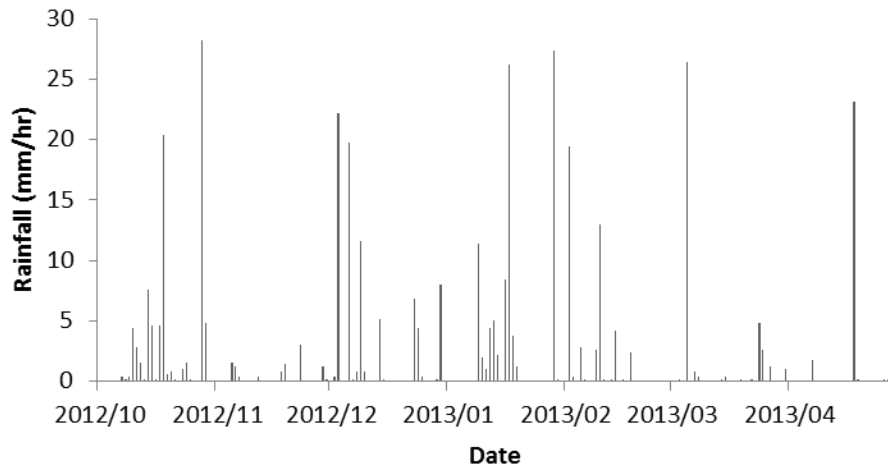


Figure 5.6 SBAS rainfall intensities over the modelling period

The basalts 1<sup>st</sup> order hillslope (Figure 5.7), shows very little variation between the interfluves (mid-crest) and the riparian zone with a difference of only 4 mm in water use. The interfluve has 603 mm whilst the riparian has 607 mm. For the greater part of the season (October to February), the interfluve show more water use but towards the end of the season (February to April), the riparian catena element had the greatest actual ET<sub>SEB</sub>.

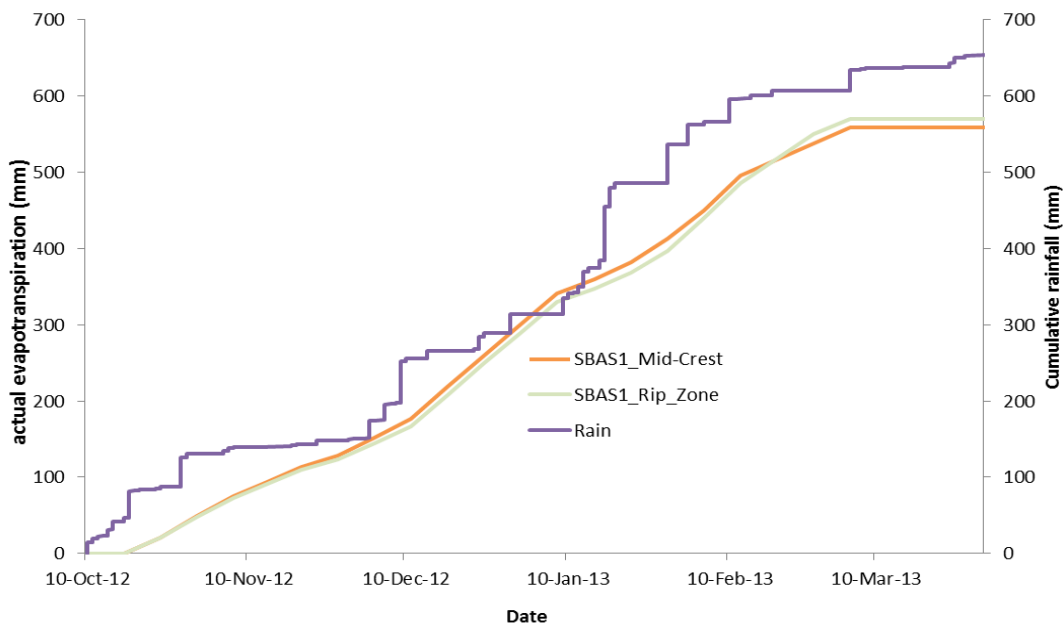


Figure 5.7 actual ET<sub>SEB</sub> per catena element for basalt 1<sup>st</sup> order hillslope

The 2<sup>nd</sup> order hillslope showed remarkable differences in water use between the interfluvial and the riparian zone from Mid-November until April (Figure 5.8). The interfluvial had 609 mm whilst the riparian zone had 573 mm making a difference of 36 mm. More water use was shown on the interfluvial. When rasters were clipped for the basalt site, the crest and midslope were combined thereby giving more pixels. Assessing the results with respect to proportional area, the riparian was much smaller compared to the interfluvial, thereby suggesting more water use on the riparian zone compared to the interfluvial.

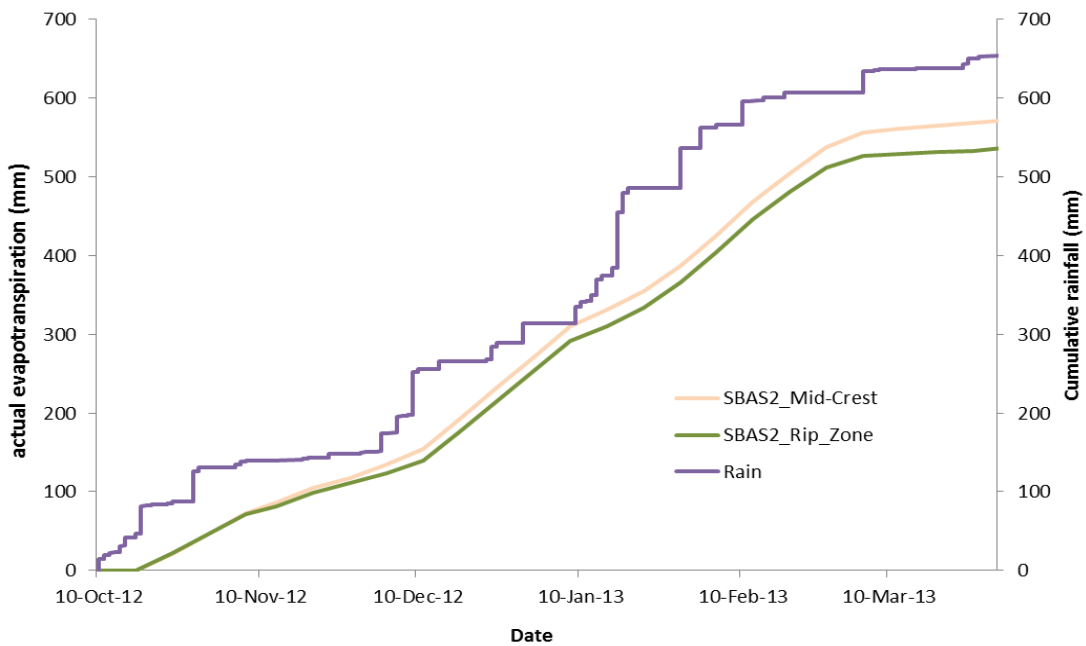


Figure 5.8 actual ET per catena element for basalt 2<sup>nd</sup> order hillslope

The 3<sup>rd</sup> order hillslope (Figure 5.9) showed some variation between the interfluvial and the riparian catena element with greatest water use shown on the interfluvial. Similar to the 1<sup>st</sup> and 2<sup>nd</sup> order, the midslope and crest were combined. The riparian zone had a much smaller area compared to the interfluvial (mid-crest combined). This therefore, implied the presence of more woody cover on the riparian, hence more water use if assessed by areas of the same size.

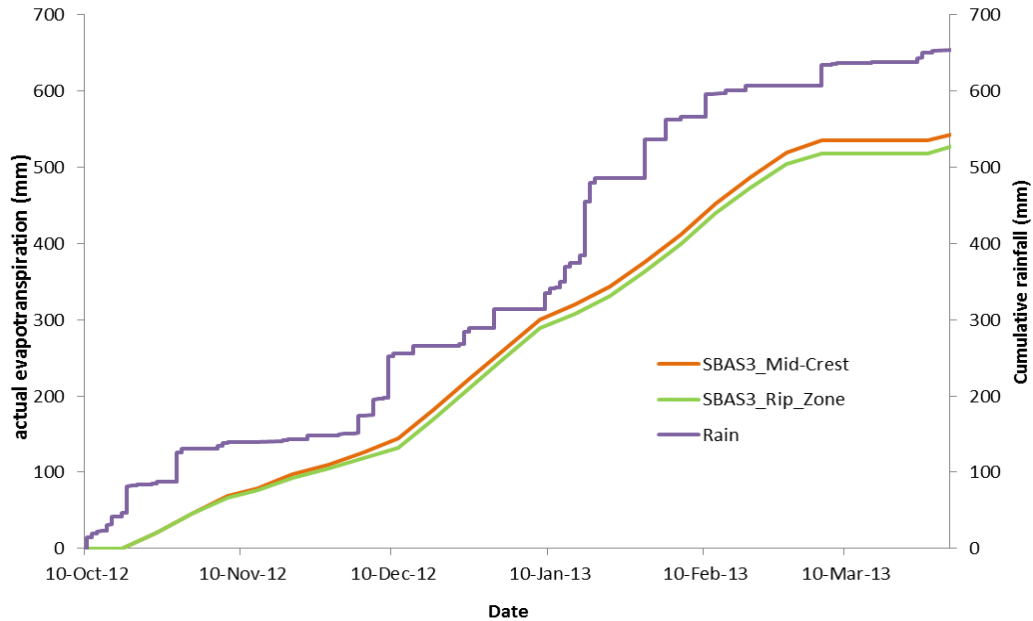


Figure 5.9 actual  $ET_{SEB}$  per catena element for basalt 3<sup>rd</sup> order hillslope

A comparison of water use on the hillslopes at the basalt site showed that actual  $ET_{SEB}$  was lower at the low order hillslopes. This implied more storage potential since there were deeper soils compared to higher orders. A comparison of water use between the two geologies showed that high actual  $ET_{SEB}$  was recorded at the southern granite supersite showing a high cumulative value of 809 mm at the 1<sup>st</sup> order riparian zone whilst the highest recorded at the basalt site was 609 mm resulting in a difference of 200 mm between the two sites. The granite site was characterized by more woody vegetation on its catena elements compared to the basalts.

#### 5.4 Modelled Hydrological Fluxes using Hydrus 1D

The objective of the modelling was to estimate the hydrological fluxes and catena element water budgets and upscale this to a hillslope scale. Time series water balances for the catena elements are presented in Appendix B (Figures 9.5 to 9.8). From the model output, the cumulative fluxes from the domain boundaries allowed insight into components of the water budget for each of the modelled catena elements. Results are presented.

### 5.4.1 Simulated results for 1st order granite hillslope

The 1<sup>st</sup> order hillslope showed a positive change in storage of 48 mm at the crest whilst the midslope and the riparian zone lost water. Based on soil depth, the crest was anticipated to have the least storage compared to the downslope elements since it had shallow soils. As shown on the Table (5.1), the midslope and riparian zones had negative storage because of water loss through actual  $ET_H$  (470 mm) and (546 mm), respectively compared to the crest (294 mm). However, the crest had the greatest free drainage (Figure 5.11) compared to the other downslope elements. At the hillslope scale, it has been shown that more water was being lost through actual  $ET_H$  than free drainage. This was therefore, evidence of how savannah vegetation is able to extract large amounts of water while the soil is wet. This was illustrated by watermark responses (Figure 4.5) through the quick drying cycles soon after rainfall events especially in the shallow and intermediate soils.

Table 5.1 Catena element water budgets for 1<sup>st</sup> order granite hillslope

	SGR1 Crest	SGR1 Mid	SGR1 Rip
Unit	mm	mm	mm
P	637.6	637.6	637.6
$ET_H$	294.9	470.17	546.73
R	0	0	0
FD	294.66	178.36	108.23
$\Delta S$	48	-11	-17

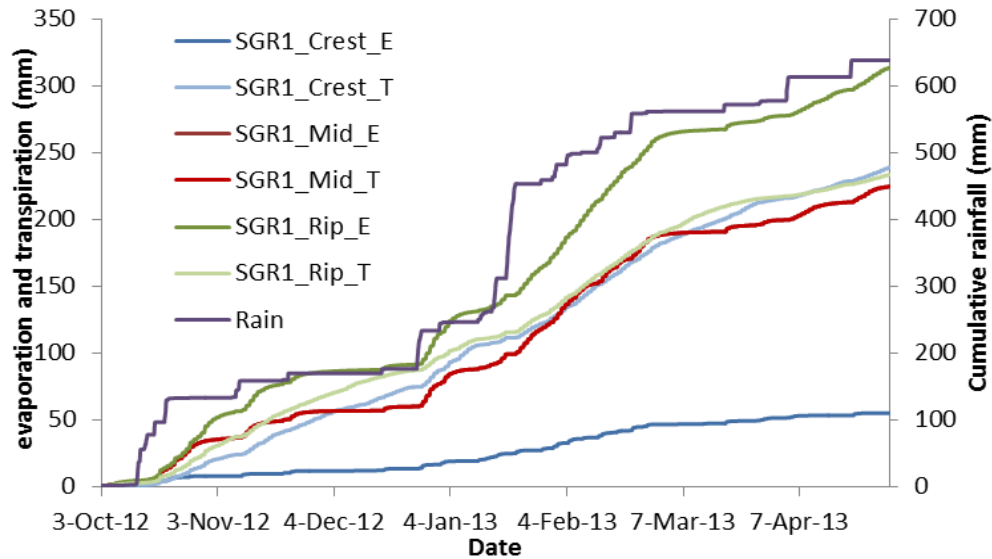


Figure 5.10 Simulated cumulative evaporation and transpiration fluxes on SGR1 hillslope catena elements

The simulation results show evaporation and transpiration fluxes from the vadose zone into the atmosphere at the 3 catena elements of the 1<sup>st</sup> order hillslope (Figure 5.10). In Table (5.1) above,  $ET_H$  was highest at the riparian zone followed by the midslope whilst the crest had the least. The same results were shown (Figure 5.10) but partitioned into evaporation and transpiration components at each catena. At the riparian zone a large proportion of the  $ET_H$  loss was from evaporation from the soil surface than through transpiration. This was not anticipated since the riparian zone was characterized by more woody cover and herbaceous vegetation. An element of uncertainty could have been brought into the model through the estimation of rooting depths (Table 9.2) and densities. The crest and midslope elements were losing water through transpiration than evaporation.

Free drainage increased moving upslope on this hillslope (Figure 5.11). The crest had the greatest amount of free drainage (Table 5.1). This was not anticipated. The crest comprised a Cartref soil form (Table 4.1), hence the presence of an E horizon, according to van Tol (2008), it indicates a perched water table and also implies that flow is restricted in some areas of the lithocutanic B resulting in more lateral flow and less free drainage. The crest responded to about 5 of the rainfall events whilst the midslope only responded to 3 events and the riparian zone

responded to only two. This suggests more fine textured soils downslope as illustrated by the texture data (Figure 4.2a). These data showed that the majority of these soils were only responding to high intensity events (October and January). This means if there are seasons characterized by low to medium intensity events, there will be less free drainage (potential recharge) especially in the lower elements of this hillslope. In a study by Peterson (2011), direct groundwater recharge was shown to be more dominant on the crest zones of the catena. This would explain why the crest responded more frequent than the downslope catena elements.

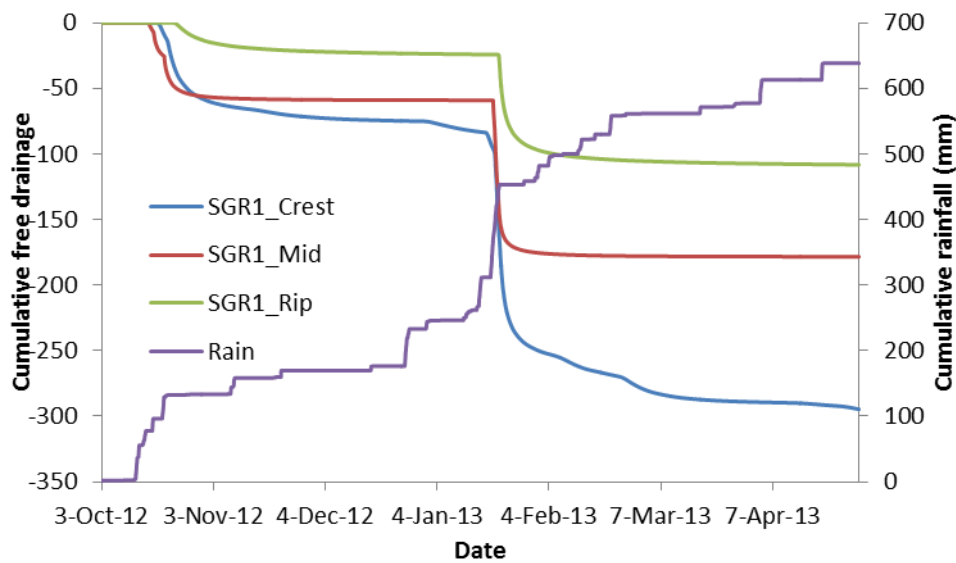


Figure 5.11 Simulated cumulative free drainage fluxes on SGR1 hillslope catena elements

#### 5.4.2 Simulated results for 2<sup>nd</sup> order granite hillslope

The crest on the 2<sup>nd</sup> order hillslope had the greatest change in storage (45 mm) followed by the midslope (10 mm) whilst the riparian zone was losing water (Table 5.2). Similar to the 1<sup>st</sup> order crest, less storage was anticipated at the crest due to the shallow soils because of shallow rock shown through ERT results. The greatest  $ET_H$  was experienced at the midslope (507 mm). The riparian zone was losing most water to  $ET_H$ , as well as free drainage as shown by the simulation results.

Table 5.2 Catena element water budgets for 2<sup>nd</sup> order granite hillslope

	SGR2 Crest	SGR2 Mid	SGR2 Rip
Unit	mm	mm	mm
P	637.7	637.6	637.6
ET <sub>H</sub>	420.04	507.39	354.43
R	0	0.012	22
FD	172.69	120.05	272.4
ΔS	45	10	-11

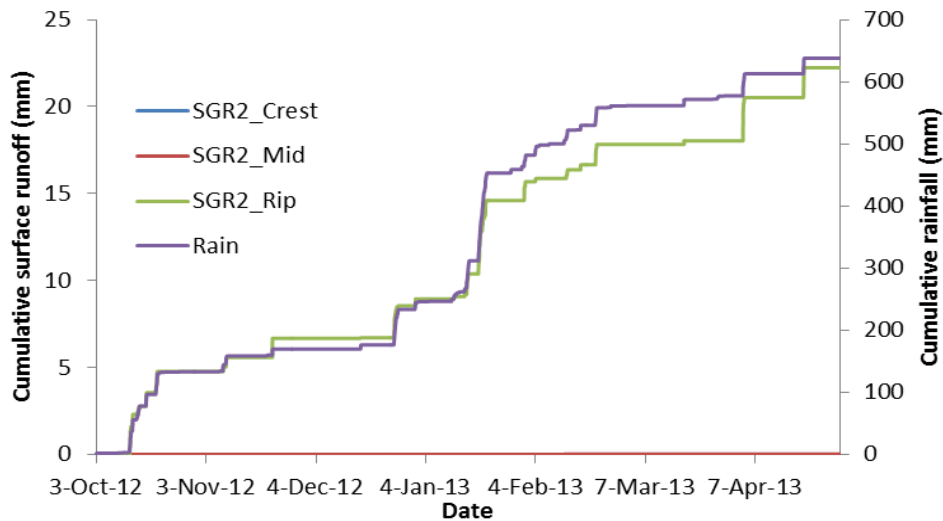


Figure 5.12 Cumulative surface runoff on SGR2 hillslope catena elements

The 2<sup>nd</sup> order riparian zone was the only catena element experiencing surface runoff on this hillslope (Figure 5.12). This catena element had a Cartref soil form, therefore, interflow was anticipated due to a flow restriction in some parts of the B horizon so this runoff could have been as a result of infiltration excess flow. Taking a closer look at the runoff responses on this catena element shows that it was responding to almost all rainfall events not just high intensity ones and this implied a responsive soil. Soils at this catena element were classified as interflow soils with a possibility of overland flow under high intensity events but these data are proving otherwise. This, therefore, means there was a possibility of overland flow but not necessarily in response to high intensity events.

Water use was greatest on the midslope at this 2<sup>nd</sup> order hillslope (Table 5.2) which was least expected since losses were mainly through evaporation from the soil surface than through transpiration especially at the midslope (Figure 5.13). Meanwhile, the crest and riparian zones were losing most water through transpiration.

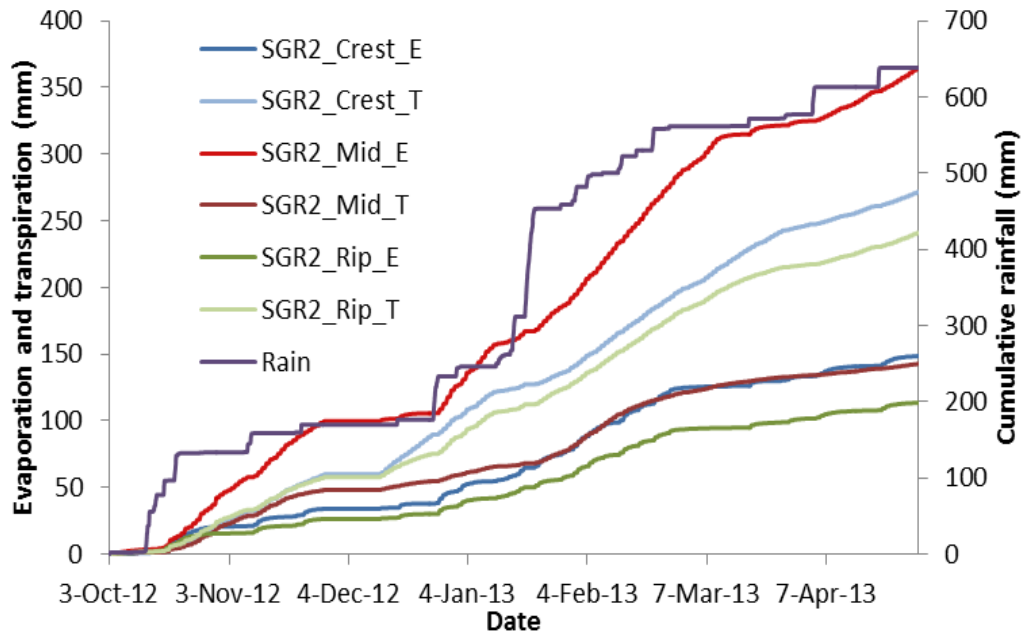


Figure 5.13 Simulated cumulative evaporation and transpiration fluxes on SGR2 hillslope catena elements

The riparian zone at the 2<sup>nd</sup> order hillslope was experiencing the greatest free drainage of water (Figure 5.14). Free drainage was greatest at the riparian zone (Cartref soil form) which was also the case at the 1<sup>st</sup> order crest. This could therefore, be a phenomenon associated with the Cartref soil form despite the water flow restriction in some parts of the B horizon. In terms of free drainage responses to rainfall events, the crest and midslope only responded to high intensity events (i.e. some of the October 2012 and January 2013 events). Meanwhile, the riparian zone responded to most of the events but only during those two months. Similar to the 1<sup>st</sup> order, under normal low to medium intensity events less free drainage was anticipated on this hillslope.

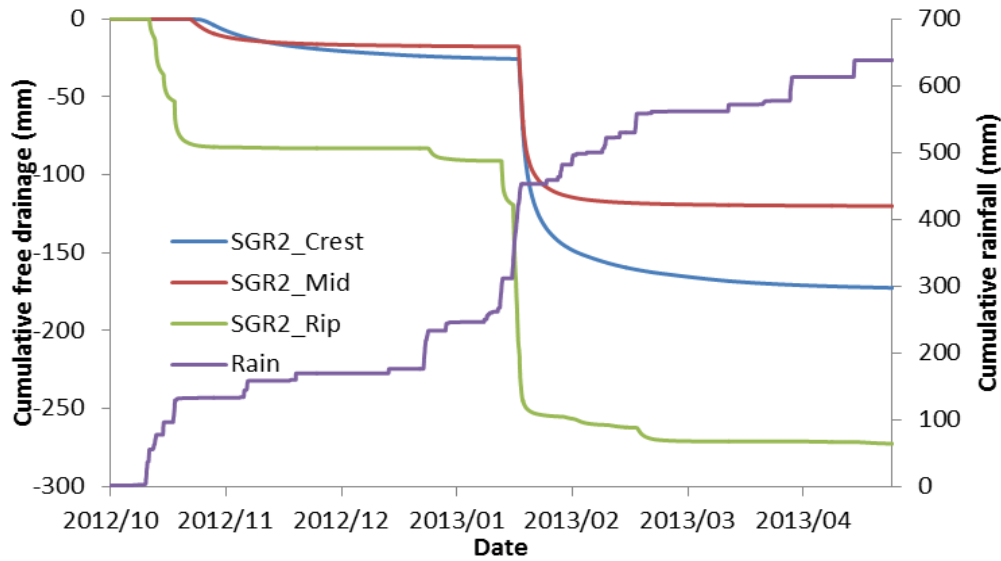


Figure 5.14 Simulated cumulative free drainage fluxes on SGR2 hillslope catena elements

### 5.4.3 Simulated results for 3<sup>rd</sup> order granite hillslope

The 3<sup>rd</sup> order hillslope showed greatest storage change (Table 5.3) on the riparian catena element (54 mm), followed by the crest (48 mm). The midslope has negative storage losing water through  $ET_H$  showing the highest water use compared to the other catena elements. Similar to the 1<sup>st</sup> and 2<sup>nd</sup> order hillslopes; large proportions of water were lost through  $ET_H$  but in terms of storage, this hillslope had the greatest storage (combined) compared to the lower order hillslopes. Factors, such as area covered, soil hydraulic properties and vegetation density could have been responsible for this storage. (NB: the midslope had a different amount of precipitation compared to the other elements because the runoff from the crest was added to the midslope precipitation)

Table 5.3 Catena element water budgets for 3<sup>rd</sup> order granite hillslope

	SGR3 Crest	SGR3 Mid	SGR3 Rip
Unit	mm	mm	mm
P	637.6	640.8	637.6
ET <sub>H</sub>	457.46	496.12	382.24
R	3	0	0
FD	129.38	152.39	201.84
ΔS	48	-8	54

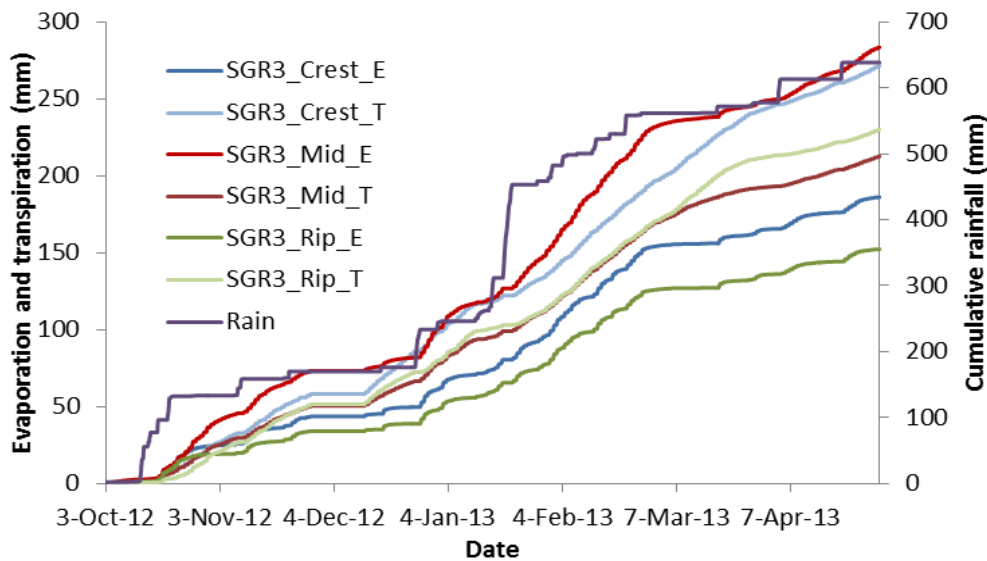


Figure 5.15 Simulated cumulative evaporation and transpiration fluxes on SGR3 hillslope catena elements

Similar to the 2<sup>nd</sup> order hillslope, ET<sub>H</sub> was greatest at the midslope of this 3<sup>rd</sup> order hillslope and it is likely that more water was lost through soil evaporation (Figure 5.15). Meanwhile, the crest and the riparian zone lost more through transpiration than evaporation which was also the case on the 2<sup>nd</sup> order hillslope due to the increased density of woody cover and herbaceous plants on these elements.

Free drainage was highest at the riparian zone in comparison with the other elements (Figure 5.16). This augments the hydropedological classification of this catena element as a potential

recharge soil (Table 4.3). The midslope and riparian zones only responded twice to two high intensity rainfall events (in October and January). The crest only responded to the event in January. These data shown for the crest augments the low  $K_{sat}$  values (Figure 4.4d) on the c horizon. This means therefore, flow was restricted in this horizon implying less water would drainage from this catena element but would either flow laterally at the A/B interface with some lost through  $ET_H$ . Similar to the 1<sup>st</sup> and 2<sup>nd</sup> order hillslope, less free drainage was anticipated when there were low to medium intensity events (<10 mm/hr).

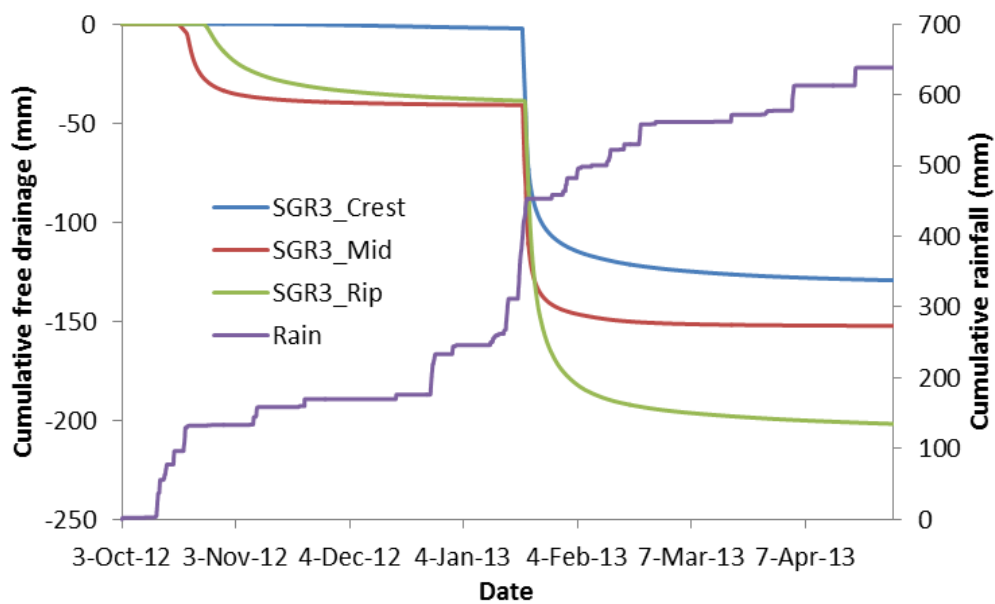


Figure 5.16 Simulated cumulative free drainage fluxes on SGR3 hillslope catena elements

#### 5.4.4 Simulated results for basalt 3<sup>rd</sup> order hillslope

The basalt 3<sup>rd</sup> order riparian catena element showed the greatest  $ET_H$ , (386 mm) and runoff (82 mm) but had the least free drainage and overall water balance compared to the other elements (Table 5.4). Meanwhile, the midslope had the greatest change in water storage (102 mm). The riparian zone showed a net loss in storage and this was attributed to  $ET_H$  (386 mm). One important observation here was the runoff output by the model. Due to the low gradient topography on this site, the possibility of runoff generation was minimal. This was therefore,

considered as ponded water judging from field observations especially after high intensity rainfall events (January 18<sup>th</sup> and January 19<sup>th</sup> event).

Table 5.4 Catena element water budgets for 3<sup>rd</sup> order basalt hillslope

	SBAS3 Crest	SBAS3 Mid	SBAS3 Rip
Unit	mm	mm	mm
P	701	701	701
ET <sub>H</sub>	106.6	103.85	386.3
R	36	43.62	82
FD	532	450.6	236.83
ΔS	26	102.94	-4

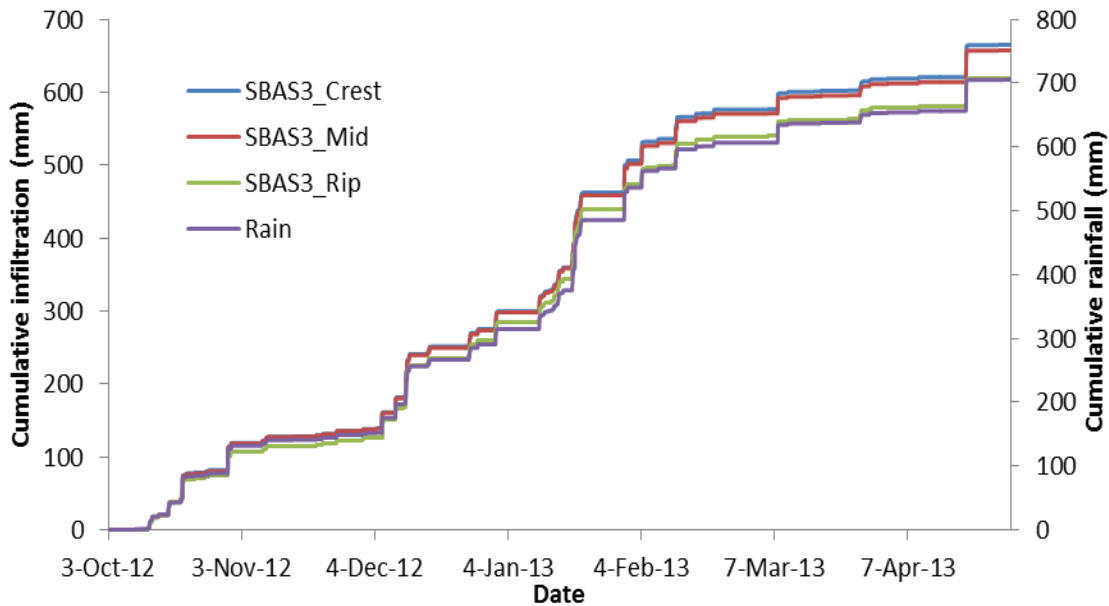


Figure 5.17 Cumulative infiltration on SBAS3 hillslope catena elements

The riparian cumulative infiltration for the 3<sup>rd</sup> order basalt hillslope (Figure 5.17) was largest and this augmented the conductivity data (Figure 4.18) which showed high  $K_{unsat}$  on the riparian zone compared to the other catena elements. Before the high intensity January events, the crest showed less infiltration whilst the midslope and riparian zones showed more infiltration possibly due to surface contributions from upper slopes (Table 5.4).

Water use on the 3<sup>rd</sup> order hillslope (Figure 5.18) showed that more water was being taken up through transpiration than evaporation at the riparian zone, although there was not much difference from water loss through evaporation and transpiration at this catena element. As discussed earlier, responses for the crest and midslope were almost similar and both having more water lost through evaporation than transpiration due to less vegetation density compared to the riparian zone.

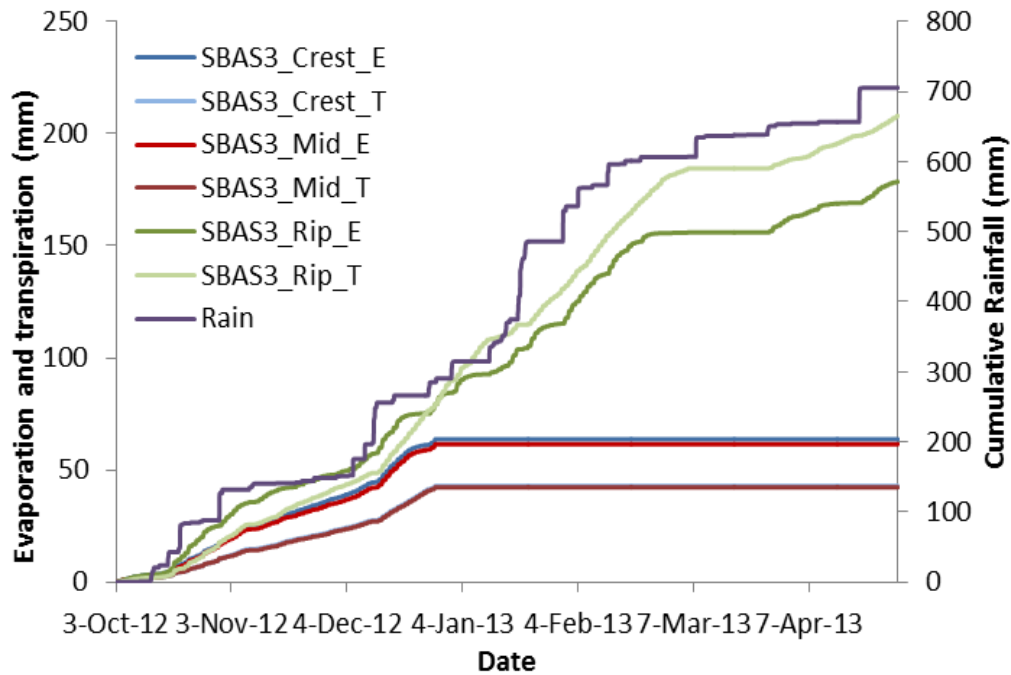


Figure 5.18 Simulated cumulative evaporation and transpiration fluxes on SBAS3 catena elements

Free drainage on this 3<sup>rd</sup> order basalt hillslope does not show much variation on the crest and midslope (Figure 5.19). The riparian zone had the least free drainage and it showed a response to about 5 rainfall events whilst the crest and midslope responded to most of the events. Due to high  $K_{unsat}$  at this element free drainage was anticipated to be high compared to the crest and midslope. This means that large amounts of water are being lost through  $ET_H$  therefore, less water will be left in the subsurface to allow for free drainage.

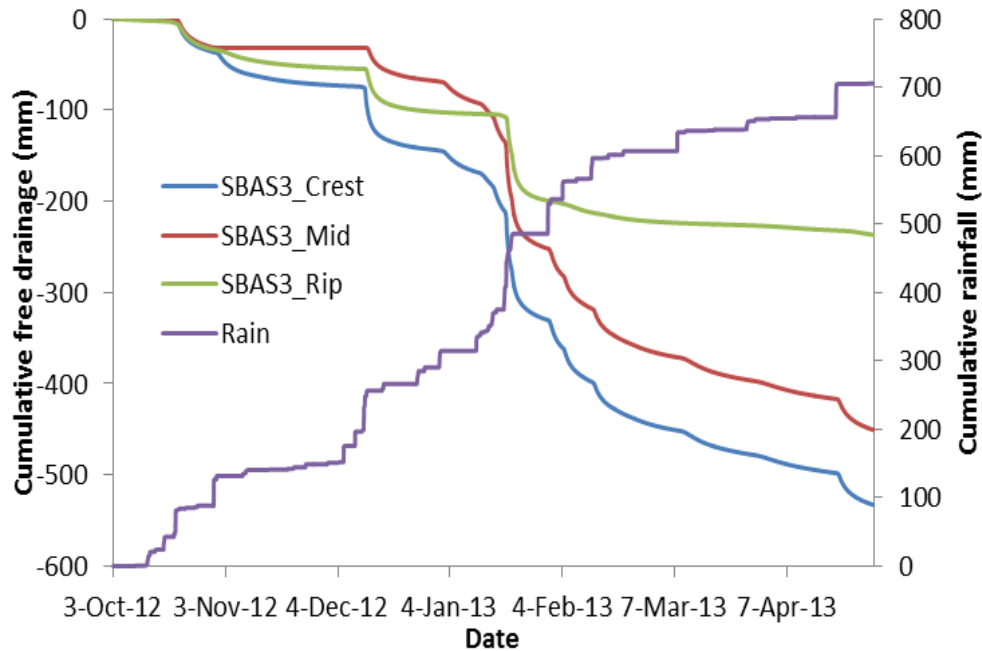


Figure 5.19 Simulated cumulative free drainage fluxes on SBAS3 hillslope catena elements

## 5.5 Model Validation

Model performance was validated by comparing output from the simulated data with observed watermark data. Observation nodes on the domain were set at the same depths where soil moisture sensors were installed in profiles in the field (Appendix A: Table 9.1).

### 5.5.1 Observed vs Simulated Matric potential

Figures 5.20 to 5.23 show comparisons between observed watermark data and simulated output. This was a qualitative interpretation of model performance. Observation nodes were set at the same depths as the installed soil moisture sensors (Figure 9.4). Observed data measured by watermarks can be used for a general trend in responses but they are not very accurate for extreme wet or dry conditions.

There was not much variation in observed and simulated data on the 1<sup>st</sup> order hillslope (Figure 5.20). The crest showed a mismatch on three events in November, December and February where some degree of saturation was shown on the simulated responses (<100 mm). In general the responses seem to be the same.

The 2<sup>nd</sup> order hillslope also did not show much difference between the observed and simulated responses especially at the midslope (Figure 5.21). The crest showed a slight mismatch on the deep and intermediate channels. The riparian zone showed the same trend only that the observed data was filtered to get rid of the extreme values but here it showed the profile was actually getting saturated at some points.

3<sup>rd</sup> order responses showed a relative agreement between observed and simulated data (Figure 5.22). The crest shallow soils got saturated in response to most events in the simulated results. The original data was filtered to get rid of extreme values. Meanwhile, the midslope showed a similar trend in responses for both the observed and simulated results. Riparian zone results showed more or less the same responses, although the simulated results had lower matric potentials than the observed. The differences could be attributed to the fact that watermarks do not work well with extreme conditions both on the wet and dry ends.

Basalt responses (Figure 5.23) showed a more or less similar trend but a magnitude lower in matric potentials. This could be attributed to the fact that saturated hydraulic conductivity was not measured at this site therefore default values for the textural classes were used.

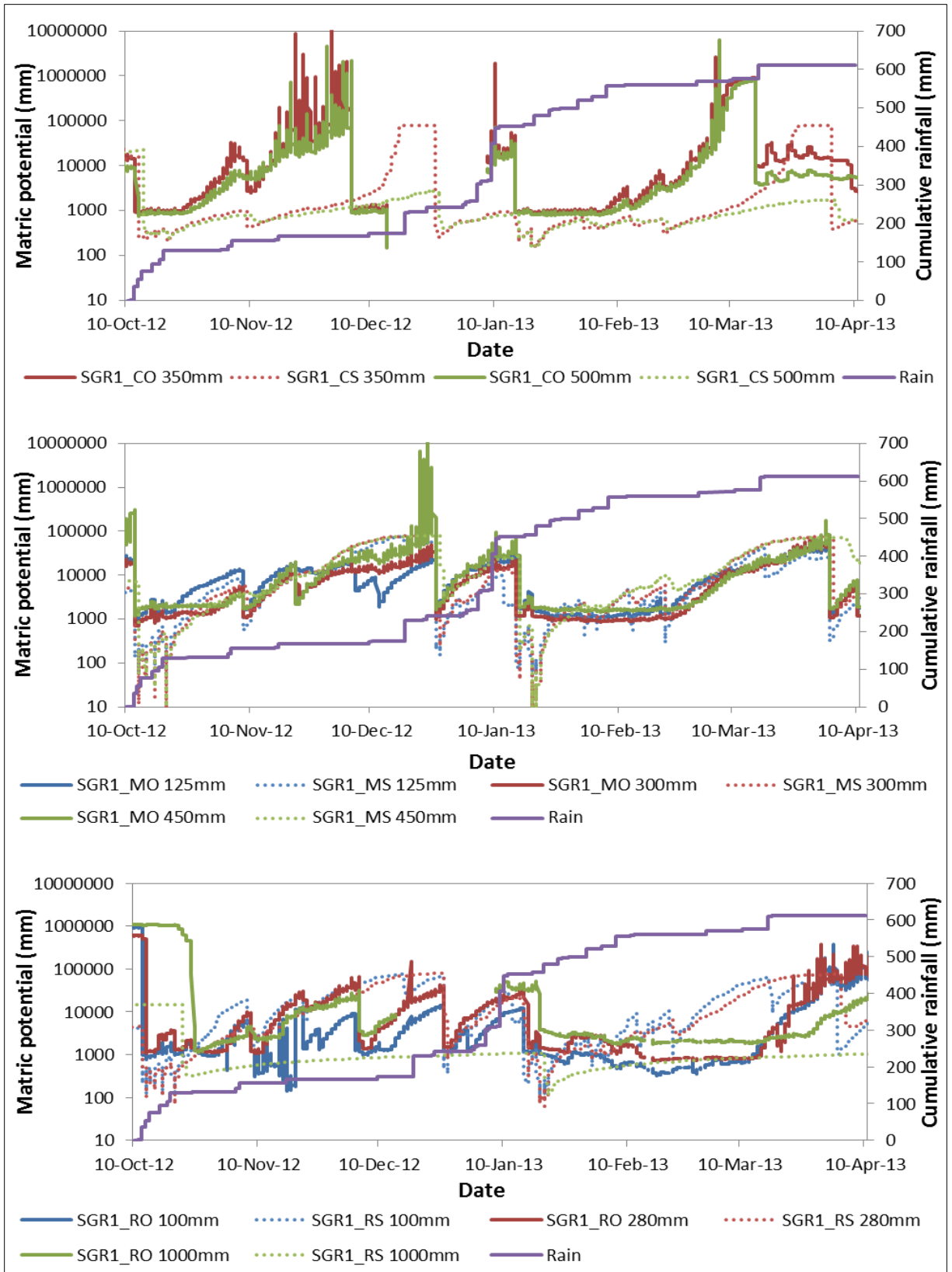


Figure 5.20 Observed and simulated responses for 1<sup>st</sup> order granite hillslope

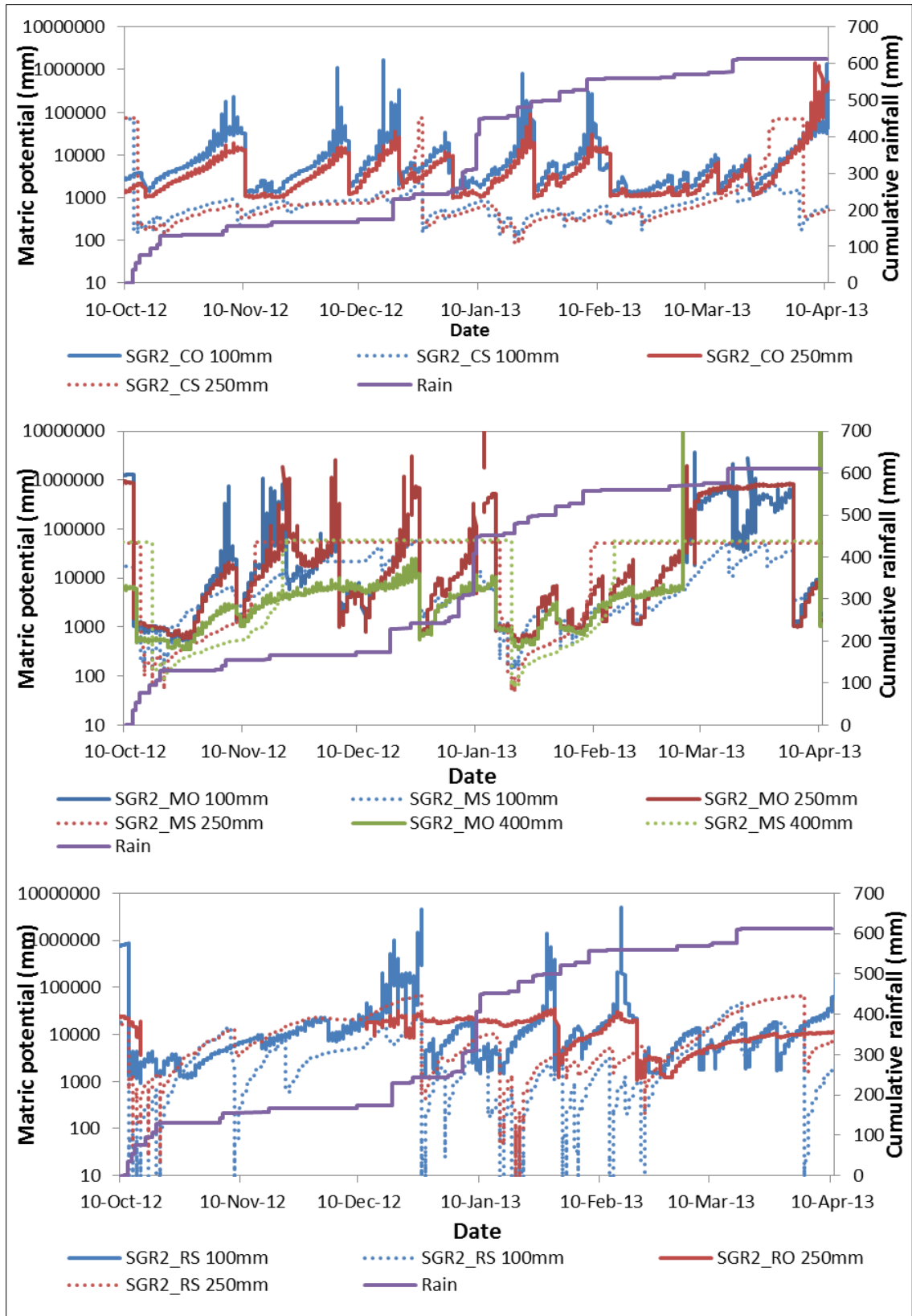


Figure 5.21 Observed and simulated responses for 2<sup>nd</sup> order granite hillslope

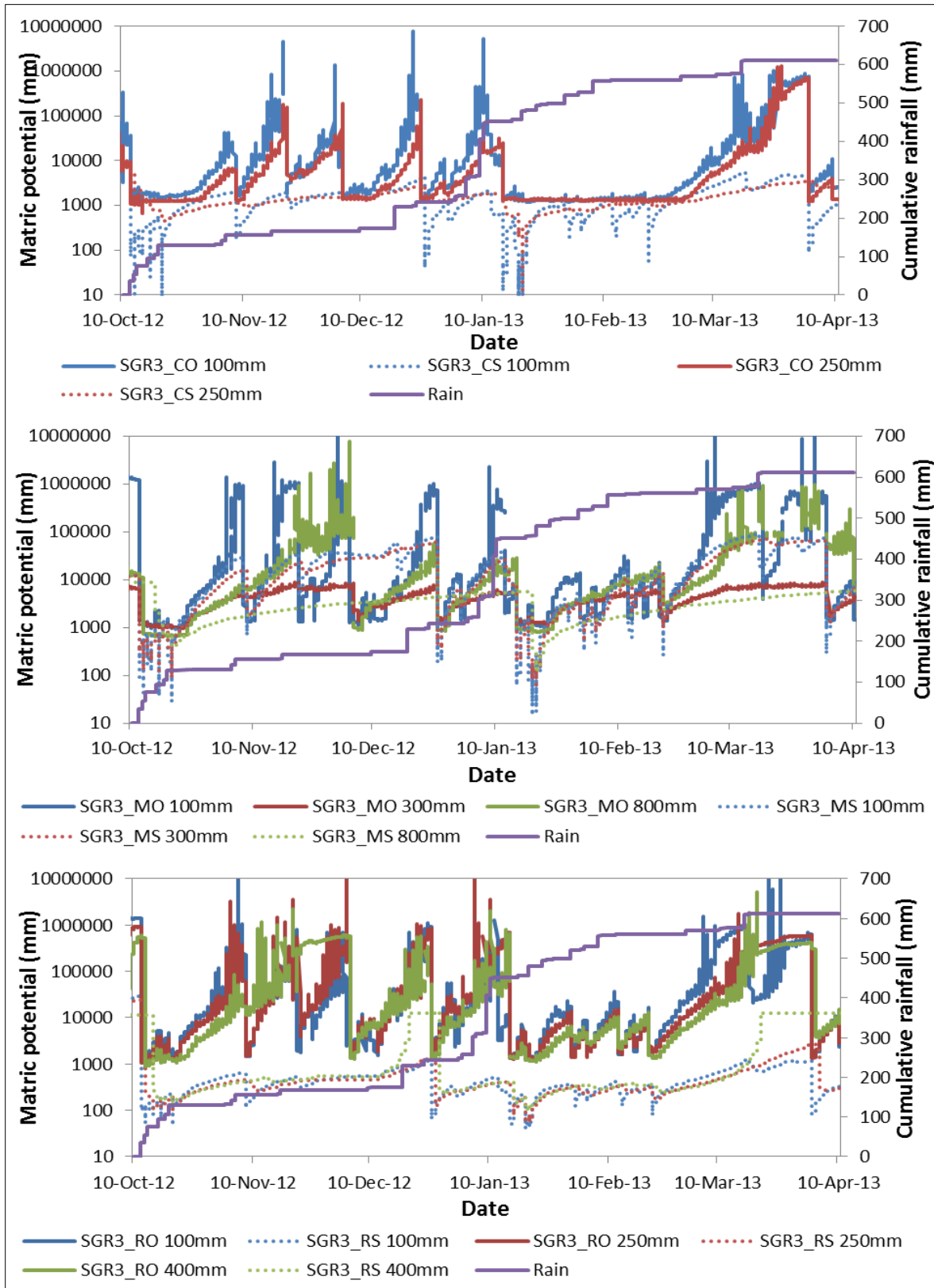


Figure 5.22 Observed and simulated responses for 3<sup>rd</sup> order granite hillslope

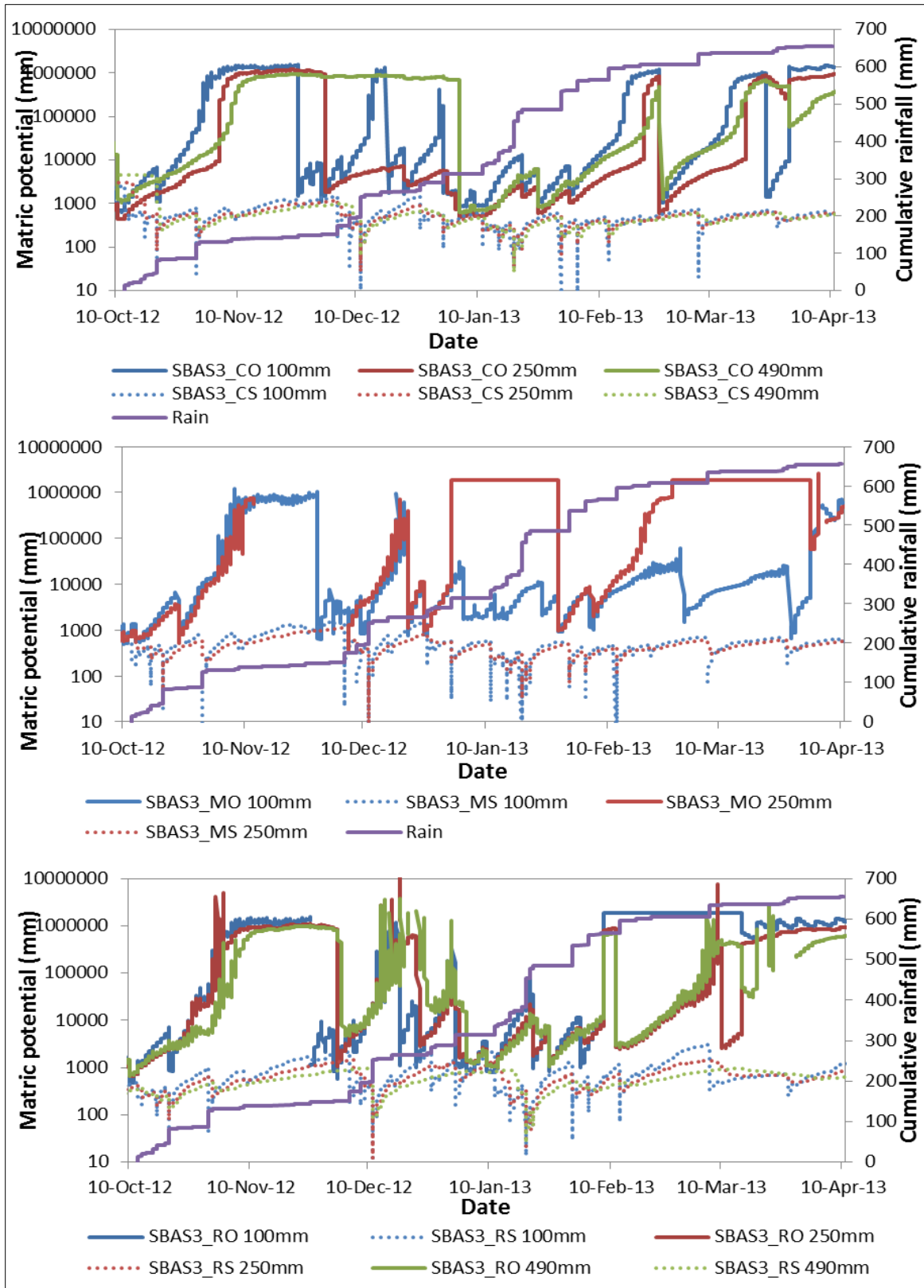


Figure 5.23 Observed and simulated responses for 3rd order basalt hillslope

## 5.5.2 Model sensitivity analysis

In order to assess how sensitive HYDRUS 1D was to input parameters; a sensitivity analysis was performed for one of the catena elements (Refer to section 3.15 for more details on calculations). The results from the analysis are presented in Table (5.5).

Table 5.5 Sensitivity analysis using 2<sup>nd</sup> order granite midslope catena element

SGR2 Mid							
	Original run	+50%ET	-50%ET	+50Rain	-50Rain	Soil low K	Soil high K
Unit	mm	mm	mm	mm	mm	mm	mm
P	638	638	638	956	319	638	638
ET <sub>H</sub>	507	546	347	595	326	517	505
R	0	0	0	0	0	0	0
FD	120	93	230	320	0	105	124
ΔS	10	-2	60	42	-7	16	9
Percent change from original							
Unit		%	%	%	%	%	%
P		0	0	50	-50	0	0
ET <sub>H</sub>		8	-32	17	-36	2	0
R		0	0	0	0	0	0
FD		-23	92	167	0	-13	3
ΔS		-120	500	320	-170	60	-10
Total		143	592	504	206	75	13
max-min		449		298		62	

P – Precipitation, ET<sub>H</sub> – evapotranspiration simulated using Hydrus, R – runoff, FD – free drainage and ΔS – the change in storage

The results illustrated in Table (5.5) above show that HYDRUS 1D was most sensitive to an increase or decrease in actual ET. A 50 % increase in the amount of actual ET has shown a negative water balance (-2 mm) and a 50 % decrease in actual ET giving a water balance of 60 mm. A calculation of the differences between the maximum and minimum percentage changes from original was 449 mm for actual ET (Table 5.5) which was the highest value of all three

parameters. This shows how sensitive the model was to the parameter (actual ET), hence accurate characterization, modelling or measure of actual ET is therefore, of fundamental importance for credible output results.

Moderate sensitivity was shown from a 50 % increase and decrease in rainfall giving water balances of 42 mm and -7 mm, respectively. Calculated difference between percent changes of variables from original was 90 which was also an intermediate value for the three parameters under analysis. The model also showed that an increase or decrease in rainfall yielded an increase and decrease in the amount of actual  $ET_H$  and free drainage, respectively, which showed its sensitivity to rainfall. The accurate recording and measurement of rainfall in the study sites for use on this model therefore, becomes important.

Although not anticipated, soil hydraulic properties were shown to be the parameter that the model was least sensitive to. Soil properties are known to be the first order controls of hydrological responses therefore, the anticipation was for the model to be highly sensitive to changes in soil hydraulic properties but results turned out otherwise. Nevertheless, the model did show some sensitivity to soil hydraulic properties therefore, precision is still called for in the determination of these since changes were detected in all components of the water balance by a change of the  $K_{sat}$  values.

The model was parameterized by point measurements to give spatial data, an element of uncertainty was therefore, introduced. This therefore, indicates the need for more replicates for a representative average for the area under observation. In conclusion, HYDRUS 1D was shown to have different levels of sensitivity to different input parameters. In this study uncertainty was therefore, introduced where actual  $ET_{SEB}$  used to drive the model was modelled using SEBAL and by so doing this means that output from another model was used to inform another model, hence there is some uncertainty involved in the model output. The uncertainty in SEBAL is in the selection of end members for canopy cover which has a significant effect on estimation of the net heat flux which in turn affect the amount of actual ET (Timmermans *et al.*, 2006). According to Hughees (2008) knowing the uncertainties of a model helps in deciding whether or not it would be viable to integrate the output data depending on how credible the results are.

## 5.6 Updated Conceptual Models from Observed and Simulated Data

Conceptual models were updated using both the observed data ( $K_{sat}$ ,  $K_{unsat}$  and hydrogeological surveys) and simulated data. Results presented below show the initial concepts (desktop) and the updated concepts embraced after observations, measurements and the modelling.

The 1<sup>st</sup> order hillslope was dominated by interflow soils (Figure 5.24). Results from the model showed more water leaving the domain through free drainage (potential recharge) and less was shown for lateral flow. The simulated results showed that free drainage was experienced after the two high intensity events in October, hence the high percentage. Therefore, under low to medium intensity events, the dominant flowpath will be subsurface lateral flow with a possibility of return flow at the toeslope of this hillslope. Unlike the 2<sup>nd</sup> and 3<sup>rd</sup> order hillslopes, the 1<sup>st</sup> order hillslope shows connectivity with the adjacent 1<sup>st</sup> order stream through lateral flow.

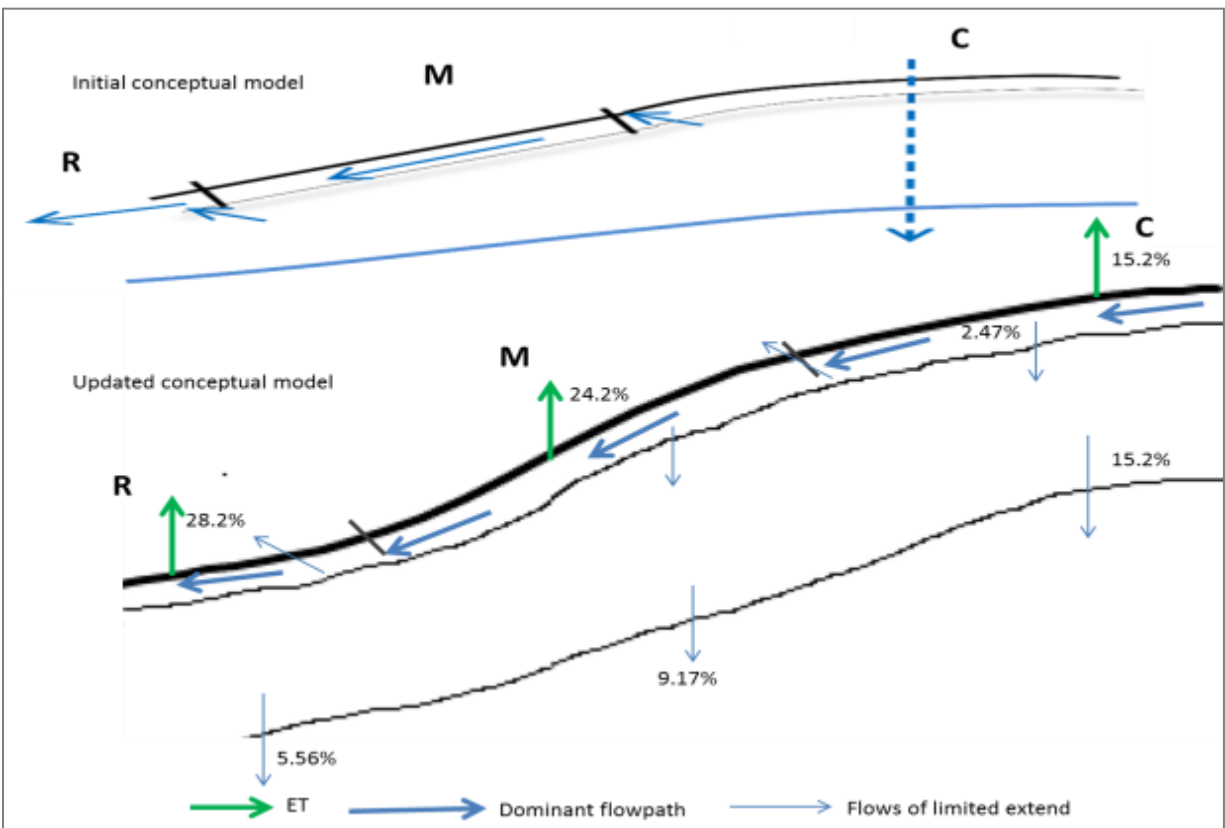


Figure 5.24 Initial and updated conceptual model for 1<sup>st</sup> order granite hillslope

The 2<sup>nd</sup> order hillslope (Figure 5.25) was dominated by interflow (lateral). Similar to the 1<sup>st</sup> order, free drainage showed high percentages as well after the high intensity rainfall events (October and January), therefore, under low to medium intensity rainfall events (<10 mm/hr), the hydrogeological interpretations were still embraced for this hillslope. The midslope was characterized as responsive but since it did not generate overland flow even after high intensity events, this implied subsurface flow. Since there were duplex soils on this catena element, flow would be restricted in the B horizon resulting in interflow at the A/B interface. High potential recharge on the riparian zone supported the hydrological disconnection between this hillslope and the adjacent stream network for the greater part of the season.

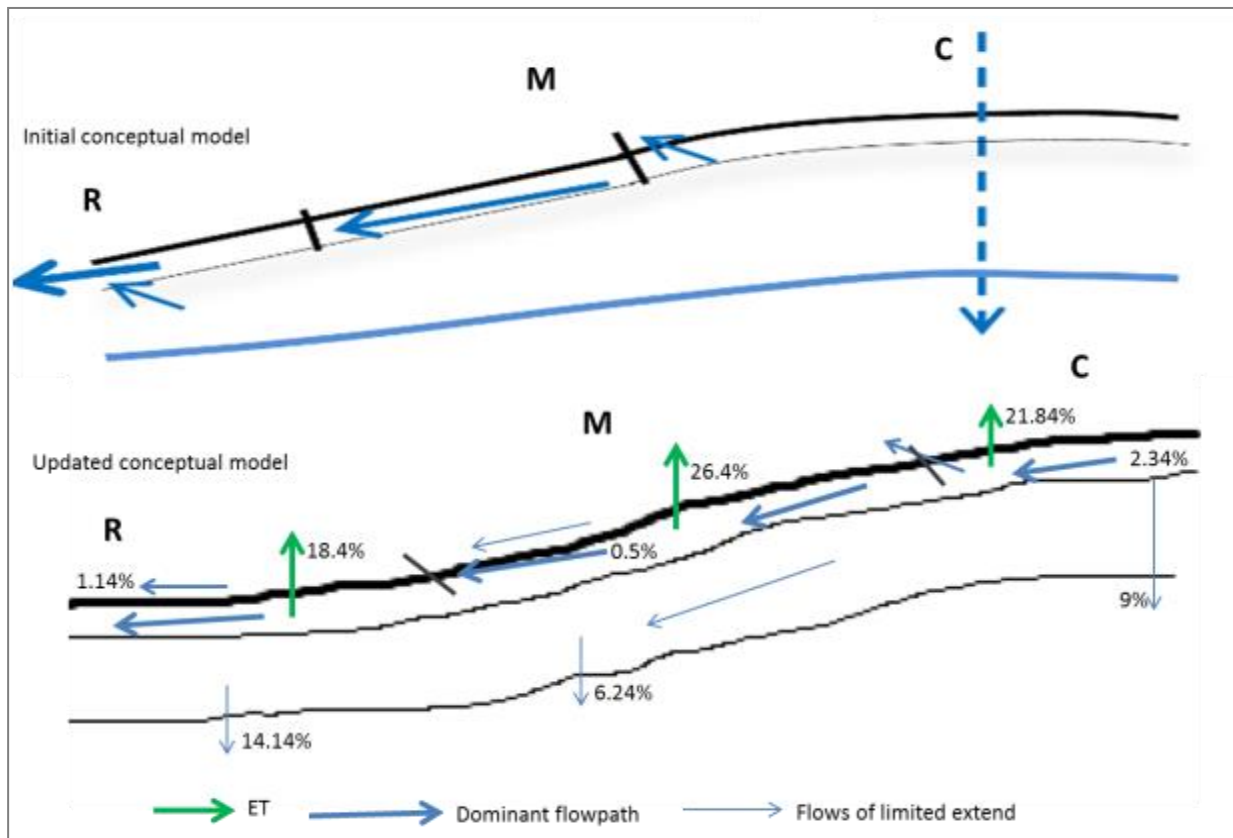


Figure 5.25 Initial and updated conceptual model for 2<sup>nd</sup> order granite hillslope

The 3<sup>rd</sup> order hillslope was initially anticipated to have recharge soils on the crest and interflow (lateral) on the midslope and riparian zone soils (Figure 5.26) overleaf. Through hydrogeological surveys and conductivity data, the crest comprises interflow soils; the midslope

was classified as responsive, whilst the riparian has recharge soils. Similar to the 1<sup>st</sup> and 2<sup>nd</sup> order, hydrogeological interpretations supported by the  $K_{sat}$  data were still embraced. Although free drainage (potential recharge) was showing high percentages this was only in response to the high intensity events (October 2012 and January 2013) events. The hydrogeological classification mentioned above was therefore, embraced.

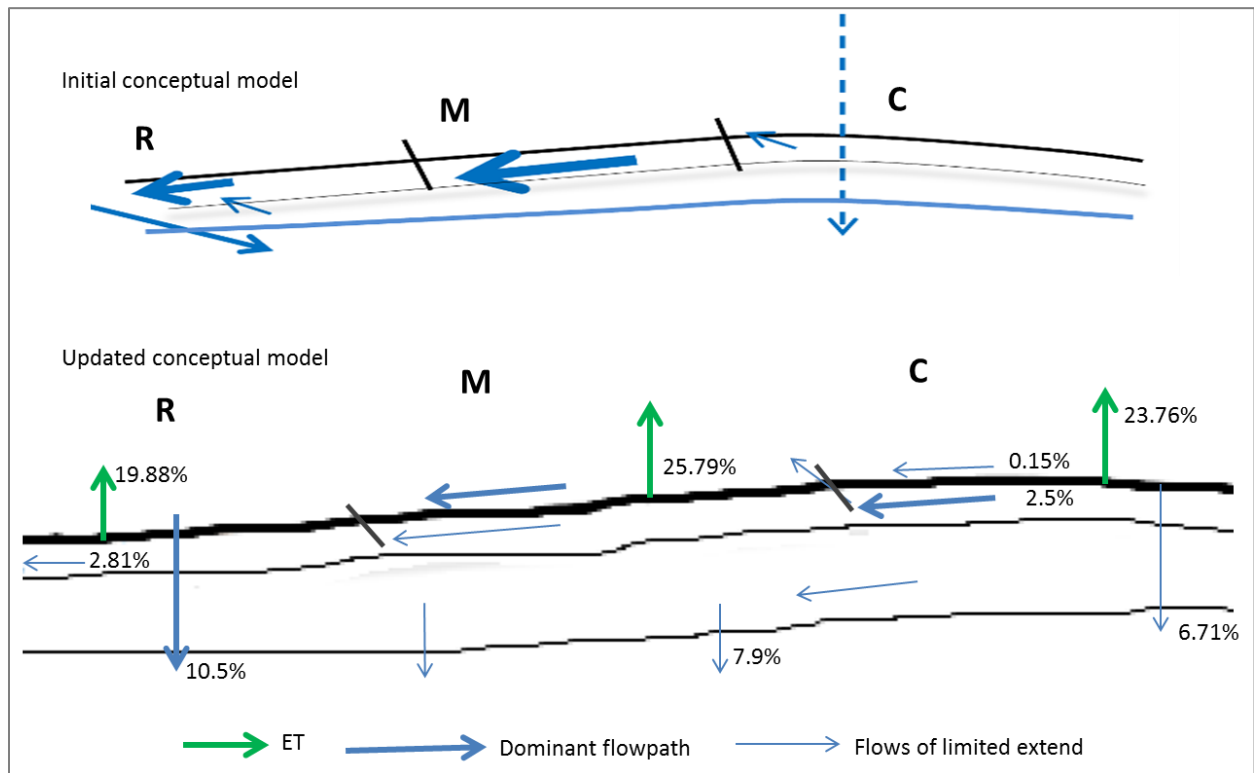


Figure 5.26 Initial and updated conceptual model for 3<sup>rd</sup> order granite hillslope

A comparison of the 3 hillslopes showed that a lot of water was being lost through  $ET_H$  with the 3<sup>rd</sup> order hillslope losing the greatest amount. This showed the extent to which savanna vegetation uses available water and the high evaporative demand. The modelled responses showed that there was free drainage only after high intensity events (October and January). This showed that a threshold rainfall amount and/or intensity is required for certain responses, such as free drainage and connectivity between hillslope and stream components. Interflow was the dominant flowpath on the granite hillslopes whilst in the basalts it was vertical subsurface flow (potential recharge).

The basalt hillslope was initially conceptualized to have potential recharge soils, through hydrogeological surveys; this concept was embraced (Figure 5.27). Meanwhile, outputs from the model showed that they could be responsive as well. Overland flow was only anticipated after high intensity events but results showed otherwise. Based on field observations, surface ponding was observed on the hillslopes after the January high intensity events. The possibility of runoff generation was minimal therefore the initial concept of vertical subsurface flow with some surface ponding is still embraced.

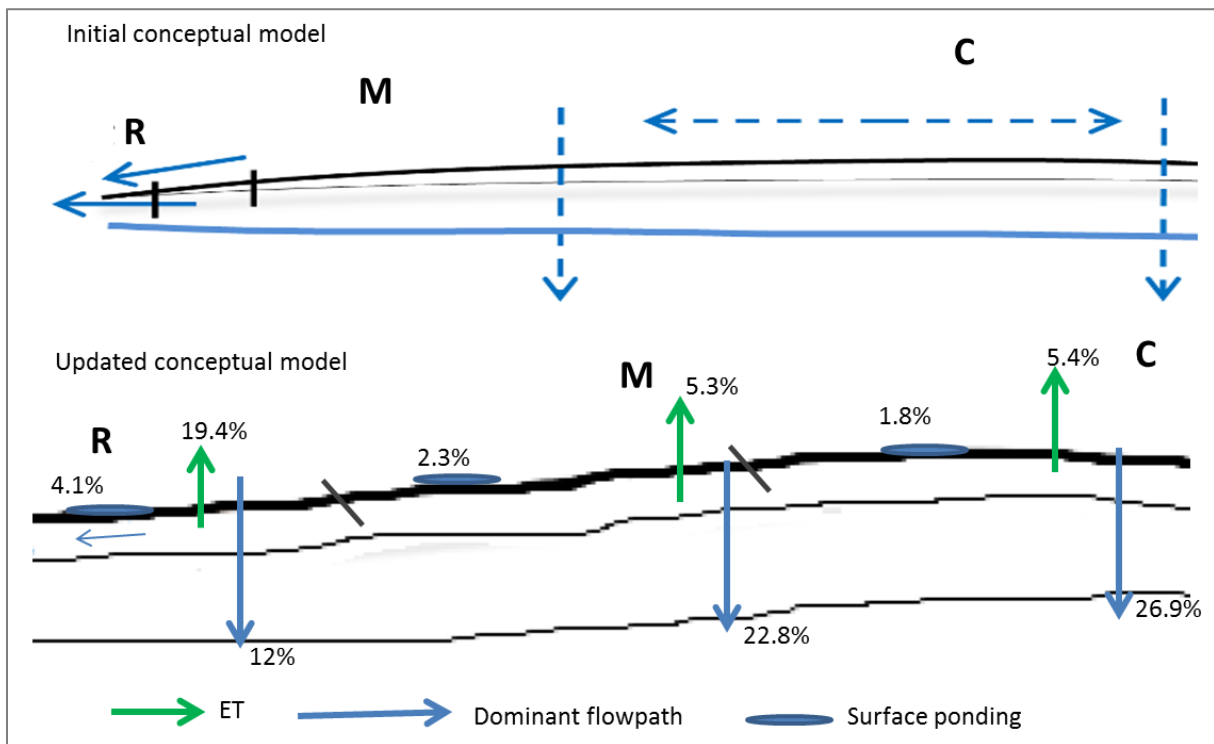


Figure 5.27 Initial and updated conceptual model for 3<sup>rd</sup> order basalt hillslope

In conclusion, part of the aim of this study was to quantify the differences in hydrological responses at different scales and different parent materials. Using the modelling exercises, fluxes were calculated to help improve the understanding of processes on the two sites. Actual  $ET_H$  was shown to be high in the granites compared to the basalt site. Meanwhile, on the granite hillslopes, the 3<sup>rd</sup> order had the highest water use compared to the 1<sup>st</sup> and 2<sup>nd</sup> order hillslopes. Free drainage (potential recharge) showed the highest percent flux than other fluxes on the

hillslopes at both sites. The observation made from this was that this was only due to two high intensity events (October and January). On the granite site the hydrogeology classes and dominant flow paths were embraced since free drainage could not be made the dominant flowpath just from big responses to two events. Lateral flow could not be quantified properly since a 2D model was required for that but estimates could be calculated.

## 6. SYNTHESIS

The review of literature showed that, although hillslope hydrology has been well studied and documented in the past it still remains challenging. According to Ridolfi *et al.* (2003), this is because processes interact and operate differently at various scales due to heterogeneity within the vadose zone and the surface biotic components, hence the need to do more research in order to gain insights into this heterogeneity.

Results of this study have shown how rainfall in savanna areas is highly variable. A comparison of rainfall received and intensities for the two sites showed much variability. The granite site showed many dry spells during the wet season compared to the basalt site. Knowledge of these in between dry periods is crucial especially in savannas where erratic rainfalls are experienced (Falkenmark and Rockstrom, 2004). This is important for water resources managers because dry spells can be managed compared to other phenomena, such as meteorological droughts therefore, this helps in strategic planning for ecosystem sustainability. The review of literature shows that the study of flow paths and flow mechanisms on hillslopes is crucial for an understanding of water storage during wet seasons and its subsequent release during dry periods (discussed above) for ecosystem sustainability, predominantly in the small catchments and water-limited environments (Lin *et al.*, 2006). Overland flow, subsurface saturated or unsaturated flow and bedrock flow were then shown to be the major flow paths on a hillslope determined by soil physical properties and parent material (Ticehurst *et al.*, 2007; van Tol *et al.*, 2013). This led to the hypothesis that vertical subsurface flow will dominate on the granite crest catena elements because they are characterized by sandy soils (high hydraulic conductivity) since most clay particles would be washed downslope by colluvial processes. Results have shown this hypothesis to be invalid and all the granite crests comprise lateral flows having an increase in amounts of free drainage only after high intensity rainfall events (October 2012 and January 2013 events). There were loamy sands on the crests as shown by the texture data but due to some impeding layers underneath shown by saturated hydraulic conductivity results and soil classification, lateral flow became dominant.

Topography has been shown to have an impact on responses at the hillslope scale (Tromp-van Meerveld and McDonnell, 2006). It was therefore, hypothesized that there will be lateral contributions to downslope catena elements due to the slope in the granites which will ultimately result in hydrological connectivity between elements. This hypothesis was valid for some catena elements of the hillslope but not all of them. The 1<sup>st</sup> order showed full connectivity, whilst the 2<sup>nd</sup> and 3<sup>rd</sup> order showed temporal connectivity on midslope and riparian elements after high intensity rainfall events. This suggested that connectivity was therefore, temporal on this site and was mainly driven by rainfall intensity.

Hillslopes on the granite supersite were longer in the higher orders which therefore, meant that the travel time for water reserves would be higher in the 3<sup>rd</sup> order compared to the 2<sup>nd</sup> and 1<sup>st</sup> order hillslopes. This was another reason why connectivity was shown in the 1<sup>st</sup> order hillslope and became intensity-driven at higher order hillslopes. Processes such as overland flow and subsurface flow are affected by travel time. This therefore, means that on a longer hillslope, such as the 3<sup>rd</sup> order, some of the overland flow or subsurface flow might be lost to evaporation before reaching the downslope elements or deeper soil layers. Meanwhile, overland flow on a low order hillslope will take less time to connect with downslope elements because of a short travel time. This also explains the disconnection between hillslopes and stream networks in the 2<sup>nd</sup> and 3<sup>rd</sup> order, hence showing the influence of scale on processes.

Due to low topography in the basalts, it was hypothesized that the hillslopes will be characterized by vertical subsurface flow and no lateral contributions from interfluves to downslope elements (disconnected elements). This hypothesis was shown to be valid and that most of the water was lost through evapotranspiration especially in the riparian zones likely due to greater woody vegetation cover there. Results from the model however, suggest connectivity between elements through overland flow on the third order hillslope. Overland flow was only anticipated on this site as a consequence of high intensity events but simulated results show otherwise. The initial concept of vertical subsurface flow with the absence of overland flow on these hillslopes is still embraced since no runoff was observed but rather ponded water due to low gradient topography.

Soils and hydrology were reported to have an interactive relationship where soils properties control hydrological responses whilst their morphology can be used as indicators of hydrological regimes (le Roux *et al.*, 2011; van Tol *et al.*, 2013). Unsaturated hydraulic conductivity was hypothesized to be high on the on the granites due to sandy soils characteristic of granite-derived soils compared to basalt soils that have a high clay content. This was shown to be true to a certain extent. Unsaturated hydraulic conductivity was high on the majority of the catena elements in the granites compared to the basalts but the 2<sup>nd</sup> and 3<sup>rd</sup> order granite midslopes had low unsaturated hydraulic conductivity due to accumulation of clay soils washed from the crest through colluvial processes.

Simulated results also show the 2<sup>nd</sup> and 3<sup>rd</sup> order granite midslopes to have more water loss through evaporation than transpiration as was the case for all other catena elements. This was attributed to the absence of a dense woody cover and herbaceous vegetation but nevertheless showing evidence of a high evaporative demand on the elements. Savanna vegetation was also shown to have an ability to extract large amounts of water once soil water is available. According to, Falkenmark and Rockstrom (2004), for those who rely on savannas for food production, transpiration cannot be easily influenced since an increase in the production of food will ultimately lead to increased plant water use. Nevertheless, evaporation can be controlled through land use management since a high demand has been shown for such ecosystems.

Water movement in the soil is driven by gradients in soil water potential (Buckingham, 1907). Finer soils are more capable of holding water therefore soil water potential was hypothesized to be lower in the basalts because clay soils have higher water retention capacity, hence less soil water potential compared to sandy soils. This was shown to be valid by the laboratory results were granite soils had high water potential, thereby water was able to move with ease in and out of the system compared to the basalt-derived soils.

Through literature review, hydrological processes were shown to vary with lithological differences (Lin *et al.*, 2006). This study also proved how the underlying parent material influences process, such as flow mechanisms, but to a lesser extent, since topography, rainfall intensity and soil hydraulic properties were shown to be the main contributors. In terms of soil

depth, the basalt hillslopes have shallow soils at high order hillslopes and vice versa whilst the granites have shallow soils upslope and vice versa. Areas with deep soils, such as the 1<sup>st</sup> order riparian zone were anticipated to have more storage (potential storage) than their counterparts with shallow soils, such as the crest but simulation results proved otherwise. The riparian catena element had negative actual storage whilst the crest had the greatest. Soil depth was however, shown to have less notable effects on actual storage due to ET. A study in the North of Kruger showed that soil hydraulic properties limit or increase the amount of water available for transpiration not necessarily soil depth (Riddell *et al.*, 2013). This therefore, means more water retention in the basalts and less transpiration compared to the granites (Lorentz *et al.*, 2006).

High rainfall intensity resulted in different responses on both sites in this study. Connectivity between catena elements, response of deeper soil layers especially in the basalts and generation of free drainage (both sites) was shown to be driven by rainfall intensity. This suggested temporal connectivity. For the greater part of the season, this study showed a disconnection between hillslopes and their adjacent stream networks. In the granites, connectivity was shown in the 1<sup>st</sup> order but moving up the orders, it becomes highly spatial and temporal implying scale influence on processes. According to, McGuire and McDonnell (2010), hydrological connectivity can be dynamic where it might occur episodically and seasonally.

Scale is also shown to have an influence by results from hillslope hydrological soil types which show interflow soils only at the 1<sup>st</sup> order suggesting uniformity in distribution. Meanwhile, moving up the stream orders variability is shown with some elements on a hillslope (such as the 2<sup>nd</sup> order riparian zone) showing responsive soils with a possibility of interflow (soil profile heterogeneity). This shows landscape complexity with an increment in stream orders. In a study by Khomo and Rogers (2009) on the Phugwane river network in KNP, geomorphology was shown to become more complex with an increase in stream order and geomorphology will influence hydrological responses. This is evidence of scale influence on these hillslope processes.

Differences in hydrological responses were shown at different scales and parent materials through characterization and quantification exercises which was the overarching aim of the

research. For an ecosystem to be effectively managed, hydrological processes need to be well understood. Semi-arid savanna ecosystems are highly sensitive to change therefore, given the ever-increasing population growth it therefore, becomes imperative not to ignore how the system functions even in small ephemeral catchments since people depend on these landscapes for subsistence.

## 7. CONCLUSIONS

### 7.1 General Conclusions

Although the study of hillslope hydrology is challenging due to a number of different processes operating and interacting in the vadose zone, it nevertheless provides a building block that exhibits some form of organization useful in classification and conceptualization of processes (Weiler and McDonnell, 2004; van Tol *et al.*, 2013). Conclusions drawn from this study are discussed below.

Rainfall intensity has an impact on hydrological responses such as connectivity and runoff generation. Since savannas are known to have erratic and variable rainfall characterized by high intensity events, this implies temporal hydrological connectivity and runoff on these sites.

Although topography and soil properties are influenced by parent material, they were shown to have an influence on hydrological responses than parent material. However, scale (incremental stream orders) was shown to have an influence on the hillslope hydrological responses, such as flow mechanisms and connectivity. Processes tend to be highly spatial and temporal on the higher orders compared to the 1<sup>st</sup> order. Hillslope storage was controlled by ET demand rather than soil depth, in savanna ecosystems. This was interesting since storage was assumed to be more significant on catena elements with deep soils.

Knowledge of these flow mechanisms and storage is fundamental in savannas since many people rely on them for biodiversity, ecosystem goods and services. This is especially important for water resources managers since water is the major driver of ecosystem functions. Knowledge of how the system works would then be used for water resource allocation, land use management and for prediction of hydrological behavior in ungauged systems that are in similar water-limited settings.

## 7.2 Recommendations

The first recommendation is the use of a user friendly 2D/3D hydrological model to simulate flow which would help in understanding storage but most importantly lateral fluxes which would help explain connectivity and give estimates of contributions through lateral flow. 1D offers a simple way to understand the functioning of a system especially the vertical fluxes. A 2D/3D model would also be useful since output results can be used to test the hydrogeological classes (van Tol *et al.*, 2013) since the classification is still in its infancy and this would also help in making improving the classification (if necessary), provided suggestions are welcome.

Understanding hillslope connectivity is important since it provides insights into flow paths and residence times therefore the use of tracers, such as stable isotopes in hillslope subsurface water would validate the present hypothesis on connectivity as provided in this study.

Soil hydraulic properties were shown to have much variability even within a very small area, thereby resulting in some uncertainty in the results. In future studies, more replicates are therefore, recommended to enable the calculation of averages for better representation and reliability of results.

The use of runoff plots would have been ideal in this study but could not be installed because of the presence of wild animals. This would have helped in the comparison of simulated results against observed data especially on the catena elements where model output show runoff, such as the granite 2<sup>nd</sup> order riparian and 3<sup>rd</sup> order crest zone.

To increase the knowledge base, it would be interesting for a similar study to be carried out in the northern supersites where less rainfall is received for a comparison of processes across rainfall gradients.

## 8. REFERENCES

- Abem Instrument AB, Sweden: Available from <http://www.abem.com/software.php> [Accessed May 2012].
- Ahmad, MD, Bastiaanssen, WGM and Feddes RA. 2005. A new technique to estimate net groundwater use across large irrigated areas by combining remote sensing and water balance approaches. *Hydrogeology Journal*. Volume 13 Number 5-6:653-664.
- Allen, RG, Pereira, LS, Raes, D and Smith, M. 1998. Crop evapotranspiration: Guidelines for computing crop water requirements. FAO Irrigation and Drainage Paper, No. 56, FAO, Rome.
- Allen, JF and Chambers, N. 2007. PLOW: A collaborative task learning agent. AAAI. Vancouver, BC.
- Amoozegar, Abit, SM, A, Vepraskas, MJ and Niewoehner, CP. 2008. Solute transport in the capillary fringe and shallow groundwater: Field evaluation. *Vadose Zone Journal* 7(3): 890-898.
- Anderson, MG and Burt, TP. 1978. Experimental investigations concerning the topographic control of soil water movement on hillslopes. *Geomorphology Supplement band* 29:52-63.
- Anderson, MG and Burt, TP. 1990. *Process Studies in Hillslope Hydrology: An overview* John Wiley and sons, Chichester.
- Ankeny, MD, Ahmed, M, Kaspar, TC and Horton, R. 1991. Simple field method for determining unsaturated hydraulic conductivity. *Soil Science of America Journal* 55:467-470.
- Artiola J, Pepper IL and Brusseau ML (Eds). 2004. *Environmental monitoring and characterization*. Elsevier Academic Press, San Diego.
- Asano, Y, Uchida, T and Ohte, N. 2002. Residence times and flow paths of water in steep unchannelled catchments, Tanakami, Japan. *Journal of Hydrology*. 261:173-192.
- Avanzi, D'Amato, G, Giannecchini, R and Puccinelli, A. 2004. The influence of the geological and geomorphological settings on shallow landslides: An example in a temperate climate environment: the June 19, 1996 event in northwestern Tuscany (Italy). *Engineering Geology*, 73(3):215-228.

- Bastiaanssen, WGM, Menentia, M, Feddesb, RA and Holtslagc, AAM. 1998. A remote sensing surface energy balance algorithm for land (SEBAL) 1. Formulation. *Journal of Hydrology* 212-213 and 198-212.
- Bastiaanssen, WGM, Ahmad, MD and Chemin, Y. 2002. Satellite surveillance of evaporative depletion across the Indus Basin. *Water Resources Research* (in press).
- Bastiaanssen, WGM, Ahmad, MD, and Feddes RA. 2005. A new technique to estimate net groundwater use across large irrigated areas by combining remote sensing and water balance approaches. *Hydrogeology Journal*. Volume 13 Number 5-6:653-664.
- Bergkamp, G. 1998. A hierarchical view of the interactions of runoff and infiltration with vegetation and microtopography in semiarid shrublands. *Catena*, 33, pp. 201–220.
- Berthold, S, Bentley, LR and Hayashi, M. 2004. Integrated hydrogeological and geophysical study of depression-focused groundwater recharge in the Canadian prairies. *Water Resources Research*. 40(6):W06505.
- Blöschl, G and Sivapalan, M. 1995. Scale issues in hydrological modelling: a review. *Hydrological processes*, 9(3-4):251-290.
- Blöschl, G. 2001. Scaling in hydrology. *Hydrological Processes* 15:709–711.
- Boisvenue, C and Running, SW. 2006. Impacts of climate change on natural forest productivity evidence since the middle of the 20th century. *Global Change Biology*. 12(5):862–882.
- Bogaart, P and Troch, PA. 2006. Curvature distribution within hillslopes and catchments and its effect on the hydrological response.
- Bouma, J. 2006. Hydropedology as a powerful tool for environmental policy research. *Geoderma*.131:275–286.
- Bracken LJ, and Croke J. 2007. The concept of hydrological connectivity and its contribution to understanding runoff-dominated geomorphic systems. *Hydrological Processes* 21:1749–1763.
- Buckingham, E. 1907. Studies on the movement of soil moisture. U.S. Department of agriculture. Soils Bulletin. 38.
- Buttle, JM. 1994. Isotope hydrograph separations and rapid delivery of pre-event water from drainage basins. *Program Physical Geography* 18:16–41.
- Buttle JM, Dillon PJ and Eerkes GR. 2004. Hydrologic coupling of slopes, riparian zones and streams: an example from the Canadian Shield. *Journal of Hydrology* 287:161–177.

- Cal Africa. 1978. Watermark ® Electric resistance granular matrix sensor. [Internet]. Cal Africa efficient irrigation scheduling systems. Available from <http://www.calafrica-sa.co.za/watermark.htm>. [Accessed: 3 March 2014].
- Cammeraat, LH. 2002. A review of two strongly contrasting geomorphological systems within the context of scale. *Earth Surface Processes and Landforms* 27 (11):1201–1222.
- Chamran, F, Gessler, PE and Chadwick OA. 2002. Spatially explicit treatment of soil water dynamics along a semi-arid catena. *Soil Science Society of America Journal* 66:1571-1583.
- Cleugh HA, Leuning R, Mu, Q and Running, SW. 2007. Regional evaporation estimates from flux tower and MODIS satellite data *Remote Sensing of Environment*, 106. Pp 285–304.
- Colgan, MS, Asner, GP, Levick, SR, Martin, RE and Chadwick OA. 2012. Topo-edaphic controls over woody plant biomass in South African savannas. Published by Copernicus Publications on behalf of the European Geosciences Union.
- Cullum, C and Rogers, K. 2011. A Framework for the Classification of drainage networks in Savanna Landscapes. Report to the Water Research Commission. Draft Final Report WRC Report No K5/1790.

- Doorenbos, J and Pruitt, WO. 1977. Crop Water Requirements FAO Irrigation and Drainage Paper 24 FAO, Rome, p. 144.
- Dye, PJ and Croke, BFW. 2003. Evaluation of Streamflow Predictions by the IHACRES Rainfall-Runoff Model in Two South African catchments Environmental Modelling and Software, 18. pp. 705–712.
- Elhaddad, A, Garcia, LA. 2008. Surface Energy Balance-Based Model for Estimating Evapotranspiration Taking into Account Spatial Variability in Weather. ASCE Journal of Irrigation and Drainage – 134(6) 681-689.
- Falkenmark, M and Rostrom, J. 2004. Balancing water for humans and nature: The new approach in Ecohydrology. ISBN 1-85383-927-2.
- Farah, HO. 2001. Estimation of regional evaporation under different weather conditions from satellite and meteorological data. PhD Thesis, Department of Water Resources, Wageningen University, pp 170.
- Freeman, MC, Pringle, CM and Jackson, CR. 2007. Hydrologic connectivity and the contribution of stream headwaters to ecological integrity at regional scales. *Journal of the American Water Resources association* 43:5–14.
- Freer, J, Moore, J and Donnelly, R. 1997. GRAZPLAN: decision support systems for Australian grazing enterprises. II. The animal biology model for feed intake, production and reproduction and the Graz Feed DSS Agricultural Systems, 54, pp. 77–126.
- Freer, J, McDonnell, JJ, Beven, KJ, Peters, NE, Burns, DA, Hooper, RP and Aulenbach, B. 2002. The role of bedrock topography on subsurface storm flow. *Water Resources Research* 38: 1269, DOI: 1210.1029/2001WR000872.
- Gómez-Plaza, A, Alvarez-Rogel, J, Albaladejo, J, and Castillo, VM. 2001. Spatial patterns and temporal stability of soil moisture across a range of scales in a semi-arid environment. *Hydrological Processes*. 14:1261–1277.
- Graham, CB, Woods, RA and McDonnell, JJ. 2010. Hillslope Threshold Response to Rainfall: A field forensic approach. *Journal of Hydrology*: 393:965-76).
- Grayson, R and Bloschl, G. (Eds.). 2000. Spatial Pattern in Catchment Hydrology: Observations and Modelling. Cambridge University Press, Cambridge, UKdoi:10.1006/rwas.2002.0172.

- Guan Spence, C, Phillips, XJ, Hedstrom, R, Granger, N and Reid, B. 2010. Storage dynamics and streamflow in a catchment with a variable contributing area. *Hydrological Processes*, 24(16):2209-2221.
- Haga, H, Matsumoto, Y, Matsutani, J, Fujita, M, Nishida, K and Sakamoto, Y. 2005. Flow paths, rainfall properties, and antecedent soil moisture controlling lags to peak discharge in a granitic unchanneled catchment. *Water Resources Research* 41: W12410. DOI:10.1029/2005WR004236.
- Hamby, DM. 1994. A review of techniques for parameter sensitivity analysis of environmental models. *Environmental Monitoring and Assessment* 32:135–154.
- Hernandez, ME and Mitsch WJ. 2007. Influence of hydrologic pulses, vegetation, and season on nitrous oxide emissions from created riparian marshes. *Wetlands*, 26, pp. 862–877.
- Hjalmar, L, Viktor, S, Ishi, B, Jan, S and Magnus, M. 2007. The role of catchment scale and landscape characteristics for runoff generation of boreal streams. *Journal of Hydrology* 344:198– 209.
- Hubbard, CM. 1998. Hydrologic Modelling of the Missouri River Basin in a Climate Change Model. MS. Thesis, University of Nebraska-Lincoln, Lincoln, Nebraska.
- Hughees, DA. 2008. Hydrological Information Requirements and Methods to Support the Determination of Environmental Water Requirements in Ephemeral River Systems. WRC Report 9. KV 205/08.
- Jacobs, SM, Bechtold, JS, Biggs, HC, Grimm, NB, Lorentz, S, McClain, ME, Naiman, RJ, Perakis, SS, Pinay, G and Scholes, MC. 2007. Nutrient Vectors and Riparian Processing: A Review with Special Reference to African Semiarid Savanna Ecosystems. *Ecosystems* (10:1231–1249 DOI:10.1007/s10021-007-9092-1).
- Jakeman, AJ, Letcher, RA and Norton, JP. 2006. Ten iterative steps in development and evaluation of environmental models. *Environmental Modelling and Software* 21 (5):602-614.
- Jencso, KG, McGlynn, BL, Gooseff, MN, Wondzell, SM, Bencala, KE and Marshall, LA. 2009 Hydrologic connectivity between landscapes and streams: transferring reach and plot scale understanding to the catchment scale. *Water Resources Research* 45:W04428. doi:10.1029/2008WR007225.

- Jewitt, G and Görgens, AHM. 1995. Can Vaal Dam Basin Runoff be Augmented by Convective Cloud-seeding? Proceedings of the 7<sup>th</sup> South African National Hydrology Symposium. Rhodes University, Grahamstown.
- Johnson, RC. 1991. Effects of Upland Afforestation on Water Resources The Balquhiddy Experiment 1981–1991. Rep. 116 Institute of Hydrology, Wallingford, UK, p. 73.
- Karvonen, T, Koivusalo, H, Jauhiainen, M, Palko, J. and Wepling, K. 1999. A hydrological model for predicting runoff from different land use areas. *Journal of Hydrology*. 217, pp. (253-265).
- Khomo, L and Roger, KH. 2009. Stream order controls geomorphic heterogeneity and plant distribution in a savanna landscape. *Austral Ecology*, 34, pp. 170–178.
- Kokwaro, JO and Gillett, JB. 1980. Notes on the Anacardiaceae of Eastern Africa. *Kew Bull*, 34:745–760.
- Lane, SN and Richards, KS. 1998. Two-dimensional modelling of flow processes in a multi-thread channel. *Hydrological Processes*, 12, pp. 1279–1298.
- Le Roux, PAL and du Preez CC. 2006. Nature and distribution of South African plinthic soils: Conditions for occurrence of soft and hard plinthic soils. *S. Afr. J. Plant Soil* 23, 120-125.
- Le Roux, PAL, van Tol, JJ, Kuenene, BT, Hensley, M, Lorentz, SA, Everson, CS, van Huyssteen, CW, Kapangaziwiri, E and Riddell, E. 2011. Hydropedological interpretations of the soils of selected catchments with the aim of improving the efficiency of hydrological models. Water Research Commission Report No. 1748/1/10.
- Le Roux, PAL, du Plessis, MJ, Turner, DP, van der Waals, J and Booyens, HB. 2013. South African Soil Surveyors Organisation Field Book for classification of South African soils. Reach Publishers, Wandsbeck, South Africa. ISBN 978-0-620-55039-0.
- Lenhart, T, Eckhardt, K, Fohrer, N and Frede, HG. 2002. Comparison of two different approaches of sensitivity analysis. *Physics, Chemistry, Earth* 27:645–654.
- Lin, HS, Kogelmann, W, Walker, C and Bruns, MA. 2006. Soil moisture patterns in a forested catchment: A hydropedological perspective. *Geoderma*.131:345-368.
- Lin, HS, Bouma, J, Owens, P and Verpraskas, M. 2008. Hydropedology: Fundamental issues and practical applications. *Catena* 73, pp. (151 – 152).
- Liu, YB, Batelaan, O, De Smedt, F, Poórová, J and Velcická, L. 2005. Automated calibration applied to a GIS based flood simulation model using PEST. In: van Alphen J, van Beek

- E, Taal M (Eds) *Floods, from Defense to Management*. Taylor-Francis, London, pp 317–326.
- Lorentz, S, Thornton-Dibb, S, Pretorius, JJ and Goba, P. 2003. Hydrological systems modelling research programme hydrological processes: Phase II quantification of hillslope, riparian and wetland processes. Report K5/1061. Water Research Commission, Pretoria, RSA.
- Lorentz, S., Riddell, E., Koning, B., Grant, R. 2006. The Influence of Catena Soil Water Dynamics on the Vegetation Patch Structure in the Northern Plains, KNP. *HydroEcology* Karlovy Vary, Czech Republic, 11-14 September.
- Lorentz, SA, Burse, K, Idowu, O, Pretorius, C and Ngeleka, K. 2008. Definition and upscaling of key hydrological processes for application in models. Report No.K5/1320. Water Research Commission, Pretoria.
- Lorentz, SA, Riddell, ES, Nel, JM and le Roux, PAL. 2010. Groundwater, surface water and vadose zone interactions in selected pristine catchments in the Kruger National Park. Unpublished Water Research Commission proposal. University of Kwa-Zulu Natal. South Africa.
- Loke, MH. 1999. *Electrical imaging survey environment and engineering studies: A practical guide to 2-D and 3D surveys: Geometrics*, San Jose.
- Loke, MH. 2004. Tutorial: 2-D and 3-D electrical imaging surveys, available at: [www.geoelectrical.com](http://www.geoelectrical.com).
- Maranga, EK. 1986. An ecological perspective of the phytosociology of woody Acacia / herbaceous-understory complex. In: Hansen, R. M., Woie, B. M. and Child, R. D. (eds.), Proc. Conf. Agricultural Research Centre, Egerton College, Njoro, Kenya, April 1986, pp. 243-252.
- Marquez, J, Martinez-Carter, E, Dalmaso, A and Pastran OS. 2005. Protected areas of the province of San Juan II. The vegetation of the Provincial Park Iischigualasto. *Multequina* (Argentina) 14:1-27.
- Marsh, WM and Kaufman, MM. 2012. *Physical geography: Great systems and global environments*. Cambridge University Press, Cambridge, UK.

- Matríguez-Mena, M, Albaladejo, J and. Castillo, VM. 2001. Factors influencing surface runoff generation in a Mediterranean semi-arid environment: Chicamo watershed, SE Spain, *Hydrological Processes*, 12, 741-754, doi:10.1002/(SICI)1099-1085(199804)12:5<741:AI DHYP 622> 3.0.CO;2-F.
- McDonnell J. 2003. Where does water go when it rains? Moving beyond the variable source area concept of rainfall-runoff response. *Hydrological Processes* 17:1869-1875.
- McGlynn, BL, McDonnell, JJ and Brammer, DD. 2002. A review of the evolving perceptual model of hillslope flow paths at the Maimai catchments, New Zealand, *J. Hydrology* 257:1-26.
- McGuire, KJ, McDonnell, JJ, Weiler, M, Kendall, C, McGlynn, BL, Welker, JM and Seibert, J. 2005. The role of topography on catchment scale water residence time, *Water Resources Research*, 41, W05002, doi:10.1029/2004WR003657.
- McGuire, KJ and McDonnell, JJ. 2010. Hydrological connectivity of hillslopes and streams: Characteristic time scales and nonlinearities. *Water Resources Research*, Vol. 46, W10543, doi: 10.1029/2010WR009341.
- McNamara, JP, Chandler, D, Seyfried, M and Achet, S. 2005. Soil moisture states, lateral flow, and streamflow generation in a semi-arid, snowmelt-driven catchment. *Hydrological Processes*, 19(20):4023-4038.
- Moleele NM, Mainah, J. 2003. Resource use conflicts: the future of the Kalahari ecosystem *Journal of Arid Environments* 54, pp. 405–423.
- Montgomery, DR, Dietrich, WE, Torres, R, Anderson, SP, Hener, JT, and Loague, K. 1997. Hydrologic response of a steep unchanneled valley to natural and applied rainfall', *Water Resources Research*., 33, 91-109.
- Mosley, MP. 1979. Streamflow generation in a forested watershed, *Water Resources Research*, 15:795– 806.
- Mosley, MP. 1982. Subsurface flow velocities through selected forest soils, South Island, New Zealand, *J. Hydrology*., 55:65– 92.
- Muleta, MK and Nicklow, JW. 2005. Sensitivity and uncertainty analysis coupled with automatic calibration for a distributed watershed model. *Journal of Hydrology* 306 (1e4):127-145.
- Mulligan, M and Wainwright. 2004. Modelling and model building. Environmental modelling: Finding simplicity in complexity, 7-73.

- Newman, BD, Campbell, AR. and Wilcox, BP. 1998. Lateral subsurface flow pathways in a semiarid ponderosa pine hillslope, *Water Resources Research*. 34:3485–3496.
- Newman, BD, Wilcox, BP, Archer, SR, Breshears, DD, Dahm, CN, Duffy, CJ, McDowell, NG, Phillips, FM, Scalon, BR and Vivoni, ER. 2006. Ecohydrology of water-limited environments: A scientific vision. *Water Resources Research* 42:1-15.
- Nicolau, JM. 2002. Runoff generation and routing on artificial slopes in a Mediterranean-Continental environment: the Teruel coalfield, Spain *Hydrological Processes*, 16, pp. 631–647.
- Nieber, JL, Bauters, TWJ. Steenhuis, TS and Parlange, JY. 2000. Numerical simulation of experimental gravity-driven unstable flow in water repellent sand. *Journal of Hydrology* 231:295-307.
- O'Brien, K. 2006. Are we missing the point? Global environmental change as an issue of human security. *Global Environmental Change*, 16(1):1-3.
- O'Keefe, J and Rogers, KH. 2003. Heterogeneity and Management of the Lowveld Rivers in Du Toit, JT, Rogers, K and Biggs HC (Eds) *The Kruger Experience. Ecology and Management of savanna Heterogeneity*. Washington DC, Island Press.
- Orchard, CM, Lorentz, SA, Jewitt, GPW and Chaplot, VAM. 2013. Spatial and temporal variations of overland flow during rainfall events and in relation to catchment conditions. *Hydrological Processes*, 27(16):2325-2338.
- Pachepsky, YA and Rawls, WJ. 2002. Soil consistence and structure as predictors of water retention. *Soil Science Society of America*. J. 66:1115-1126.
- Peterson, R. 2011 Personal Communication relating to unpublished data for MSc in Geohydrology at the University of Western Cape.
- Petry, TM and Bryant, JT. 1993. Evaluation and use of the Decagon WP4 dewpoint potentiometer. In Proceedings of the Fall Meeting of the Texas Section of ASCE (pp 3-5).
- Podwojewski, P, Janeau, JL, Grellier, S, Valentin, C, Lorentz, S and Chaplot, V. 2011. Influence of grass soil cover on water runoff and soil detachment under rainfall simulation in a sub-humid South African degraded rangeland. *Earth Surface Processes and Landforms*, 36(7):911-922.

- Pollard, S, Shackleton, C, and Carruthers, J. 2003. Beyond the fence: People and the Lowveld landscape. In: du Toit J, Biggs H, Rogers KH, Eds. The Kruger experience: ecology and management of Savanna heterogeneity. Washington, DC: Island Press. pp 422–460.
- Pringle, C, Mary, C, Freeman, Catherine, M and Rhett Jackson, C. 2007. hydrologic connectivity and the contribution of stream headwaters to ecological integrity at regional scales.
- Puigdefábregas, J, del Barrio, G, Boer, MM, Gutiérrez, L and Solé Benet, A. 1998. Differential responses of hillslope and channel elements to rainfall events in a semi-arid area. *Geomorphology* 23:337–51.
- Riddell, ES, van Niekerk, A, Nel, JM, Thibela, D, de Klerk, M, Peterson, R. and Lorentz, SA. 2011. Surface Water, Groundwater and Vadose Zone Interactions in Selected Pristine Catchments in the Kruger National Park. WRC Progress Report 2 - Geophysics Data, K5/2051.
- Riddell, ES, van Niekerk, A, Nel, JM, Jumbi, FT, Fundis, D and Lorentz, SA. 2013. Surface Water, Groundwater and Vadose Zone Interactions in Selected Pristine Catchments in the Kruger National Park. WRC Progress Report 9. K5/2051.
- Ridolfi, L, Dodorico, Poroorato, A and Rodrigez-Iturbe, I. 2003. Stochastic soil moisture dynamics along a hillslope. *Journal of Hydrology* 272:264-275.
- Rodriguez-Iturbe, I. 2000. Ecohydrology: A hydrologic perspective of climate-soil-vegetation dynamics. *Water Resources Research*, 36:3-9.
- Rodríguez-Iturbe, I and Porporato, A. 2004. Ecohydrology of water-controlled ecosystems: soil moisture and plant dynamics. Cambridge University Press.
- Sanjari G, Yu, B, Ghadiri, H, Cielsiolka, CAA and Rose, CW. 2009. Effects of time controlled grazing on runoff and sediment loss. *Australian Journal of Soil Research* 47:796–808.
- Scholes, RJ and Walker, BH. 1993. An African savanna: Synthesis of the Nylsvley study. Cambridge University Press, Cambridge, England.
- Scholes, RJ and Archer, SR. 1997. Tree-grass interactions in savannas. *Annual Review of Ecology and Systematics* 28:517-544.
- Schulze R.E. 1995. Hydrology and Agrohydrology: A Text to Accompany the ACRU 3.00 Agrohydrological Modelling System. Water Research Commission, Pretoria.
- Sieber, A and Uhlenbrook, S. 2005. Sensitivity analyses of a distributed catchment model to verify the model structure. *Journal of Hydrology* 310:216–235.

- Šimůnek, J, Šejna, M, Saito, H, Sakai M, and van Genuchten, MTh. 2013. The HYDRUS-1D Software Package for Simulating the Movement of Water, Heat, and Multiple Solutes in Variably Saturated Media, Version 4.17, HYDRUS Software Series 3, Department of Environmental Sciences, University of California Riverside, Riverside, California, USA, pp. 342.
- Sivapalan, M and Kalma, JD. 1995. Scale problems in hydrology: Contributions of the Robertson Workshop. *Hydrological Processes*, 9(3-4):243-250.
- Sivapalan, M, Blöschl, G, Zhang, Lu and Vertess. 2003: Downward approach to hydrological prediction. *Hydrological Processes*. 17, 2101–2111. Published online in Wiley InterScience (www.interscience.wiley.com). DOI: 10.1002/hyp.1425.
- Smethurst, PJ, Langergraber, G, Petrone, KC. and Holz, GK. 2009. Hillslope and stream connectivity: simulation of concentration-discharge patterns using the HYDRUS model. 18th World IMACS/MODSIM Congress, Cairns, Australia 13-17 July 2009.
- Smit, IPJ, Riddell, ES, Cullum, C and Petersen, R. 2013. ‘Kruger National Park research supersites: Establishing long-term research sites for cross-disciplinary, multiscaled learning. *Koedoe* 55(1), Art. #11077 pages. <http://dx.doi.org/10.4102/koedoe.v55i1.1107>.
- Smithers J and Schulze RE. 1995. ACRU Agrohydrological Modelling System User Manual. WRC Report TT 70/95, Water Research Commission, Pretoria.
- Soil Classification Working Group. 1991. Soil classification. A taxonomic system for South Africa. Ministry of Agriculture and Natural Resources. No. 15. Department of Agriculture and Development, Pretoria.
- Soulsby, C, Tetzlaff, D, Dunn, SM and Waldron, S. 2006. Scaling up and out in runoff process understanding: Insights from nested experimental catchment studies. *Hydrological Processes*, 20(11):2461-2465.
- Spence, C. 2007. On the relation between dynamic storage and runoff: A discussion on thresholds, efficiency, and function. *Water Resources Research*, 43(12).
- Stieglitz, M, Shaman, J, McNamara, J, Engel, V, Shanley and Kling, GW. 2003. An approach to understanding hydrologic connectivity on the hillslope and the implications for nutrient transport. *Global Biogeochemical Cycles* 17 (4):16.1–16.15.
- Suleiman AA, Bali KM, Kleissl J. 2009. Comparison of ALARM and SEBAL Evapotranspiration of Irrigated Alfalfa. 2009 ASABE Annual International Meeting.

- Tasumi, M, Trezza, R, Allen, RG and Wright, JL. 2003. Some U.S. Validation Tests on the SEBAL Model for Evapotranspiration via Satellite. Proceedings of the ICID Workshop on Remote Sensing of Evapotranspiration for Large Regions. P 13.
- Tetzlaff, D, Soulsby, C, Bacon, PJ., Youngson, AF, Gibbins, C and Malcolm, IA. 2007. Connectivity between landscapes and riverscapes—a unifying theme in integrating hydrology and ecology in catchment science? *Hydrological Processes*, 21(10):1385-1389.
- Tetzlaff, D, McDonnell, JJ, Uhlenbrook, S, McGuire, KJ, Bogaart, PW, Naef, F and Soulsby, C. 2008. Conceptualizing catchment processes: simply too complex? *Hydrological Processes*, 22(11):1727-1730.
- Thompson, SE, Harman, CJ, Troch, PA, Brooks, PD and Sivapalan, M. 2011. Spatial scale dependence of ecohydrologically mediated water balance partitioning: A synthesis framework for catchment ecohydrology. *Water Resource Research*, 47, W00J03, doi:10.1029/2010WR009998.
- Ticehurst, JL, Cresswell, HP, McKenzie, NJ and Clover, MR. 2007. Interpreting soil and topographic properties to conceptualize hillslope hydrology. *Geoderma* 137, pp. (279 – 292).
- Timmermans, WJ, Kustas, WP, Anderson MC and French, AN. 2006. An intercomparison of the Surface Energy Balance Algorithm for Land (SEBAL) and the Two-Source Energy Balance (TSEB) modelling schemes. *Remote Sensing of Environment* 108 (2007):369–384.
- Todd, KD. 1980. *Groundwater Hydrology*. University of California, John Wiley and Sons. New York.
- Troch, PA, Martinez, GF, Pauwels, V, Durcik, M, Sivapalan, M, Harman, C and Huxman, T. 2009. Climate and vegetation water use efficiency at catchment scales. *Hydrological Processes*, 23(16):2409-2414.
- Tromp-van Meerveld, I and McDonnell, JJ. 2006. Threshold relations in subsurface stormflow: The fill and spill hypothesis. *Water Resources Research* 42:1-11.
- Tyson, PD and Dyer, TGJ. 1978. The predicted above-normal rainfall of the seventies and the likelihood of drought in the eighties in South Africa. *S. Afr. J. Sci.*, 74 pp. 372–377

- Uchida, T, McDonnell, JJ and Asano, Y. 2006. Function intercomparison of hillslopes and small catchments by examining water source, flowpath and mean residence time. *Journal of Hydrology* 327: 627–642. DOI: 10.1016/j.jhydrol.2006.02.037.
- Uhlenbrook, S, Frey, M, Leibundgut, CH and Maloszewski, P. 2002. Hydrograph separations in a mesoscale mountainous basin at event and seasonal timescales. *Water Resource Research*.38(6):1–14.
- Uhlenbrook, S, Wenninger, J and Lorentz, SA. 2005. What happens after the catchment caught the storm? Hydrological processes at the small, semi-arid Weatherley catchment, South-Africa. *Advances in Geoscience* 2:237-241.
- van Genuchten, MT, Leij, FJ and Yates, SR. 1991. The RETC code for quantifying the hydraulic functions of unsaturated soils. EPA/ 600/ 2-91/ 065. RS Kerr Environmental Research Laboratory, US environmental Protection Agency, Oklahoma, USA.
- van Genuchten, MT and Šimůnek, J. 1996. Evaluation of pollutant transport in the unsaturated zone, in Proceedings of Regional Approaches to Water Pollution in the Environment, NATO ASI Ser., Ser 2, Environment, edited by. Rijtema PE and Elias, V, Kluwer, Norwell, Mass., in press.
- van Tol, 2008. Soil indicators of hillslope hydrology in the Bedford and Weatherly catchments. Personal Communication relating to unpublished data for MSc in Agriculture at the University of Free State.
- van Tol, JJ, Le Roux, PAL, Hensley, M and Lorentz, SA. 2010. Soil as an indicator of hillslope hydrological behavior in the Weatherley Catchment, Eastern Cape, South Africa. *Water SA* 36:513-519.
- van Tol, JJ, Le Roux, PAL and Hensley, M 2011. Soil indicators of hillslope hydrology. Principles, application and assessments in soil science. In Tech, Rijeka, Croatia, 209-240.
- van Tol, JJ, Le Roux, PAL and Hensley, M. 2012. Pedotransfer functions to determine water conducting macroporosity in South African soils. *Water Science and Technology*, 65(3).
- van Tol, JJ, Le Roux, PAL, Lorentz, SA and Hensley, M. 2013. Hydropedological Classification of South African Hillslopes. *Vadose Zone Journal*. doi:10.2136/vzj2013.01.0007.
- Venter, FJ. 1990. A classification of land for management planning in the Kruger National Park (PhD thesis). University of South Africa, Pretoria, South Africa.

- Venter, FJ, Scholes, RJ and Eckhardt, HC. 2003. The Abiotic template and its associated vegetation pattern. In: The Kruger experience: Ecology and management of savanna heterogeneity (Eds du Toit, JT, Rogers, KH and Biggs, H) pp. 83–129. Island Press, Washington, DC.
- Venter, FJ, Naiman, RJ, Biggs, HC and Pienaar, DJ. 2008. The evolution of conservation management philosophy: Science, environmental change and social adjustments in Kruger National Park. *Ecosystems*, 11(2): 173-192.
- Wainwright, J., Mulligan, M. (Eds.), 2004. Environmental Modelling: Finding Simplicity in Complexity. Wiley, Chichester.
- Walker, BH and Noy-Meir, I. 1981. Aspects of the stability and resilience of savanna ecosystems. In: Eds. Huntley, BJ and Walker, BH, Ecology of tropical savannas, Ch. 25: 556-590. *Springer-Verlag*, Berlin, Germany.
- Weiler, M and McDonnell, J. 2004. Virtual experiments: a new approach for improving process conceptualization in hillslope hydrology. *Journal of Hydrology* 285(1–4):3–18.
- Weninger, J, Uhlenbrook, S, Tilch, N and Leibundgut, C. 2004. Experimental evidence of fast groundwater responses in a hillslope/floodplain area in the Black Forest Mountains, Germany. *Hydrological Processes*, 18(17):3305-3322.
- Weninger, J, Uhlenbrook, S, Lorentz, S and Leibundgut, C. 2008. Identification of runoff generation processes using combined hydrometric, tracer and geophysical methods in a headwater catchment in South Africa. *Journal of hydrological science*. 53:65 – 80.
- Werner, Patricia A, Walker, BH and Stott, PA. 1991. "Introduction" Savanna Ecology and Management: Australian Perspectives and Intercontinental Comparisons. Oxford: Blackwell Publishing. ISBN 978-0-632-03199-3.
- Western, WA, Grayson, RB, Blöschl, G, Willgoose, GR and McMahon, TA. 1999. Observed spatial organization of soil moisture and its relation to terrain indices. *Water Resources Research*.35:797–810.
- Western, AW, Zhou, SL, Grayson, RB, McMahon, TA, Blöschl, G and Wilson, DJ. 2004. Spatial correlation of soil moisture in small catchments and its relationship to dominant spatial hydrological processes. *Journal of Hydrology* 286(1):113-134.
- Woods, R and Rowe, L. 1996. The changing spatial variability of subsurface flow across a hillside. *Journal of Hydrology*. (NZ) 35(1):51-86.

- Wright, JL and Jensen, ME. 1972. Peak water requirements of crops in southern Idaho. American Society of Civil Engineering, *Journal of Irrigation and Drainage*. 98(IR2):193-201.
- Zhang, L. 2002. Modelling and prediction. *Hydrological Processes* 13: doi:10.1006/rwas.2002.0172. University of Nevada–Las Vegas, Department of Geoscience, Las Vegas, NV 89154, USA.

## 9. APPENDICES

### 9.1 Appendix A: Results from Geophysical Surveys (ERT) on Basalt Supersite

Due to time and logistic constraints, geophysical surveys could not be done on the southern basalt supersite during the 2012-2013 period therefore, just for comparison sake between the two geologies surveys that were done in 2011 are presented (courtesy of Lucie Porentu)

1<sup>st</sup> order hillslope (Figure 9.1), has a shallow vadose zone, hence shallow soils but comparing it with the other hillslopes on this supersite, it has the deepest soils.

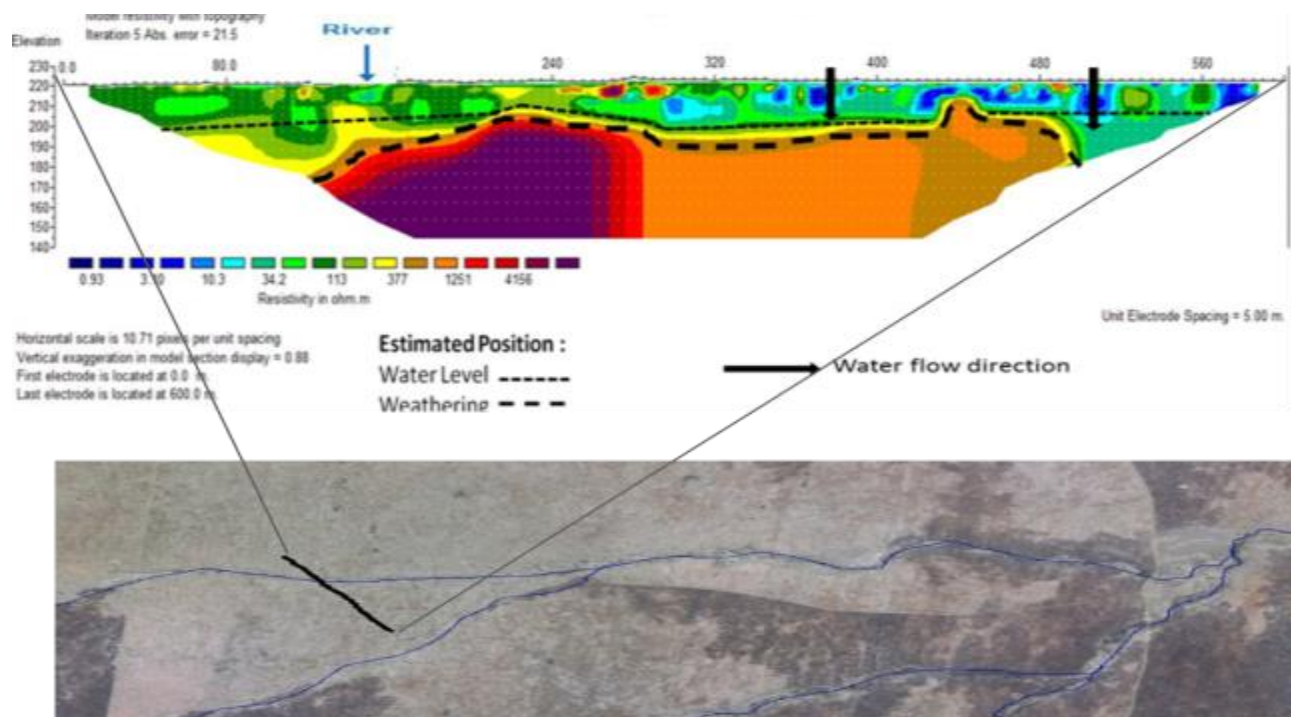


Figure 9.1 Electrical resistivity for basalt 1<sup>st</sup> order hillslope

### SBAS2

The 2<sup>nd</sup> order hillslope (Figure 9.2) appears to have a relatively flat topography with very shallow soils especially at the midslope and parts of the crest (400-560). On this hillslope, it shows that the

interfluves are characterized by shallow soils and they get deeper down the slope towards the stream.

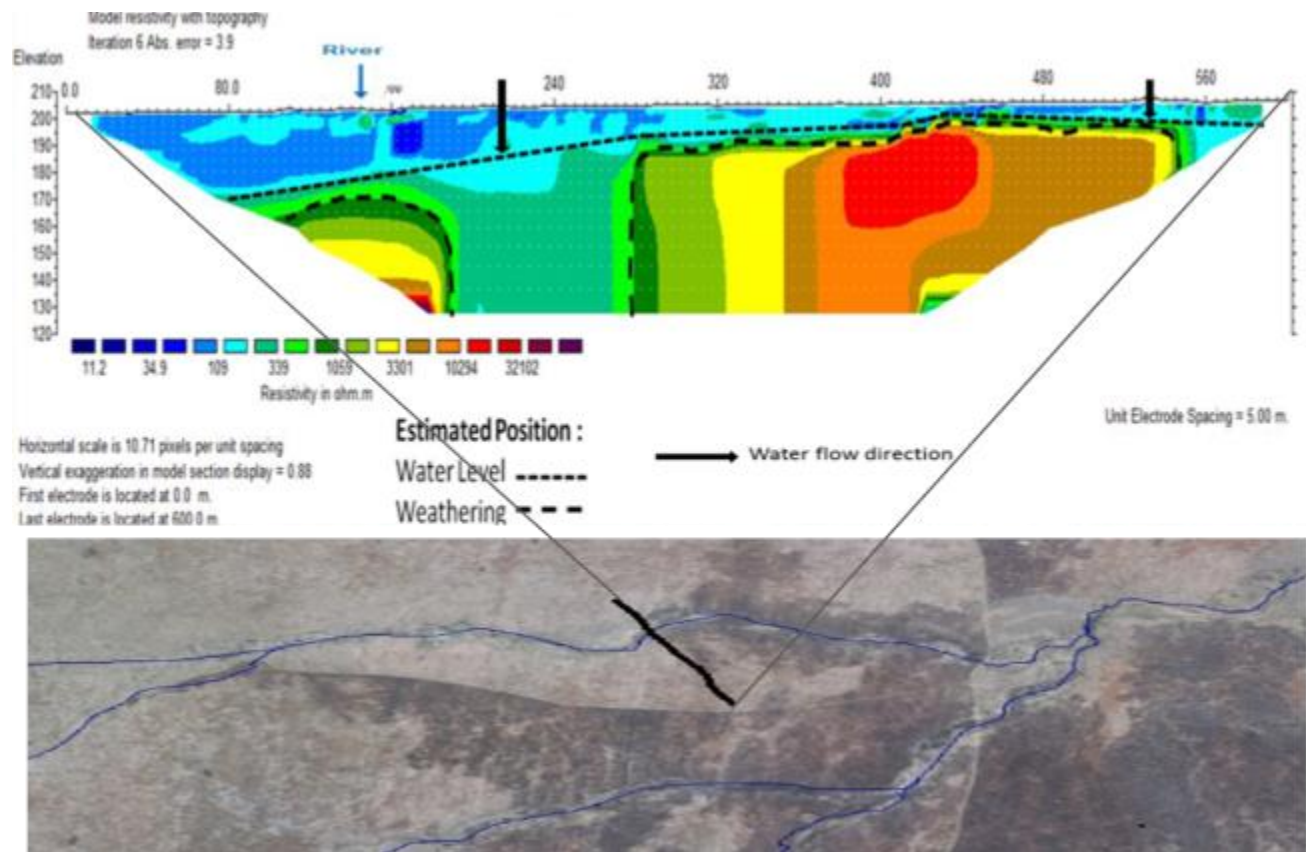


Figure 9.2 Electrical resistivity for basalt 2<sup>nd</sup> order hillslope

### SBAS3

This 3<sup>rd</sup> order hillslope pseudosection (Figure 9.3) indicates a low gradient topography with a very shallow vadose zone, thereby implying very shallow soils (Mispah soil forms). It shows very high resistivity values of the bedrock which lies close to the surface with a shallow weathered zone.

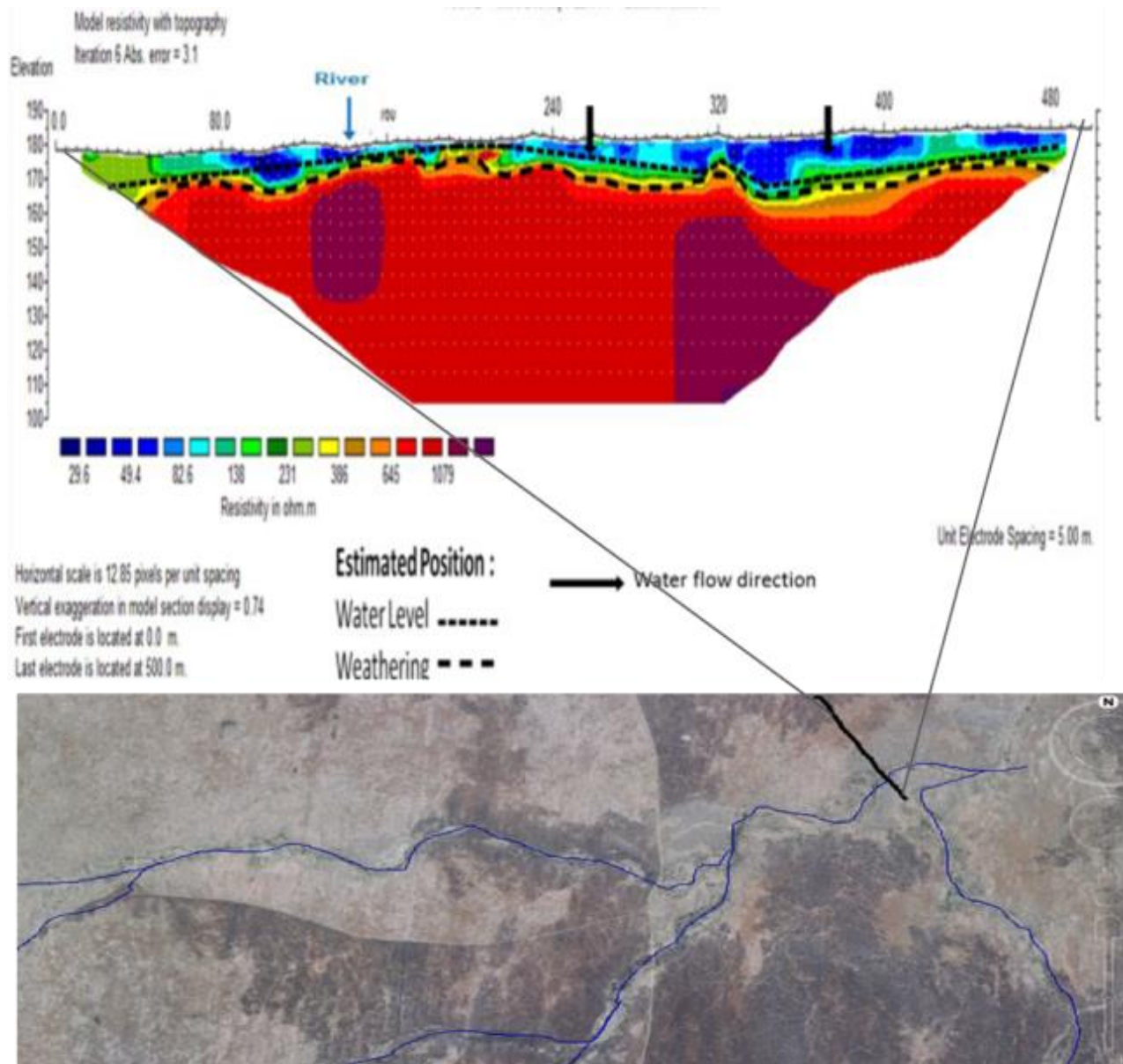


Figure 9.3 Electrical resistivity for basalt 3<sup>rd</sup> order hillslope

Soil surveys have shown that there is potential vertical subsurface flow (recharge) but due to the low gradient topography on these hillslopes, when this water reaches the underlying rock, it cannot flow laterally therefore, most of it is expected to be lost through evapotranspiration.

## 9.2 Depth of installed soil moisture sensors, taxonomical classification and diagnostic horizons

Table 9.1 Catena elements taxonomy classes, diagnostic horizons and depths of installed sensors and thickness of horizons

Profile Number	Horizon	Diagnostic horizon	Soil Form	Depth(mm)	Depth of Sensor (mm)
SGR1_Crest	A	Orthic	Catref	0-250	125
	B	E		250-500	350
		Lithocutanic		500+	500
SGR1_Midslope	A	Melanic	Bonheim	0-200	125
	B	Pedocutanic		200-550	300
		unspecified		550+	450
SGR1_Riparian	A	Melanic	Bonheim	0-200	100
	B	Pedocutanic		200-600	280
		unspecified		600+	1000
SGR2_Crest	A	Orthic	Pinedene	0-200	100
	B	yellow brown apedal		200-400	250
		(unspecified with signs of wetness)		400+	
SGR2_Midslope	A	Orthic	Sterkspruit	0-200	100
	B	Prismacutanic		200-400	250
					400
SGR2_Riparian	A	Orthic	Catref	0-50	100
	B	E		50-200	250
		Lithocutanic		200+	
SGR3_Crest	A	Orthic	Pinedene	0-250	100
	B	Yellow brown apedal		250-500	250
	C	(unspecified with signs of wetness)		500+	350
SGR3_Midslope	A	Orthic	Sterkspruit	0-100	100
	B	Prismacutanic		100-400	300
					800
SGR3_Midslope	A	Orthic	Sterkspruit	0-100	100
	B	Prismacutanic		100-400	300
					400
SGR3_Riparian	A	melanic	Bonheim	0-300	100
	R	Pedocutaanic		300-500	250
		unspecified		500+	400

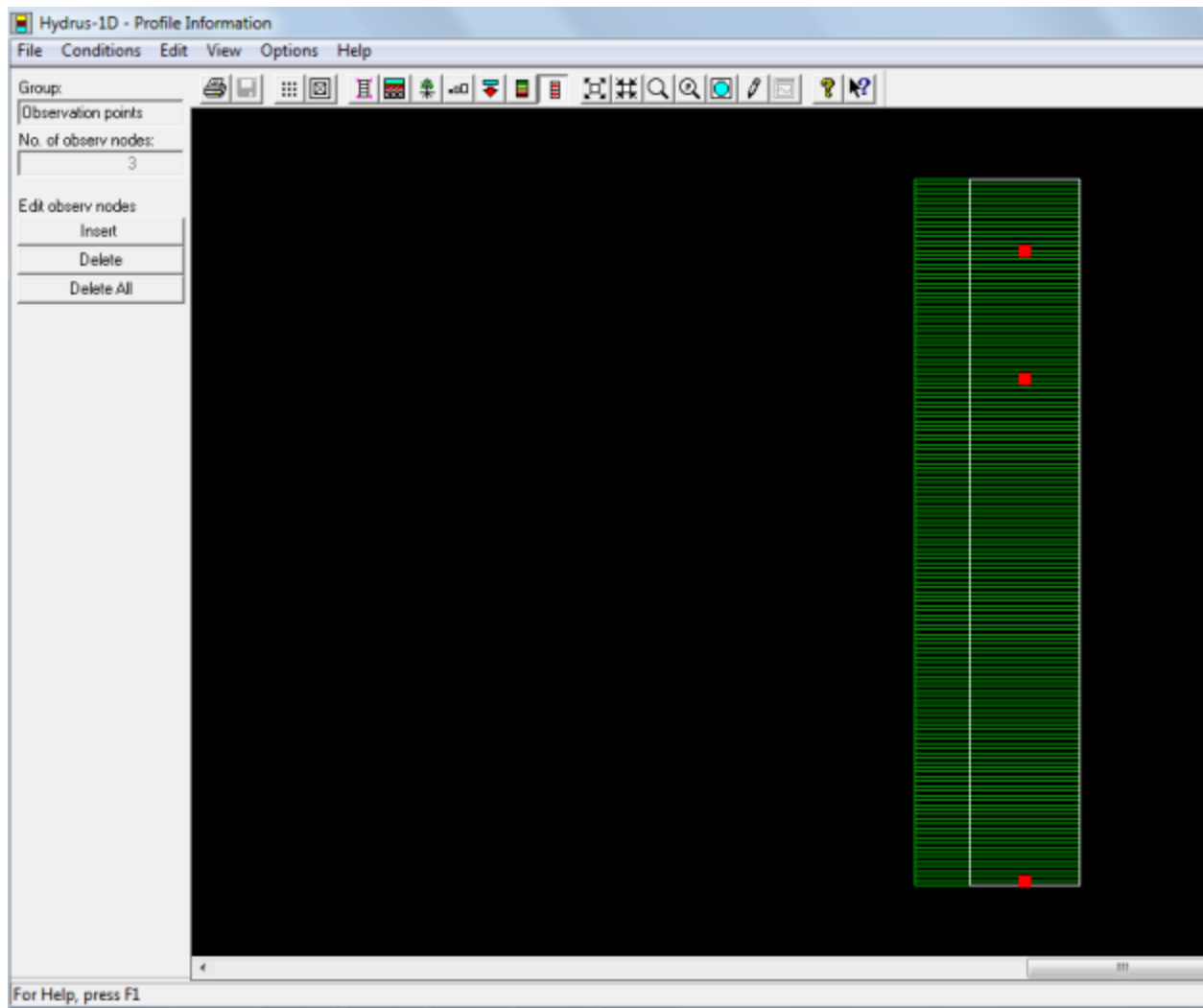


Figure 9.4 Domain set-up with location of observation nodes for 1<sup>st</sup> order riparian.

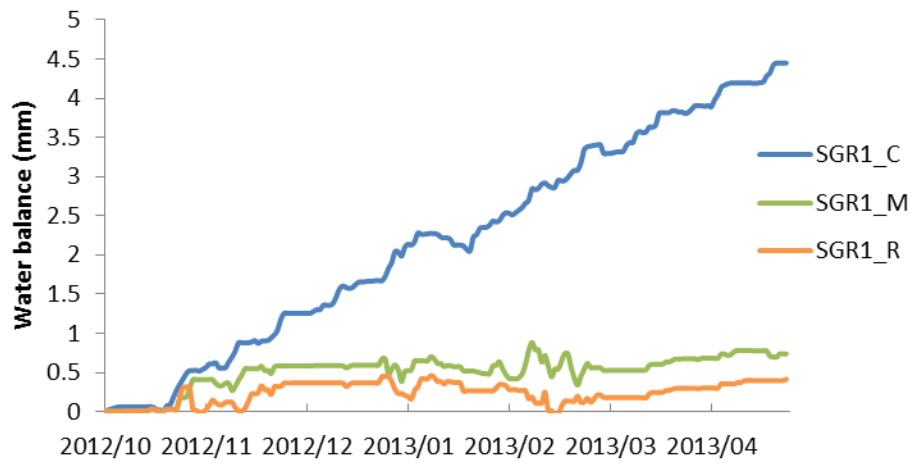


Figure 9.5 Time series water balances for granite 1<sup>st</sup> order Hillslope



Figure 9.6 Time series water balances for granite 2<sup>nd</sup> order hillslope

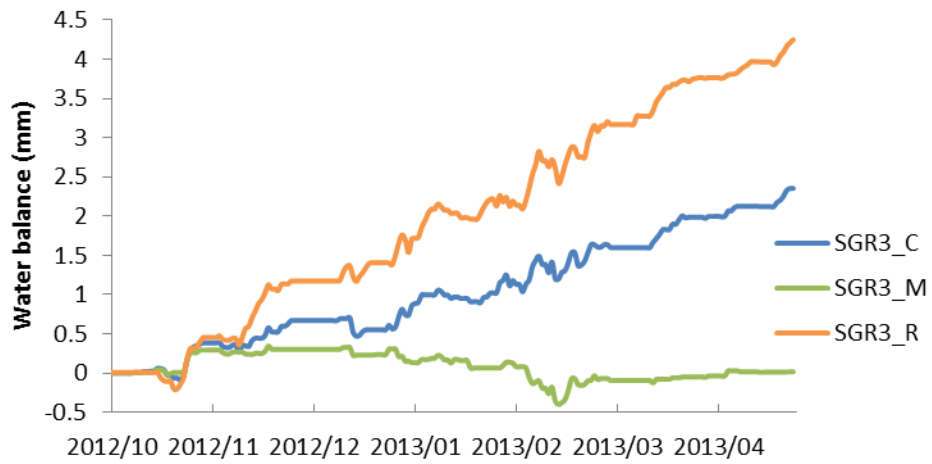


Figure 9.7 Time series water balances for granite 3<sup>rd</sup> order hillslope

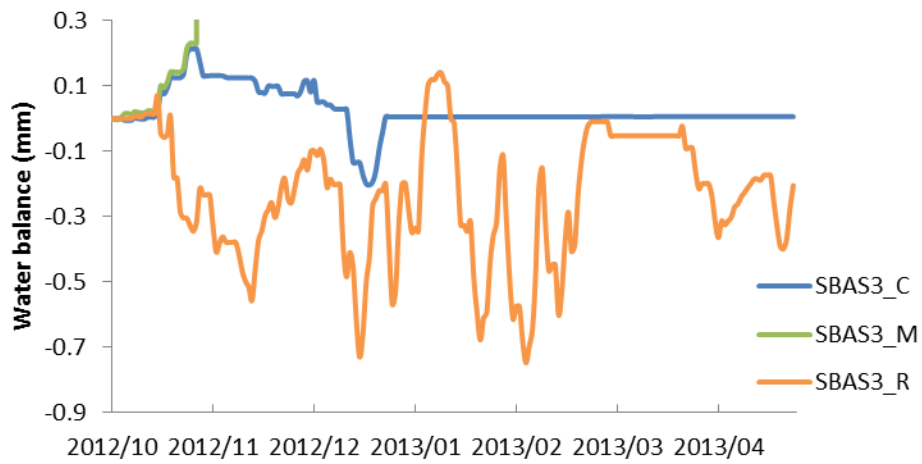


Figure 9.8 Time series water balances for basalt 3<sup>rd</sup> order hillslope

### 9.3 $K_{sat}$ Replicates on Granite Supersite Measured Using the Mobile Permeameter

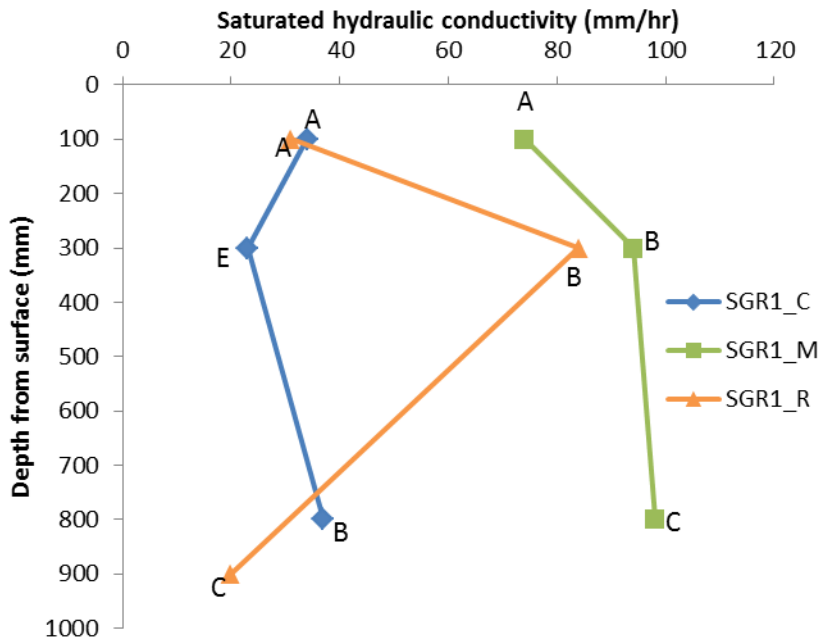


Figure 9.9 Saturated hydraulic conductivity per horizon on granite 1<sup>st</sup> order hillslope

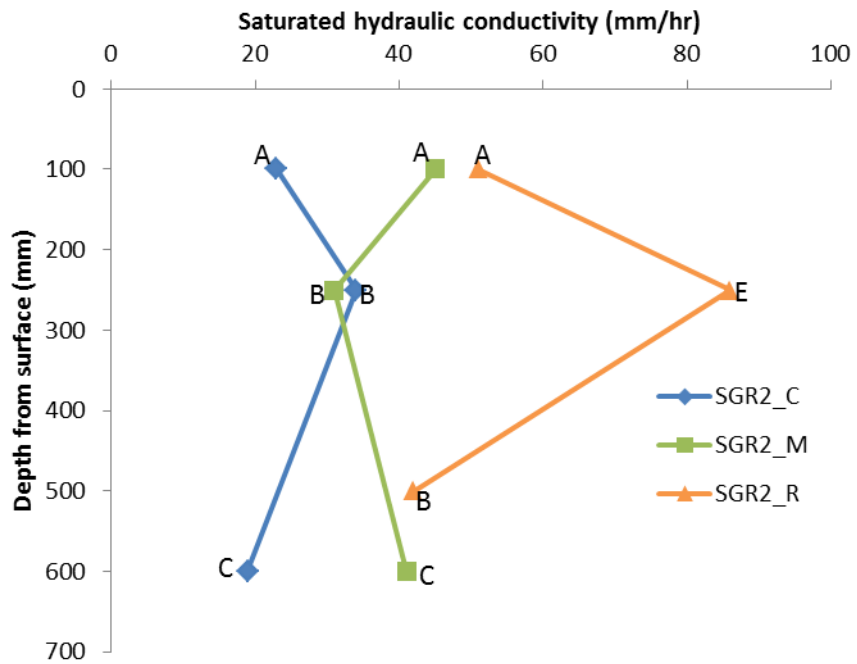


Figure 9.10 Saturated hydraulic conductivity per horizon on granite 2<sup>nd</sup> order hillslope

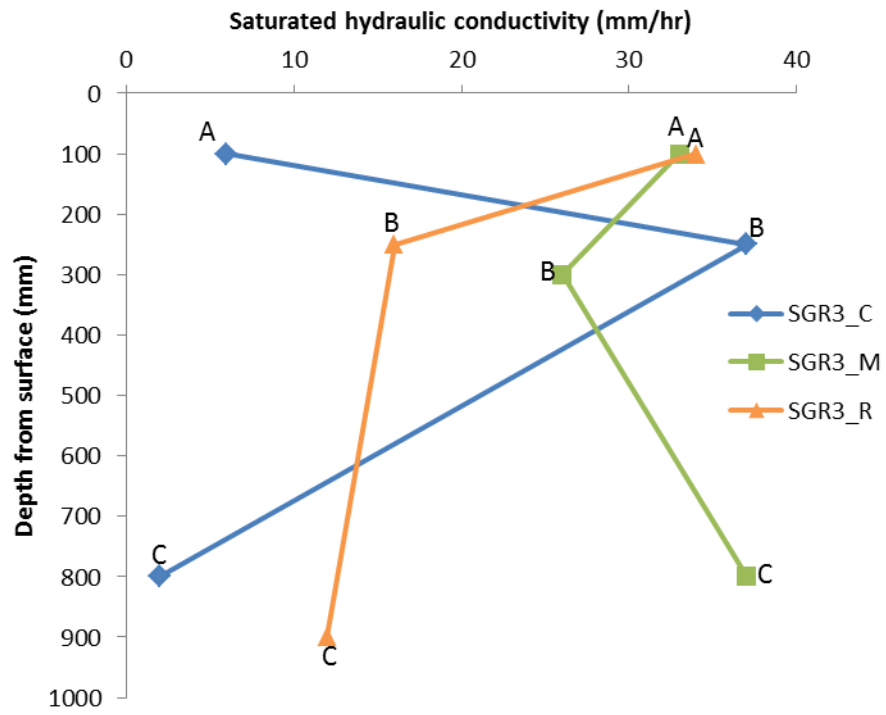


Figure 9.11 Saturated hydraulic conductivity per horizon on granite 3<sup>rd</sup> order hillslope

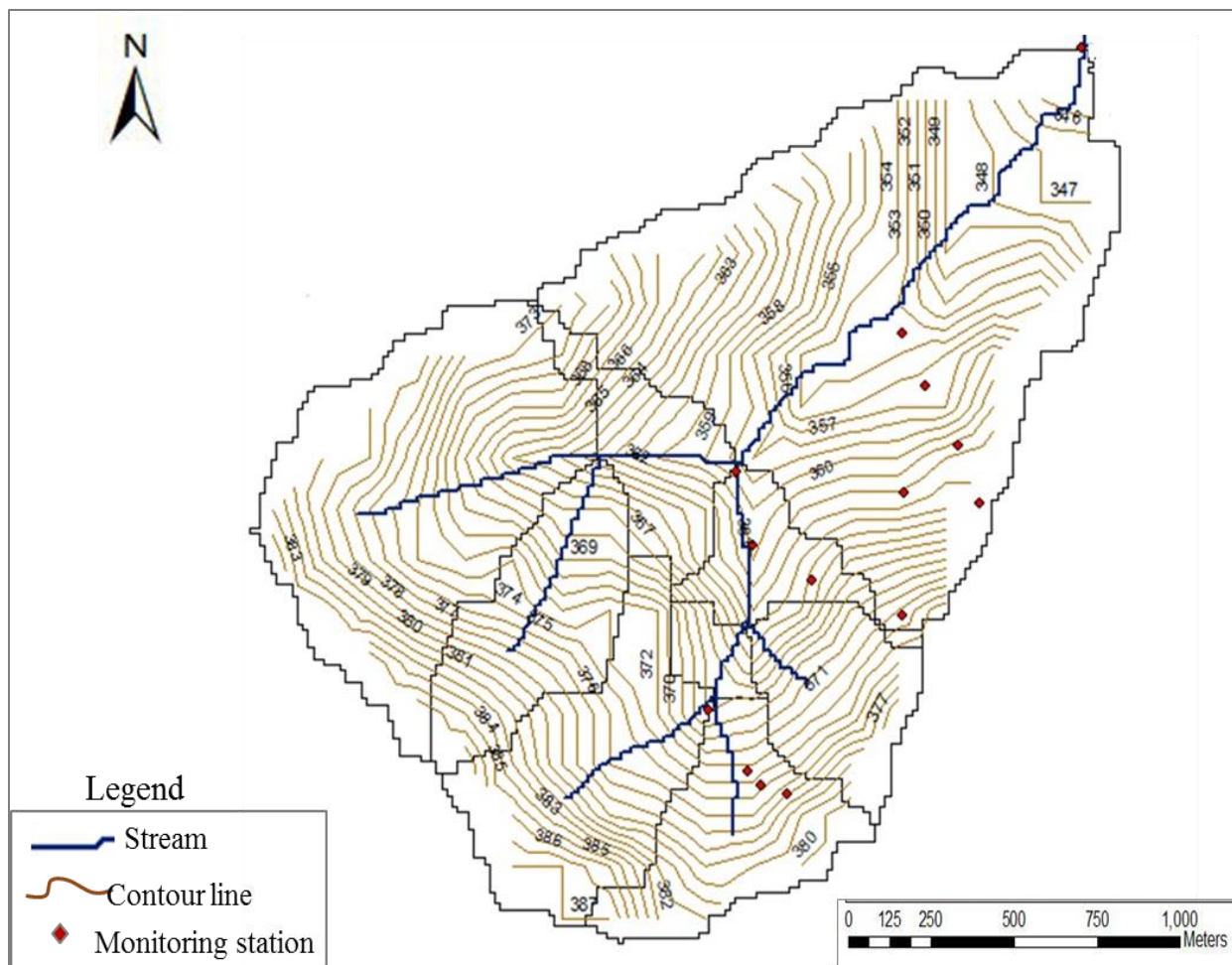
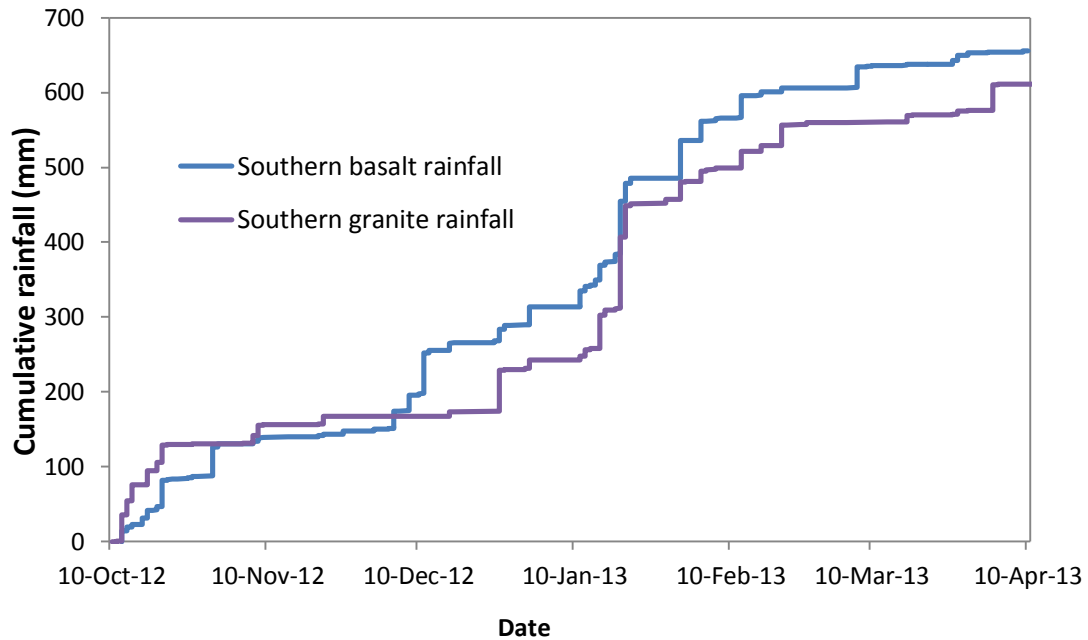


Figure 9.12 The southern granite contour map



Figure

9.13 Cumulative Rainfall for the granite and basalt supersite

Table 9.2 Rooting depths used for flow simulation in HYDRUS

	SGR1	SGR2	SGR3	SBAS3
Crest	500mm	600mm	630mm	300mm
Midslope	600mm	600mm	300mm	300mm
Riparian	600mm	250mm	600mm	300mm